SYNTHESIS, CHARACTERIZATION AND BIOLOGICAL ACTIVITY OF SOME CARBAZONE SCHIFF BASES AND THEIR METAL COMPLEXES

MOHD. RIZAL BIN RAZALI

A DISSERTATION SUBMITTED TO DEPARTMENT OF CHEMISTRY IN FULFILMENT OF THE DEGREE OF MASTER OF SCIENCE

FACULTY OF SCIENCE
UNIVERSITY OF MALAYA
KUALA LUMPUR

2009

ACKNOWLEDGEMENT

ABSTRACT

All the metal complexes in this study are synthesized by the general method which the ligand was first prepared by refluxing the precursors of the Schiff base. It was then followed by the addition of the appropriate metal salt to form metal complexes. The characterization of the series of the Schiff base complexes of Ni(II), Cu(II), Zn(II) and Cd(II) with ligand systems containing nitrogen, sulphur and oxygen donor atoms were also carried out.

Formation of the Schiff base ligands were confirmed by the presence of v(C=N) band at the range 1550-1650 cm^{-1} in the IR spectra. In some cases the absence of a band around 1700 cm^{-1} that can be attributed to C=O stretching indicates the complete condensation of the carbonyl group. The reductions in the relative intensity of the *thione* sulphur and *keto* oxygen bands were evidence of the complexation.

The ^{1}H and ^{13}C NMR spectroscopy technique was employed to prove the formation of the Schiff base ligands. The electronic spectra of metal complexes with Schiff bases containing several donors atom displayed charge transfer at the range of 26000-30000 cm^{-1}. In the case of Ni(II) ad Cu(II) complexes, low intense visible bands were seen between 17000-20000 cm^{-1}. Studies of the magnetic properties of several metal complexes were also conducted. Magnetic susceptibilities of Cu(II) complexes showed that the Cu(II) are paramagnetic. The magnetic moments obtained were consistent with those reported for Cu(II).

The crystal structure of some metal complexes revealed that the Schiff bases always behaved as bidentate ligands which chelated through the azomethine nitrogen and deprotonated sulphur or oxygen. Determination by X-ray diffraction have showed that, in the solid state of the complexes, the bis(1*H*-Indole-3-carbaldehyde)thiocarbohydrazone and 1*H*-Indole-3-carbaldehyde thiosemicarbazone exhibit as *thiol* tautomer while bis(1*H*-Indole-3-carbaldehyde)carbohydrazone existed as an *enol* tautomer.

The crystal structure showed that the $Ni_{Ind3Thio}$ possessed self assembly via the hydrogen bonds to furnish infinite layer structure. Besides, the structure for bis(1*H*-Indole-3-carbaldehyde)carbohydrazone formed infinite zigzag chain structure due to hydrogen bonds between the independent molecules.

The toxicity study and antiulcerogenic activity were carried out. The metal complexes have showed significantly property in preventing the ulcer disease especially for the Zn(II) and Cd(II) complexes.

ABSTRAK

Kesemua kompleks logam di dalam kajian ini telah disintesis dengan kaedah yang biasa digunapakai iaitu ligan bes Schiff disediakan dengan merefluks sebatian permulaan. Kemudian, garam logam yang sesuai ditambah ke dalam ligan untuk memperolehi kompleks-kompleks logam yang diingini. Kesemua bes Schiff dan siri nikel(II), kuprum(II), zink(II) dan kadmium(II) kompleks logamnya dicirikan dengan menggunakan teknik-teknik kimia fizik.

Pembentukan bes Schiff dipastikan dengan kewujudan regangan v(C=N) dalam julat 1550-1650 cm^{-1} di dalam spektrum inframerah. Di dalam kes-kes tertentu, ketiadaan regangan dalam julat 1700 cm^{-1} yang mewakili regangan v(C=O) dapat memberi petunjuk bahawa kondensasi telah berlaku sepenuhnya tehadap kumpulan karbonil. Kewujudan kompleks logam juga dipastikan dengan perubahan regangan kepada atom sulfur dan oksigen di dalam spektrum kompleks logam.

Analisis spektroskopi ^{1}H dan ^{13}C NMR telah dijalankan untuk memastikan pembentukan bes Schiff. Spektrum elektronik untuk kompleks logam dengan bes Schiff yang mengandungi beberapa atom penderma menunjukkan pemindahan cas di dalam julat 26000-30000 cm^{-1} . Untuk kes-kes nikel(II) dan kuprum(II), regangan yang lemah dapat dilihat sekitar julat 17000-20000 cm^{-1} . Sifat kemagnetan untuk beberapa kompleks logam juga turut dijalankan. Regangan magnetik untuk kuprum(II) membuktikan bahawa kompleks kuprum(II) adalah paramagnetik. Nilai kesan momen yang diperolehi oleh kuprum(II) ini menyamai dengan yang telah dilaporkan sebelum ini.

Struktur kristal untuk beberapa kompleks logam menunjukkan bahawa bes Schiff akan bersifat ligan bidentat melalui atom nitrogen azometina dan pemprotonan sulfur ataupun oksigen. Pembelauan sinar-X menunjukkan bahawa, di dalam keadaan pepejal ligan-ligannya seperti bis(1*H*-Indole-3-carbaldehyde)thiocarbohydrazone dan 1*H*-Indole-3-carbaldehyde thiosemicarbazone wujud sebagai tautomer *thiol* manakala bis(1*H*-Indole-3-carbaldehyde)carbohydrazone wujud sebagai tautomer *enol*.

Struktur kristal menunjukkan bahawa Ni$_{\text{Ind3Thio}}$ dengan sendirinya melalui ikatan hidrogen membentuk struktur lapisan yang berkepanjangan infiniti. Selain daripada itu, struktur bis(1*H*-Indole-3-carbaldehyde)carbohydrazone membentuk struktur rantaian zigzag disebabkan kewujudan ikatan hidrogen di antara molekul-molekul yang bebas.

Kajian terhadap ketoksidan and aktiviti antiulser telah dijalankan. Kompleks-kompleks logam menunjukkan hasilan yang baik dalam mencegah ulser terutamanya kompleks-kompleks zink(II) dan kadmium(II).

TABLE OF CONTENTS

LIST OF TABLES

LIST OF FIGURES

These following abbreviations were used at various parts in the subsequent text:

Å	Ångström
B.M	Bohr Magneton
cm	Centimeter
c	Concentration
ºC	Degree Celsius
DMF	N,N-Dimethylformamide
DMSO	Dimethylsulfoxide
g	Gram
h	Hour
IR	Infra-red
Ind3Thio	bis(1H-Indole-3-carbaldehyde)thiocarbohydrazone
Ind3Thiosemi	1H-Indole-3-carbaldehyde thiosemicarbazone
Ind3Carbo	bis(1H-Indole-3-carbaldehyde)carbohydrazone
K	Kelvin
kg	Kilogram
mg	Milligram
ml	Milliliter
mm	Millimeter
mmol	Millimole
min	Minute

MW	Molecular Weight
NMR	Nuclear Magnetic Resonance
ORTEP	Oak Ridge Thermal-Ellipsoid Plot Program
ppm	Parts Per Million
%	Percentage
% I	Percentage of Inhibition
S.E.M.	Standard Error Mean
UI	Ulcerative Index
UV-Vis	Ultraviolet-Visible
χ_g	Mass Susceptibility
χ_m	Molar Susceptibility

Introduction

Indoles constitute on important class of heterocyclic compounds because of its applications in several fields such as medicine and the cosmetics industry (Sundberg, 1970). Owing to their importance as biological active compounds, research has been directed to improving the activities of the compounds through replacing some of the hydrogen atoms with other functional groups. For example, replacement of hydrogen atom with methoxy group in melatonin has been proven successful in treating strokes (Raymond and Shiufun, 2004). Indoles can have substituents in several carbon positions and among these sustituents, one of the most useful is the formyl substituent.

The condensation of aldehydic or ketonic group with the primary amine has afforded compounds known as 'Schiff bases'; such chemicals have been known for more than 150 years (Schiff, 1864). One reason for the abundance of Schiff bases in the chemical literature can be attributed to the convenient synthesis of the carbon-nitrogen double bond, which generally proceeds under mild conditions, without catalysts and sometimes, even without the application of heat.

Studies of Schiff bases comprising of indoles have shown their usefulness arising from their antioxidant, anticancer activity and antimalarial properties. The present work involves the synthesis of Schiff base based on the condensation of indole-3-carboxaldehyde with thiocarbohydrazone, thiosemicarbazone or carbohydrazone. These carbazones are primary amines which have *thiolic-thionic* tautomerism or *ketoic-enolic* tautomerism; the compounds, owing to the presence of azomethine nitrogen, can

1

function as chelating ligands to metal ions in their deprotonated forms. Moreover, it was reported before that the sulphur donor ligands have been given considerable attention because of their important role in biology aspect.

The ability to coordinate in either neutral *thione* or deprotonated *thiol* as well as in either neutral *keto* or deprotonated *enol* form plays an important part in the transition metal chemistry of the ligand.

Metal Schiff base complexes were also discovered long time ago (Ettling, 1840); systematic studies were undertaken by Pfeiffer and co-workers in 1931 to 1942. Whereas such systems are now not in the forefront of chemistry, they remain as appropriate research topics owing to interesting structural, electronic and magnetic features that can be elucidated by most spectroscopic methods.

The present trend in chemical research on Schiff-base complexes has gyrated towards elucidation of antifungal activity and antibacterial activity (Sathisha et al., 2008). That is, such metal complexes may have the possibility to serve as antibiological agents. This dissertation contributes to this field by reporting the nature of the chemical interaction between the metal ions and the deprotonated Schiff bases. In this report, the ligands and their metal complexes were characterized by physico-chemical techniques including IR, ^{1}H and ^{13}C NMR, UV-visible and magnetic susceptibility. For crystalline compounds, their solid-state structures were elucidated by X-ray diffraction.

The toxicity of the compounds was evaluated on *Sprague-Dawley* rats. Furthermore, the Schiff bases and their metal complexes were also screened for antiulcerogenic activity to examine the protective effect of the ligands and their metal complexes against ethanol-induced gastric lesions in *Sprague-Dawley* rats.

Literature Review

2.1 Indole

First obtained in 1866 by Adolf von Baeyer, indole was originally prepared by zinc-dust pyrolysis of oxindole which had been obtained by the reduction of isatin, an oxidant product of the natural dyestuff, indigo. Interest in indole chemistry revived around 1930 when it was discovered that the essential amino acid, tryptophan, the plant growth hormone, heteroauxin and several groups of important alkaloids are indole derivatives. It was shown that 3-methylindole is produced with indole during pancreatic digestion or putrefactive decomposition of proteins and, hence, both are found in the intestines and feces. Interest has centered on medicinal and biochemical aspects of indole chemistry.

The new metal complexes of 1*H*-Indole-3-ethylensalicylaldimine, in which the study forms part of a line of work on biochemical applications of coordination compounds has been synthesized and characterized (Martin R. et al., 1986). This same group also prepared metal complexes from 1*H*-indole-3-ethylensalicylaldimine with their 3-methoxy, 5-methoxy and 5-bromo derivatives to investigate the thermal stability of these complexes (Martin Z. et al., 1989).

Based on this work, nickel complexes were synthesized from bis(1*H*-indole-3-ethylene)-3'-ethoxysalicylaldimine ligand **(I)** in order to compare the ligand with those of related compounds and to see how the nature and position of alkoxy groups affect its properties (Gili et al., 1990).
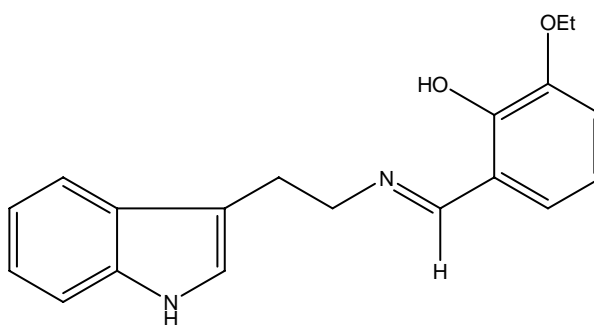
(I)

Gili and co-workers reported the structural characterization of the N-[2-(3-ethyl-indole)]-pyridoxaldimine and its copper(II) and nickel(II) complexes (Gili et al., 1992). They suggested that the complexes exhibit as four coordinated structure supported with some spectroscopic data such as IR, NMR, UV, EPR and TGA data.

Recently, divalent transition metal complexes have been synthesized and studied with indole-2-carboxylic acid and 4-substituted hydrazinethiocarbamide (Ahmed I. T., 2006). An octahedral structure was suggested for Co(II), Ni(II) and Cu(II) ternary complexes.

On the aspect of biological activities, indole and its derivatives represent one of the most active classes of compounds possessing a wide spectrum of antiparasitic activities. Indole alkaloids as apicidin **(II)** have shown potent antimalarial activity against *P. falciparum*. Studies on apicidin have suggested that the indole region is a key constituent of enzyme binding and HDAC activity (histone deacetylase), a nuclear enzyme that regulates gene transcription and the assembly of newly synthesized chromatine (Singh S.B. et al., 1996).
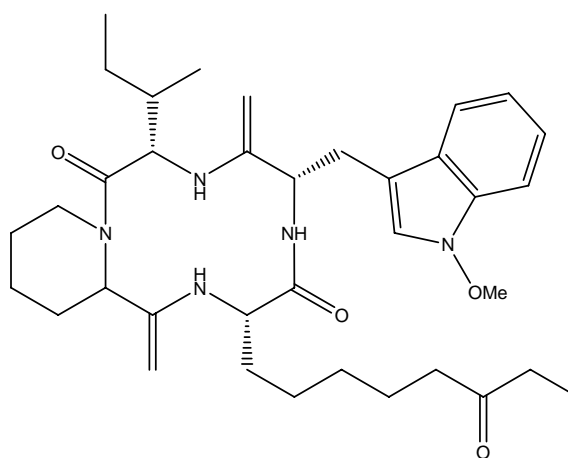
(II)

Scavenging activity of indole compounds such as melatonin **(III)**, tryptophan and serotonin against cisplatin (*cis*-diaminedichlroplatinum or CDDP)-induced reactive oxygen species (ROS) was studied by Fukutomi in 2006. The results indicate that melatonin inhibits CDDP-induced cytotoxicity by directly scavenging OH, and that melatonin markedly reduces renal cytotoxicity and DNA fragmentation caused by CDDP-induced ROS *in vitro* (Fukutomi et al., 2006).
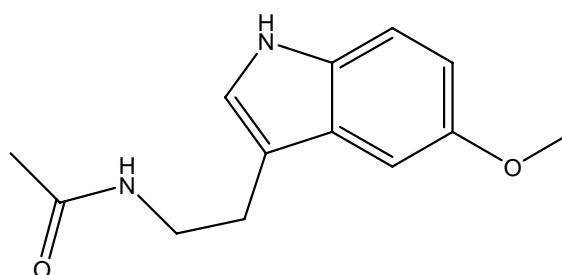
(III)

Previously, it was reported that the indole compound melatonin, which is secreted from the pineal body to have antioxidant activity (Macchi and Bruce, 2004; Boutina et al., 2005). Indole compounds, such as the melatonin precursors, tryptophan

and serotonin, and the melatonin metabolite 6-OH-MLT, also have antioxidant activity (Noda et al., 1999; Betten et al., 2001). Hardeland and Poeggeler noted that melatonin exhibited antioxidant activity by donating electrons to –OH groups to become indolyl cation radicals (Hardeland et al., 1993; Poeggeler et al., 1994)

2.2 Thiocarbohydrazide

Thiocarbohydrazide was discovered in 1908 by R. Stolle and structural study on this chemical was started by Wilson and Gula. The synthesis of thiocarbohydrazide has been done by Beyer in 1954 and Sandstrom was among the first to use thiocarbohydrazide in heterocyclic synthesis. The wide use of thiocarbohydrazide was due to indefinite shelf life. In the beginning of the scientific research, the exposures of thiocarbohydrazide were goes around physical properties such as the uses in Transmission and Scanning Electron Microscope (TEM and SEM).

Some biological activity studies using thiocarbohydrazide as a starting material were detected around 1970s. Since 1971, the researcher found that ligand with sulphur containing showed properties in inhibitory tumors (Rosenberg, 1971). Most of the research at that time only concentrate on using the platinum ions to test for the tumors. After a year, there was another effort to test the ligand that contain sulphur atom on the cancer cells (Williams, 1972). They have proved that platinum with sulphur-containing ligand showed an important rule in treat a cancer cell.

In 1989, copper(II) complexes with thiocarbohydrazide ligand were tested for antitumor properties (Patil et al., 1989). After that period, the usage of metal ions were widely used especially to examine antitumor properties using Ni(II), Co(II), Pd(II), Zn(II) and others. There be some believe that the ligands which contain a sulphur atom have good activity in antitumor properties.

Around 2004, the Schiff base ligands which contain sulphur atom were continuously used in testing some medical properties. The Schiff base ligand obtained by the condensation of thiocarbohydrazide along with 2-hydroxyacetophenone and synthesis of metal complexes using this ligand were used for antimicrobial activity (Hussen and Azza, 2004). From this Schiff base **(IV)**, the metal complexes that formed were binuclear or mononuclear with *mono*, *bi-*, or *tri-* dentate and the complexes always exhibited as tetrahedral or octahedral structures.
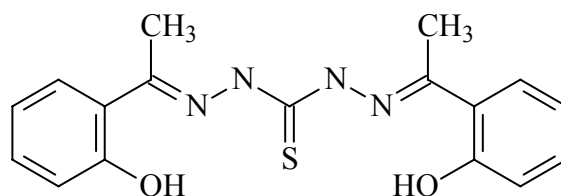
(IV)

In the antimicrobial activity, the Co(II) and Cu(II) complexes that were used in this screening showed that these ligand and metal complexes possessed antimicrobial towards bacteria and fungi. In presenting of –OH group in this Schiff base, the complexes may exist as *thiol* form and the chelation may involved the hydroxyl group, azomethine nitrogen and sulphur atom.

The synthesis of Co(II), Cu(II), Ni(II) and Zn(II) complexes from bis(1,1'-disubstituted ferrocyl)thiocarbohydrazone were used in antibacterial and antifungal (Zahid et al., 1987). The structural study on these complexes showed that the octahedral bidentate complexes gave an excellent property in preventing bacterial.

The complexes synthesized from Co(II), Ni(II) and Cu(II) ions and bis(3-acetlycoumarin)thiocarbohydrazone also apply in the test for anticancer (Sathisha et al., 2004). Determination by the FT-IR, NMR and UV-Vis spectra suggested the structure as **(V)**. These compounds were found to have show cytotoxic activity when screened using the *in vitro* method and Ehrlich Ascites Carcinoma model.

(V)
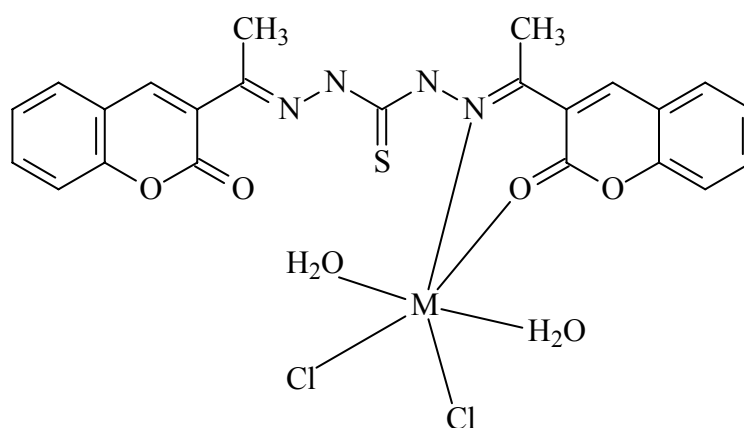
Later on, the same group condensed thiocarbohydrazide with isatin to form another type of Schiff base (Sathisha et al., 2008). With IR, NMR, UV-Vis, magnetic susceptibility and ESR study, they conclude that the complexes that formed exist in two

geometries, four coordinated **(VI)** and six coordinated **(VII)**, based on the metal ions that were used.
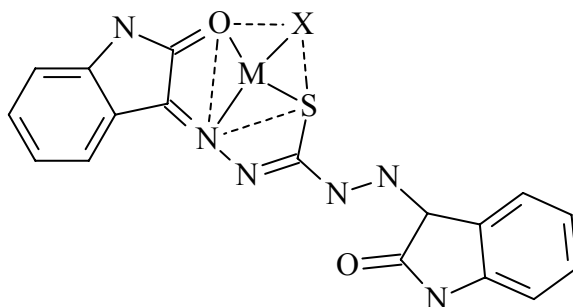
where M= Ni(II), Cu(II)
X= Cl

(VI)
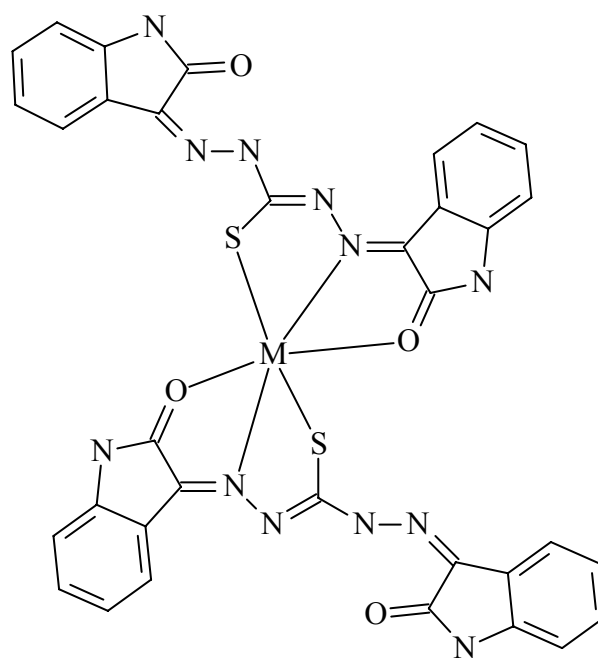
where M= Co(II), Zn(II)

(VII)

The observation of study on the Swiss Albino Mice showed that the octahedral Co(II) complexes gave a good result in not only for anticancer test, but also in antibacterial and antifungal properties.

Beside the use of late transition metal elements, there are also several studies on the geometry for early transition metal elements. In 2007, the VO^{2+} was used in synthesizing the complexes using pyrol-2-carbaldehyde thiocarbohydrazone (Khlood and Nashwa, 2007). The complexes exhibit a square pyramidal structure for VO^{2+} and normally square planar and octahedral structures for late transition metal elements. Furthermore, only this group shows that the bidentate thiocarbohydrazone formed an octahedral environment when chelated to *N,N,S-* from one ligand **(VIII)**.
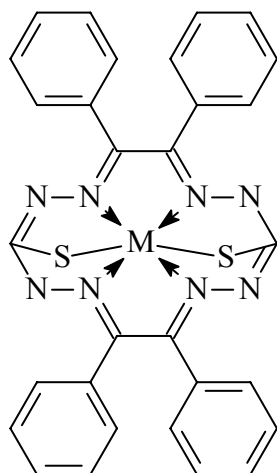
where M= Co(II), Ni(II), Cu(II), Cd(II)

(VIII)

Diana and co-workers in 2008 also studied the structure of the thicarbohydrazide Schiff base ligand. The study on the complexes showed that the complexes exist as binuclear complexes containing the ligands in their tripyldeprotonated forms (Diana et al., 2008). The complexes appear as a four or six coordinated with nonequivalent donor atoms site (*ONN-* and *ONS-*).

2.3 Thiosemicarbazide

Studies of the biological activities of thiosemicarbazide were started in 1946 when they found that thiosemicarbazide to be effective against Mycobacterium tuberculosis and their orthopox virus recognized (Domagk et al., 1946).

Later, in 1960s, the Schiff bases that were synthesized from isatin and thiosemicarbazide were used to investigate anti-virus properties (Bauer et al., 1962; Bauer et al., 1963; Bauer et al., 1965; Bauer et al., 1969). In 1980s, the investigation continued against vaccinia virus *in vivo* and *in vitro* using the same ligand (Walter et al., 1981 and Zgornaik et al., 1980).

In most known metal complexes, the thiosemicarbazide moiety coordinates as a bidentate chelate through sulphur and the hydrazinic nitrogen in *cis*- configuration (Campbell, 1975). For the Schiff base of thiosemicarbazone, if the R groups **(IX)** do not possess suitable coordinating groups, the ligand usually acts as a bidentate ligand, coordinating through the imine nitrogen and the *thione/thiol* sulphur.

$$R_1 \diagdown \atop R_2 \diagup C = N - N - C \diagup^{S}_{\diagdown NH_2}$$
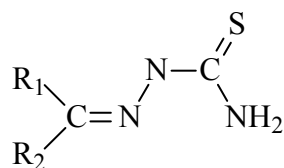
(IX)

The study of metal complexes on biological properties were started in late 1980s when Patil and co-worker synthesized the copper(II) complexes from 5-phenylazo-3-methoxy salicylidine thiosemicarbazone on antitumor properties. The researches also have been done on acetylpyridin thiosemicarbazone metal complexes for their antimalaria properties (Klayman et al., 1983). The Cu(II) complexes with pyridoxcal thiosemicarbazone have been tested to the antitumor cell and showed that the complexes are cytotoxic (Marisa et al., 2003).

In biological study, organometallic thiosemicarbazone also display an important role in antibacterial activities (Chohan et al., 2005). Thiosemicarbazone complexes work against bacteria such as *Escherichia coli*, *Bacillus subtillis*, *Staphylococcus aureus*, *Pseudomonas aeruginosa* and *Salmonella typhi*. They suggested that in increase on coordination number, the properties toward bacterial that showed by the complexes are also increased.

In 2005, the Ni(II) with naphthaquinone thiosemicarbazone **(X)** was tested on MCF-7 human breast cancer cells (Afrasiabi et al., 2005). Determination structure by IR, NMR and X-ray crystallographic data showed that the complex exhibits as an octahedral structure. It was shown that the ligand and its Ni(II) complex increase the inhibitory action on MCF-7 cell proliferation. The better result in metal complex compared to ligand suggested that metal complexation may be a vehicle for activation of the ligand as cytotoxic agent.

Kovala in 2007 have synthesized Zn(II) complexes with pyridine-2-carbaldehyde thiosemicarbazone to examine on bladder cancer cell line and mouse fibroblast L-929 cell line. They have found that the complexes exhibit in several geometries such as distorted octahedral and square pyramidal structure. The study assigned that, the complexes showed significant properties in prevent a cancer meaning that the center Zn(II) display an important role in this cytotoxic activity (Kovala et al., 2007).
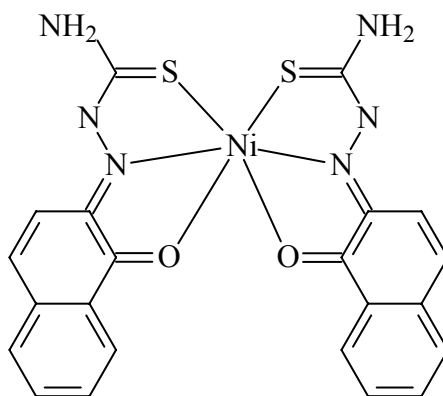
(X)

In 2007, Marisa and her research group have synthesized four coordinated complexes to test on the leukemia cell line U937. The aliphatic thiosemicarbazone forms bidentate complexes with Ni(II) **(XI)** with chelation through the *thiol* sulphur and azomethine nitrogen. The complexes existed as a square planar structure and showed significant properties in leukemia cell (Marisa et al., 2007). It was shown that the thiosemicarbazone complexes have an ability to sequester iron and to inhibit the iron-dependent enzyme ribonucleotide reductase.
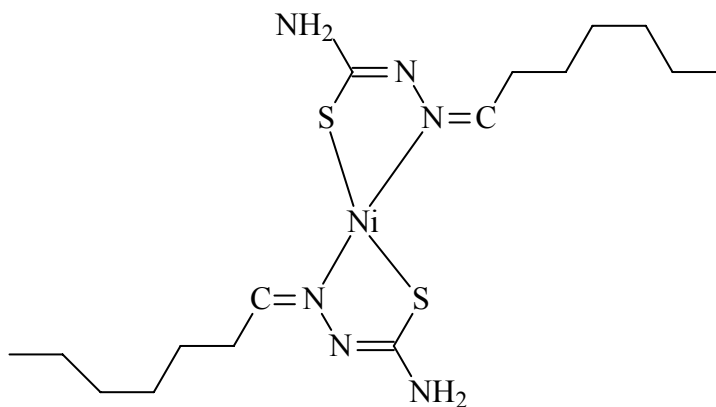
(XI)

The Pd(II) complexes have been derived from indole-3-carboxaldehyde thiosemicarbazone and were used in study of antiamoebic activity (Kakul et al., 2007). The monodentate four coordinated structure **(XII)** was screened for *in vitro* antiamoebic activity and compared with the standard amoebicidal drug, metronidazole. All metal complexes were found more active than their respective ligands indicating that complexation enhances the activity of the ligand.
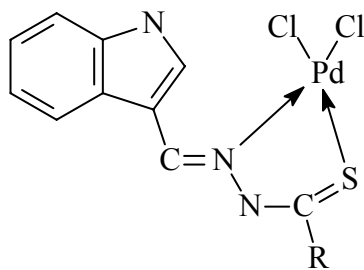
where R=NHC$_5$H$_9$, NC$_4$H$_{12}$

(XII)

Recently, a series of 5-methyl/trifluoromethoxy-1*H*-indole-2,3-dione 3-thiosemicarbazones **(XIII)**, 1-methyl-5-methyl/trifluoromethoxy-1*H*-indole-2,3-dione 3-thiosemicarbazones and 5-trifluoromethoxy-1-morpholinomethyl-1*H*-indole-2,3-dione 3-thiosemicarbazones has been synthesized (Güzel et al., 2008). The prepared compounds were evaluated for *in vitro* antituberculosis activity against *Mycobacterium tuberculosis* H37Rv. Based on their research, they found that some of the substitute in 5-methyl/trifluoromethoxy-1*H*-indole-2,3-dione 3-thiosemicarbazones and 5-trifluoromethoxy-1-morpholinomethyl-1*H*-indole-2,3-dione 3-thiosemicarbazones have showed to be most potent inhibitor of M. tuberculosis growth described in that study.
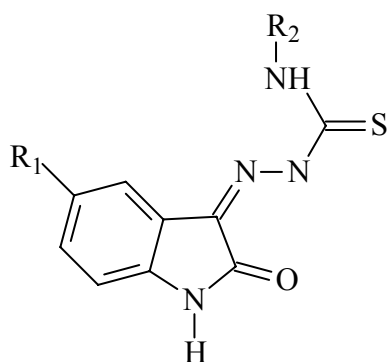
where $R_1 = CH_3$, OCF_3
R_2 = alkyl, cycloalkyl

(XIII)

Until now, there are no significant studies on biological activity especially on antiulcerogenic properties of Schiff bases of indole-3-carboxaldehyde and thiosemicarbazone unless which have been done by Kakul research group in 2007 that test on antibacterial activities.

2.4 Carbohydrazide

The discovery of carbohydrazide is close with thiocarbohydrazide and thiosemicarbazide. In 1988, the salicylaldehyde carbohydrazone ligand was used as a reagent for the determination of trace amounts of zinc in biological samples and alloys (Ureña et al., 1998).

The biological and technical importance of this chemical is generally based on their ability to form stable metal chelates (Syamal and Maurya, 1987; Singh K. et al., 1996). Ramesh in 1993, has reported the synthesis of Mn(II) and Cr(II) complexes with diacetylpyridine bis(carbohydrazone). The spectroscopic study showed that the complexes have a five coordinated structure and ligand coordinated through the pyridine nitrogen, two azomethine nitrogen and two *ketonic* oxygen atoms of the doubly deprotonated form of the ligand **(XIV)**. The study has shown that the Mn(II) and Cr(II) complexes were isostructural and have the same characteristics (Ramesh and Depali, 1993).
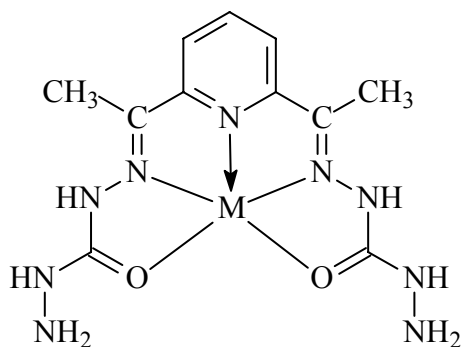
M= Mn(II), Cr(II)

(XIV)

The bimetallic Cu(II) complex derived from tetradentate ligand which was obtained by the condensation of 1,4-diformyl piperazine with carbohydrazide. The multidentate Schiff base ligand that formed binuclear Cu(II) complex **(XV)** was examined very intensively with studies of magnetic interactions.

$$H \quad\quad H$$

C—N   N—C

N—N   N—N

C   OH₂   ₂HO   C

NH₂—NH   O   Cu   Cu   O   N—NH₂

ONO₂   ONO₂
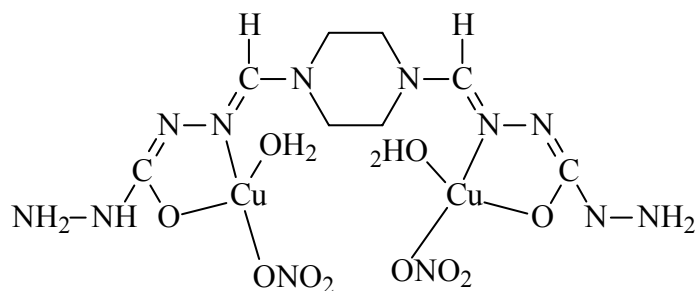
(XV)

The Co(II), Ni(II), and Cu(II) complexes were synthesized from benzaldehyde-carbohydrazone with several substituents (Gaber et al., 2004). Based on the TGA and IR studies, they found that the ligand behaves as bidentate and the metal complexes exhibit as four coordinated **(XVI)** and six coordinated **(XVII)** complexes. This research group found that carbohydrazone Schiff base ligand can form 6 coordinated complexes. They also found that the possible formation of two types of complexes with stoichiometric ratios 1:1 or 1:2 (metal:ligand).
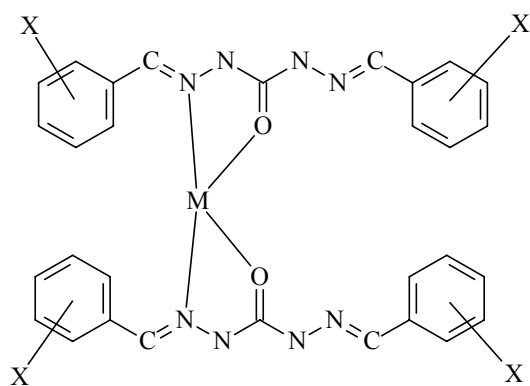
X= OH, Cl, Br   X= NO$_2$
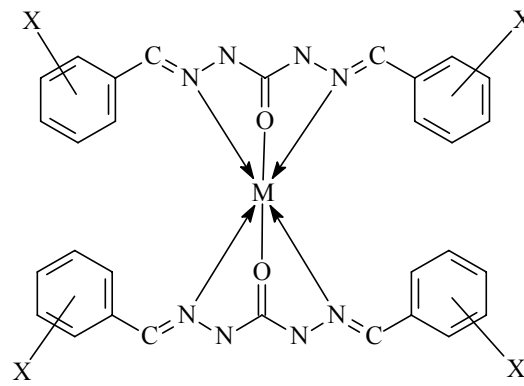
(XVI)   **(XVII)**

The study against anti-microbial has be done (Pelttari et al., 2007). It has been known before that salicaldehyde has highly potent anti-microbial activity against bacteria and fungi. In this research, they have reported that the Schiff base which was derived from salicaldehyde and carbohydrazide has shown higher activity than salicaldehyde against *Aspergillus niger*, *Bacillus cereus*, *Candida albicans*, *E.coli*, *Staphylococcus epidermidis* using the agar diffusion method.

The same group also condensed 2,3,4-trihydroxybenzaldehyde with carbohydrazide to obtain a Schiff base ligand. This compound was tested on *Staphylococcus epidermidis* and had distinctly higher activity than the parent aldehyde in the same molar concentration. The study had in general a narrower antimicrobial spectrum than the free aldehydes and are thus of interest as potential lead compounds for the development of narrow spectrum anti microbial drugs.

19

2.5 Peptic Ulcer

Peptic ulcers are erosions or open sores in the mucous lining of the stomach or duodenum. Peptic ulcer is the most common gastrointestinal disorder in clinical practice. In 1992, two Australian scientists was discovered that *Helicobacter pylori* as a causative factor for ulcer. They described that the stomach ulcers were caused by colonization with this bacterium. Besides, global expansion of consumption of alcohol and non-steroidal anti-inflammatory drugs (NSAID) and inappropriate diets have contributed to growing ulcer etiopathology (Peskar and Maricic, 1998). In this way, peptic ulcer is considered a disease of modern times, related to the addictions that are increasingly frequent in the society and to its stressful lifestyle.

Peptic ulcer being the most prevalent gastrointestinal disorder continues to occupy the key position in concern of both clinical practitioner and researchers. As a result, more and more drugs, both herbal and synthetic are coming up offering newer and better options for treatment of peptic ulcer. Considering the several side effects (arrythmias, impotence, gynaecomastia and haematopoeitic changes) of modern medicine, indigenous drugs possessing fewer side effects should be looked for as a better alternative for the treatment of peptic ulcer (Akhtar et al., 1992).

The modern approach to control gastric ulceration is to inhibit gastric acid secretion, to promote gastroprotection, to block apoptosis and to stimulate epithelial cell proliferation for effective healing (Bandhopadhyay et al., 2002). Most of the antisecretory drugs such as proton pump inhibitors (omeprazole, lanzoprazole, etc) and histamine H_2-receptor blocker (ranitidine, famotidine, etc) are extensively used to

control increased acid secretion and acid related disorders, but there are reports of adverse effects and relapse in the long run (Martelli et al., 1998; Wolfe and Sachs, 2000).

Treatment with natural products presents promise of a cure. This was demonstrated by the enormous variety of chemical substances isolated from plants that possess antiulcerogenic activity, indicating their great potential in the discovery of new therapies for ulcers (Borrelli and Izzo, 2000).

Although in most of the cases the aetiology of ulcer is unknown, it is generally accepted this results from an imbalance between aggressive factors and the maintenance of the mucosal integrity through the endogenous defence mechanism (Piper and Stiel, 1986). To regain the balance, different therapeutic agents including herbal preparations are used to inhibit the gastric acid secretion or to boost the mucosal defense mechanism by increasing mucus production.

Traditional medicine has used plants and herbs since ancient times to treat different gastrointestinal illnesses, including peptic ulcers. Recently, many efforts have been done in order to identify new anti-ulcer drugs from natural resources. Plants have originated some anti-ulcer drugs such as carbenoxolone from *Glycyrrhiza glabra*, solon from sophoradin and gefarnate from cabbage (Lewis and Hanson, 1991). Many other plants including *Quassia amara* L. (Toma et al., 2002), *Turnera ulmifolia* L. (Garcioso et al., 2002), *Syngonanthus arthrotrichus* (Batista et al., 2004) have been also reported as displaying anti-ulcerogenic activity.

However, research on antiulcerogenic activity of plant extract is limited as they are available only in a little amount. To date, research on the antiulcerogenic activity of Schiff bases and their metal complexes is yet to be fully investigated. Recently, the study on antiulcerogenic properties have been done using a bismuth complex (Sèrgio et al., 2007). Thus, our present study was carried out to examine the protective effect of synthesized ligands and their metal complexes against ethanol-induced gastric lesions in rats should be worthwhile to supplement available information with a view to contributing to the effort to discover new antiulcerogenic drugs.

Ethanol-induced gastric lesions are thought to arise as a result of direct damage of gastric mucosal cells, resulting in the development of free radicals and hyperoxidation of lipid (Terano et al., 1989). Absolute ethanol is the main factor that leads to intense damage of the gastric mucosa and it induces multiple hemorrhagic red bands (patches) of different sizes along the long axis of the glandular stomach (Mincis et al., 1995). The pathogenesis of ethanol-induced gastric mucosal damage is still unknown, but the solubility of mucus constituents, a concomitant fall in the transmucosal potential difference, increases the flow of Na^+ and K^+ into the lumen, pepsin secretion, and the histamine content in the lumen, but depresses tissue levels of DNA, RNA and proteins leading to flow stasis in damaged areas and formation of oxygen-derived free radicals, which are considered the main reasons for mucosa injury (Guth et al., 1984; Szabo, 1987).

Cimetidine was used as the standard drug in the present study of antiulcerogenic activity. Cimetidine used to prevent ulcers as a histamine H_2-receptor antagonist. Cimetidine **(XVIII)** contains an imidazole ring, and is chemically related to histamine. It

prevents the release of acid into the stomach and allows healing to occur in the area of the ulcer. It has been proven before that compounds with sulphur atom usually show significant properties in anti-bacteria and anti-cancer studies (Patil et al., 1989). The majority of drugs available in the market nowadays produce adverse reactions such as hypersensitivity, arrhythmia, impotence, gynecomastia and hematopoietic changes (Chan and Leung, 2002). Thus, the search for new therapeutic antiulcer agents are needed.
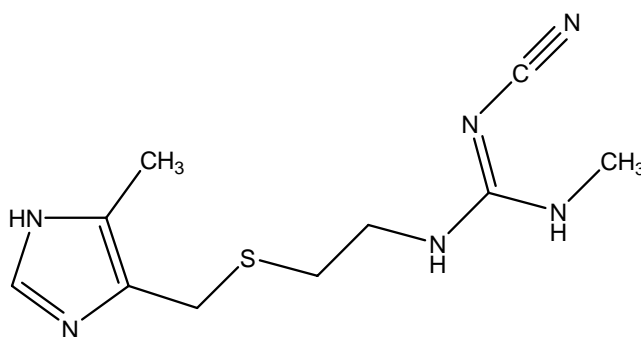
(XVIII)

Experimental

3.1 Reagents

All reagents were used as received. Ethanol was distilled before use.

3.2 Instruments

3.2.1 Carbon, Hydrogen and Nitrogen (CHN) Analysis

The microanalysis for C, H and N were done at the Chemistry Department, Universiti Teknologi Mara, Shah Alam and Universiti Pendidikan Sultan Idris, Perak.

3.2.2 Melting Point Determination

MEL-TEMP II melting point apparatus was used to determine the melting point of the compounds.

3.2.3 Fourier Transform-Infrared (FT-IR) Spectroscopy

The IR spectra were recorded in KBr pellets on a Perkin-Elmer RX1 FT IR spectrometer. All the spectra were run in the range of 400-4000 cm^{-1} at room temperature.

3.2.4 Nuclear Magnetic Resonance (^1H and ^{13}C NMR) Spectroscopy

The ^1H and ^{13}C NMR spectra were recorded in DMSO-d_6 on a Lambda JEOL 400 MHz FT-NMR/ ECA JEOL 400 MHz FT-NMR spectrometer.

3.2.5 Ultraviolet-Visible (UV-Vis) Spectroscopy

The electronic spectra were measured by means of Shimadzu 1601 spectrophotometer in the region of 300-800 nm using DMSO as solvent. The measurements using 1cm quartz cuvettes with these following parameters: measuring mode, absorbance; scan speed, fast and the concentration of the samples is 1×10^{-6} M.

3.2.6 Gouy Balance

The measurement of magnetic susceptibility has been done by Gouy balance. It was done on Magnetic Susceptibility Auto (MBS-Auto), Sherwood Sciencetific. Data were collected on a powdered sample of the compound at 25^oC. Diamagnetic and temperature independent paramagnetism corrections of the molar susceptibility were applied using Pascal's constant (Earnshaw, 1968; Carlin, 1986).

3.2.7 X-ray crystallographic data and structural determination

Single crystal X-ray diffraction data collection of selected complexes were performed on a Bruker Apex II CCD diffractometer at 100 K employing graphite-monochromated Mo Kα radiation (λ = 0.71073Å). The intensities were collected using the ω -2θ scan mode, in the range 2.4^{o} < θ <27.0^{o}. All structure were solved by direct method by using SHELXS-97 (Sheldrick, 2008) and refined by full matrix least-square methods on F^2 with the use of the SHELXL-97 (Sheldrick, 2008) program package (semi-empirical absorption corrections were applied using SADABS program).

3.3 Synthesis of the ligands

3.3.1 Synthesis of bis(1H-Indole-3-carbaldehyde)thiocarbohydrazone
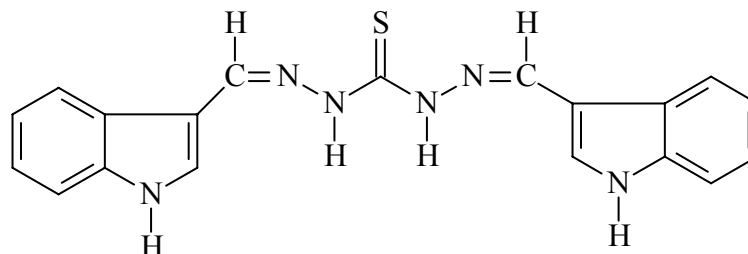
The compound was synthesized by refluxing together indole-3-carboxaldehyde (0.5g, 3.45mmol) and thiocarbohydrazide (0.18g,1.72mmol) in about 50 mL acidified ethanol for 2 hours. The yellow precipitate was collected and separated out by filtration, washed with ethanol and dried (Yield: 80-85%).

3.3.2 Synthesis of 1H-Indole-3-carbaldehyde thiosemicarbazone
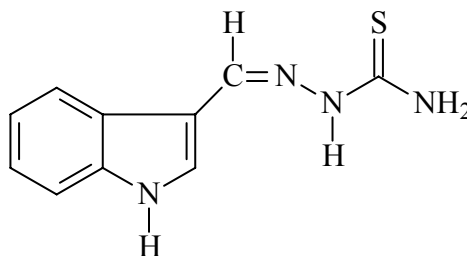
The compound was synthesized by refluxing the solution which contained indole-3-carboxaldehyde (0.50g, 3.45mmol) and thiosemicarbazide (0.31g, 3.45mmol) in 50 mL acidified ethanol for 2 hours. By evaporating at room temperature, the white precipitate was formed, filtered, washed with ethanol and dried (Yield: 75-80%).

3.3.3 Synthesis of bis(1H-Indole-3-carbaldehyde)carbohydrazone
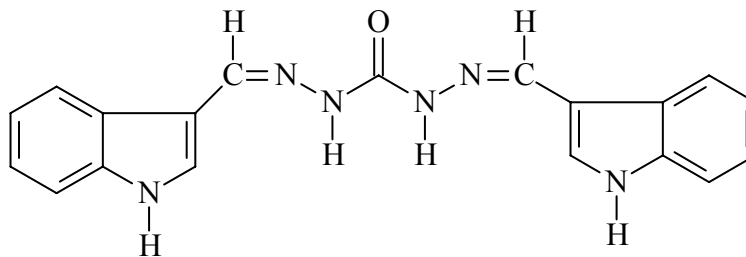
The compound was prepared by refluxing the solution of indole-3-carboxaldehyde (0.50g, 3.45mmol) and carbohydrazide (0.16g, 1.72mmol) in 50 mL acidified ethanol for 2 hours. The precipitate was collected, washed with ethanol and dried (Yield: 80-85%).

3.4 Synthesis of Metal Complexes

3.4.1 General Synthesis of M$_{Ind3Thio}$ (M= Ni, Cu, Zn, Cd)
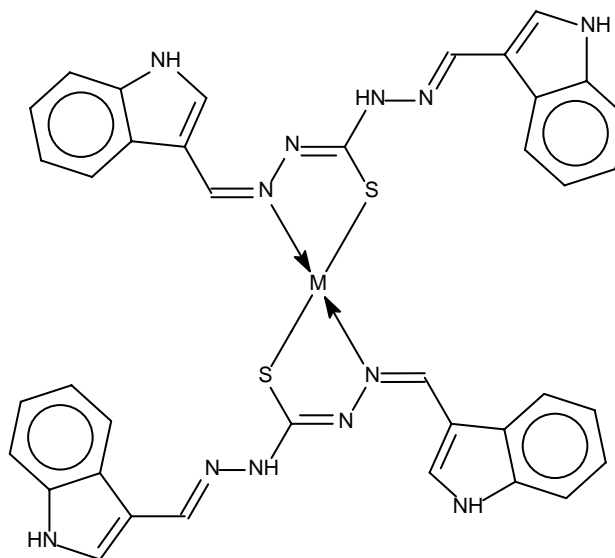
An ethanolic solution of M(II) acetate (M=Ni, Cu, Zn and Cd) was added to a solution of bis(1*H*-Indole-3-carbaldehyde)thiocarbohydrazone (1.00g, 2.65mmol) in 1:2 ratio. A few drops of triethylamine were added and the mixture then allowed to reflux for 5 hours. The precipitate were collected, filtered, washed with cool ethanol and dried. (Yield: 30-40%)

3.4.2 General Synthesis of M$_{Ind3Thiosemi}$ (M=Ni, Cu, Zn, Cd)
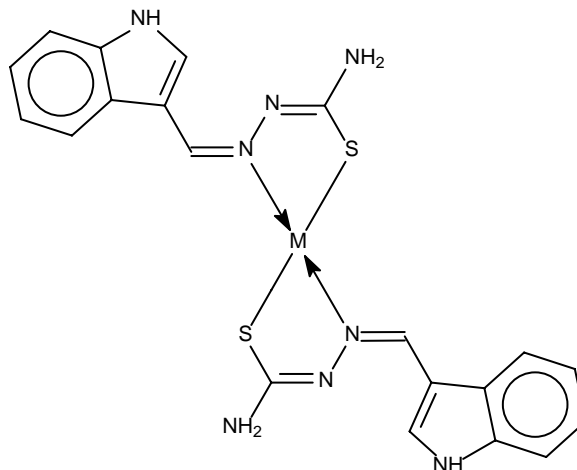
An ethanolic solution of M(II) acetate (M=Ni, Cu, Zn and Cd) was added to solution of 1*H*-Indole-3-carbaldehyde thiosemicarbazone (1.00g, 4.58mmol) ligand in 1:2 ratio. A triethylamine was added dropwise in about 3ml to the solution and the mixture then was refluxed for 5 hours. Removal of the solvent at about 70°C on a rotary evaporator gave a coloured solid. The precipitates were collected, filtered, washed with cool ethanol and dried. (Yield: 25-40%)

3.4.3 General Synthesis of M_{Ind3Carbo} (M=Ni, Cu. Zn, Cd)
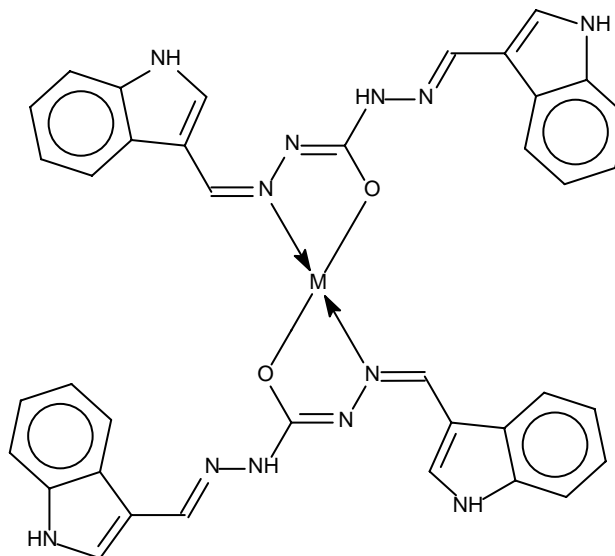
Bis(1*H*-Indole-3-carbaldehyde)carbohydrazone (1.00g, 2.26mmol) was dissolved in 30 ml ethanol and when a clear solution was obtained, M(II) acetate (M=Ni, Cu, Zn, Cd) then was added to the solution in 1:2 ratio (metal:ligand). A few drops of triethylamine were added to the solution and the mixture then was allowed to reflux for 5 hours. The precipitates that formed were collected, washed with cool ethanol and dried in *vacuo* for several hours. (Yield: 35-50%).

3.5 Toxicology Study

3.5.1 Acute toxicity testing

According to the Organization for Economic Cooperation and Development (OECD) panel of experts, as stated in the OECD Guideline for acute study, acute toxicity is defined as the adverse effects occurring within a short time of oral administration of a single dose of the substance or multiple doses given within 24 hours.

Sprague-Dawley rats were fasted for 1 day with access to water and were separated due to their sex; male and female (Ranjit and Sangita, 2004). The purpose of starving the animals is to eliminate food inside the gastrointestinal tract that may complicate absorption of the test substance. 4 groups of rats are needed for high and low dose test. All of the rats were fed orally for high dose (5 g/kg) and low dose (2 g/kg). The test substance, diluted with Tween 20, was administered by gavage to rats of both sexes using a ball-tipped intubation needle fitted onto a syringe. A control group was used and treated only with the vehicle by the same route and volume. Foods were withheld for a further 3 or 4 hours after dosing. Observations of pharmacotoxic signs were made at 10, 20, 30, 60, and 120 minutes and at 3 and 5 hours after dosing. The observations were done on mortality and behavioral changes of the rats following treatment.

3.6 Antiulcerogenic properties

3.6.1 Animals

Adult female and male *Sprague-Dawley* rats, obtained from Animal House, Faculty of Medicine, University of Malaya, were acclimatized under standard conditions of humidity, lighting and temperature and were feed with standard pellet diet and water in Animal Laboratory, University of Malaya. Rats weighing 180-225 g were fasted 48 hours before experiment but allowed free access to water. Water was then withheld 2 hours before the pretreatment.

3.6.2 Drugs

Cimetidine (50 mg kg^{-1}) which has been used as the standard anti-ulcer drug was obtained from the University Malaya Medical Center (UMMC).

3.6.3 Experimental protocol for the absolute ethanol-induced gastric ulcer model

Sprague-Dawley which mixed with male and female were randomly divided into 17 groups of 6 rats. The control group was gavaged with distilled water by orogastric intubations 30 minutes before oral administration of absolute ethanol (Noamesi et al., 1994). Treated groups were given absolute ethanol 30 minutes after administration of test solutions (5 ml kg^{-1}) prepared in 10% Tween 20 (Noamesi et al., 1994). The dose of the compound was 62.5 mg kg^{-1}. The animals were killed 30 minutes later by an overdosed of diethyl ether and their stomach rapidly removed. After fixing the stomach

in 10% buffered formalin, the stomach was excised and opened along the greater curvature and washed with water.

3.6.4 Gross gastric lesions evaluation

The gastric lesions were examined under the dissecting microscope grossly (1.8 x) with a square-grid eyepiece (10 X 10 mm^2) to access the formation of ulcer area (hemorrhagic lesions) (Das and Banerjee, 1993). The length and width (area) of each lesion was determined and the sum of the area of all lesions, in mm^2, for each stomach was expressed as the ulcerative lesion index area (mm^2) and the inhibition percentage was calculated by the following formula (El-Abhar et al., 2003):

$$\textbf{(\% I)} = \textbf{[(UI}_{\textbf{control}} - \textbf{UI}_{\textbf{treated}}\textbf{)} \div \textbf{UI}_{\textbf{control}}\textbf{]} \textbf{ x 100.}$$

Results and Discussion

4.1 Characterization of bis(1*H*-Indole-3-carbaldehyde)thiocarbohydrazone and Its Metal Complexes

4.1.1 Elemental Analysis

The elemental analysis data of C, H and N for the bis(1*H*-Indole-3-carbaldehyde)thiocarbohydrazone and its metal complexes are in a good agreement with the proposed formulations. The data results and some other physical properties are shown in Table 4.1.

Table 4.1:
The analytical data and some physical properties of bis(1*H*-Indole-3-carbaldehyde)thiocarbohydrazone and its metal complexes

Compounds	Colour	Melting Point/ ^{o}C	Found(Calculated)/%		
			C	H	N
Ind3Thio	Bright Yellow	230-236	63.12(63.51)	4.51(4.46)	23.41(23.39)
Ni$_{\text{Ind3Thio}}$	Orange	>300	59.21(59.09)	4.17(4.12)	21.66(21.63)
Cu$_{\text{Ind3Thio}}$	Brown	>300	58.54(58.73)	4.17(4.09)	22.27 (21.50)
Zn$_{\text{Ind3Thio}}$	White	>300	58.65(58.59)	4.13(4.08)	21.17(21.44)
Cd$_{\text{Ind3Thio}}$	Pale Green	>300	55.37(55.27)	3.74(3.90)	20.31(20.23)

4.1.2 IR Spectral Data

Some of the important bands for IR spectra of bis(1*H*-Indole-3-carbaldehyde)thiocarbohydrazone and metal complexes are showed in the Table 4.2.

The synthesized Schiff base ligand exhibits a frequency at 3330-3200 cm^{-1} which is attributed to the symmetric υ(N-H) stretching vibration (Mala et al., 1990). These bands appear in the spectra both of ligand and metal complexes indicating that these groups are not involved in the coordination with the metal. In addition, these band indicate that the ligand is the *thione* form tautomer (Nagaraja et al., 2007). However, the weak bands around 2341 cm^{-1} is attributed to the υ(-SH) vibration, thus the ligand exhibits as *thiol-thione* tautomerism (Scheme 1). The 2969 cm^{-1} band is due to the υ(N-H) in the indole ring (Tunde and Omolara, 1988). The small splitting of the bands in the metal complexes is due to the existence of weak interaction between the hydrogen of the N-H group of the indole and the sulphur atom of the another molecule, forming a hydrogen intermolecular bonding (Martin R., et al., 1987).

For the Schiff-base ligand, the intense band at 1608 cm^{-1} and the medium band at 1250-1180 cm^{-1} are assigned to the υ(C=N) and the υ(N-N) vibrations, respectively (Ugo R., 1967). There are two types of IR shifting of the Schiff-base ligand in this two regions differ upon coordination to each metal(II) ions. Firstly, the shift of the stretching frequency towards lower energy (30-80 cm^{-1}) of the υ(C=N) in the spectra of metal complexes. Secondly, the shifted to higher energy or positive shifts (30-50 cm^{-1}) of υ(N-N) were observed in the spectra of metal complexes.
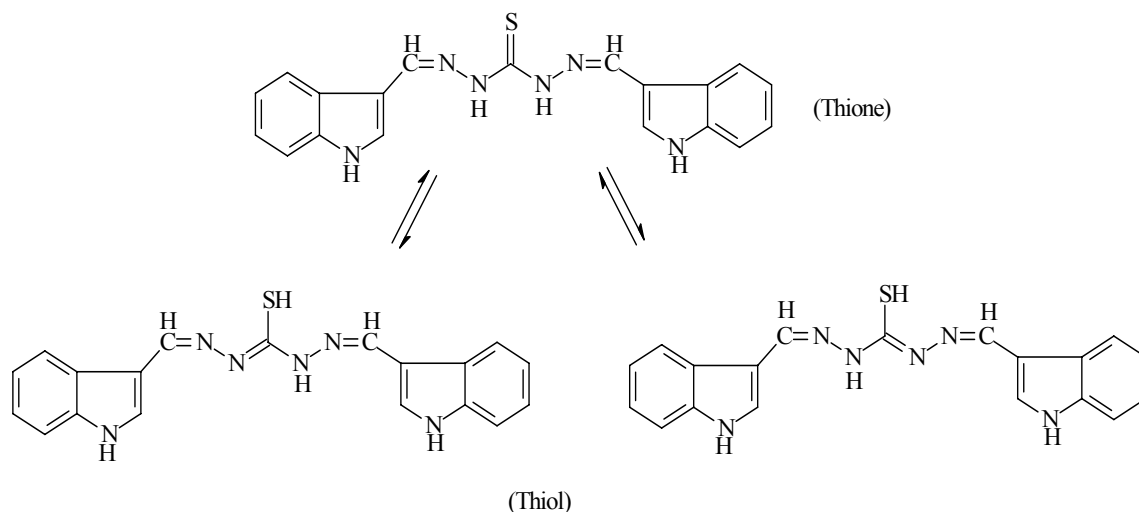
Scheme 4.1: The *thiol-thione* tautomerism

The shift to the lower energy of the $\upsilon(C=N)$ indicates that the imine nitrogen atom coordinated to the metal (II) ions (Golcu et al., 2005). The shift to the higher energy of the $\upsilon(N-N)$ vibration was due to the repulsion between the lone pairs of electron on the nitrogen atom as a result of the coordination through the azomethine nitrogen atom (Ali et al., 2003).

The important bands of the thiocarbohydrazone Schiff base ligand is the presence of the C=S group. These bands are always observed in the two regions and in some rare cases, three region in the spectra also can assigned to the $\upsilon(C=S)$ (Nabar, 1966). In this Schiff-base ligand, the $\upsilon(C=S)$ appears at 1046 cm^{-1} and 744 cm^{-1}. These results showed that the *thione* is a domain component in the mixture of *thiol-thione* tautomers (Nagaraja et al., 2007). In the metal(II) complexes spectra, the $\upsilon(C=S)$ bands were shifted to the lower energy indicating that the *thione* sulphur participates in the coordination site.

The assignment of the bands for υ(M-S) and υ(M-N) vibrations in the lower region in the metal complexes spectra seem to be complicated as ligand vibrations were interfere in this region. The regions around 600-480 cm^{-1} in the Schiff-base ligand was assigned to the in-plane and out-plane indole ring deformation (Tunde and Omalara, 1988). The simultaneous appearance of the bands around 500-450 cm^{-1} indicates the υ(M-S) vibration. The coordination of the azomethine nitrogen consistent with the presence of the new band at the range of 450-400 cm^{-1} which are assignable to the υ(M-N) vibration (Khlood et al., 2007).

In summary, the IR study of the solid state Schiff base has shown that this ligand exhibits as a *thiol-thione* tautomers form and upon complexation, the ligand is deprotonated. The IR study also showed that the Schiff base ligands were bound to the metal(II) ions *via* the sulphur and azomethine nitrogen atoms.

Table 4.2:
Important IR data for bis(1*H*-Indole-3-carbaldehyde)thiocarbohydrazone and metal complexes (cm^{-1})

Compound	υ(N-H)	υ(C=N)	υ(C=S)*	υ(C=S)**	υ(N-N)	υ(M-S)	υ(M-N)
Ind3Thio	3322	1608	1046	744	1250	-	-
Ni$_{Ind3Thio}$	3322	1592	1025	746	1111	446	421
Cu$_{Ind3Thio}$	3342	1496	1046	737	1091	483	423
Zn$_{Ind3Thio}$	3314	1595	1029	746	1096	444	425
Cd$_{Ind3Thio}$	3394	1603	1011	743	1100	480	424

Figure 4.1: IR spectrum of bis(1*H*-Indole-3-carbaldehyde)thiocarbohydrazone
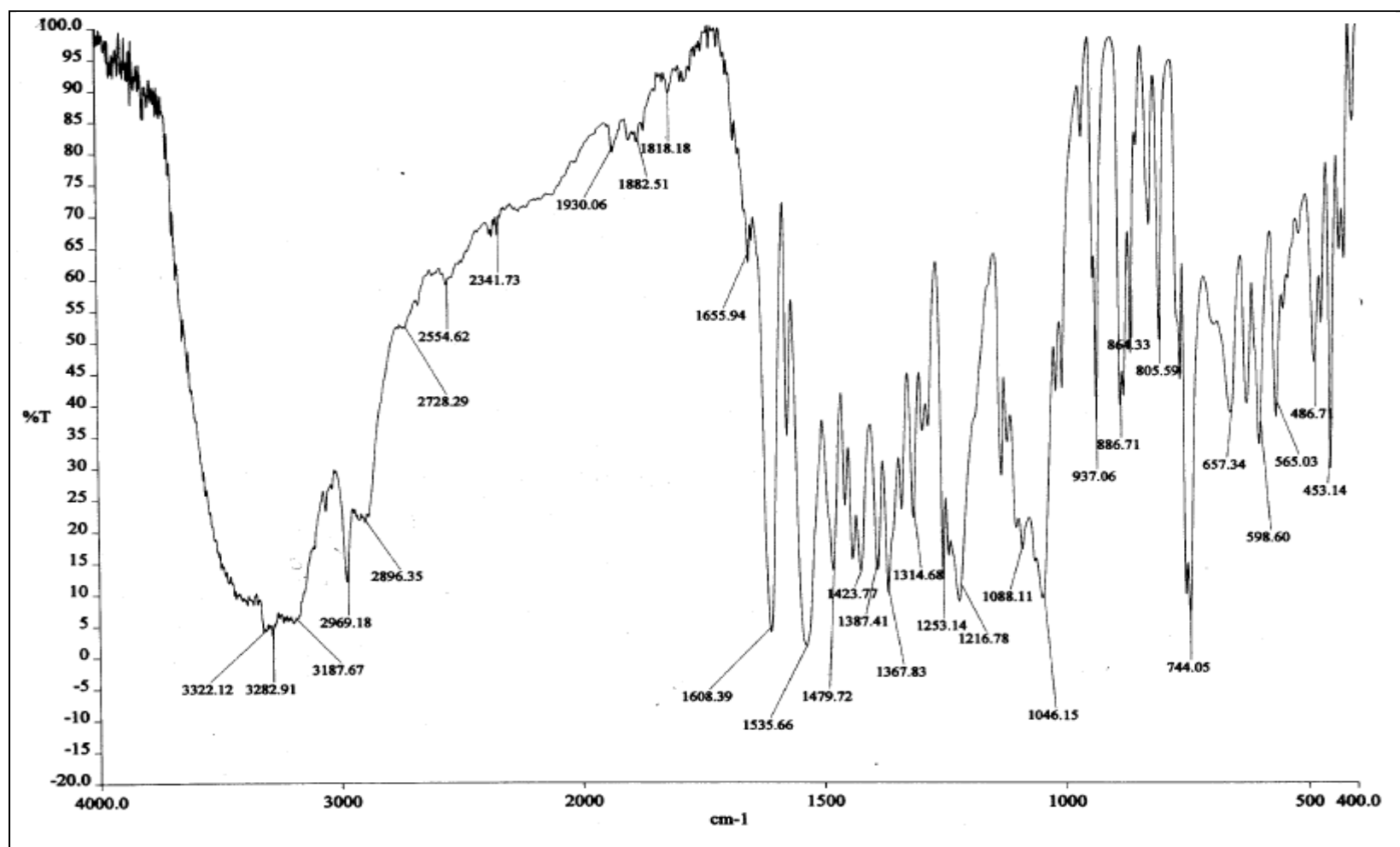
Figure 4.2: IR spectrum of Cu$_{Ind3Thio}$
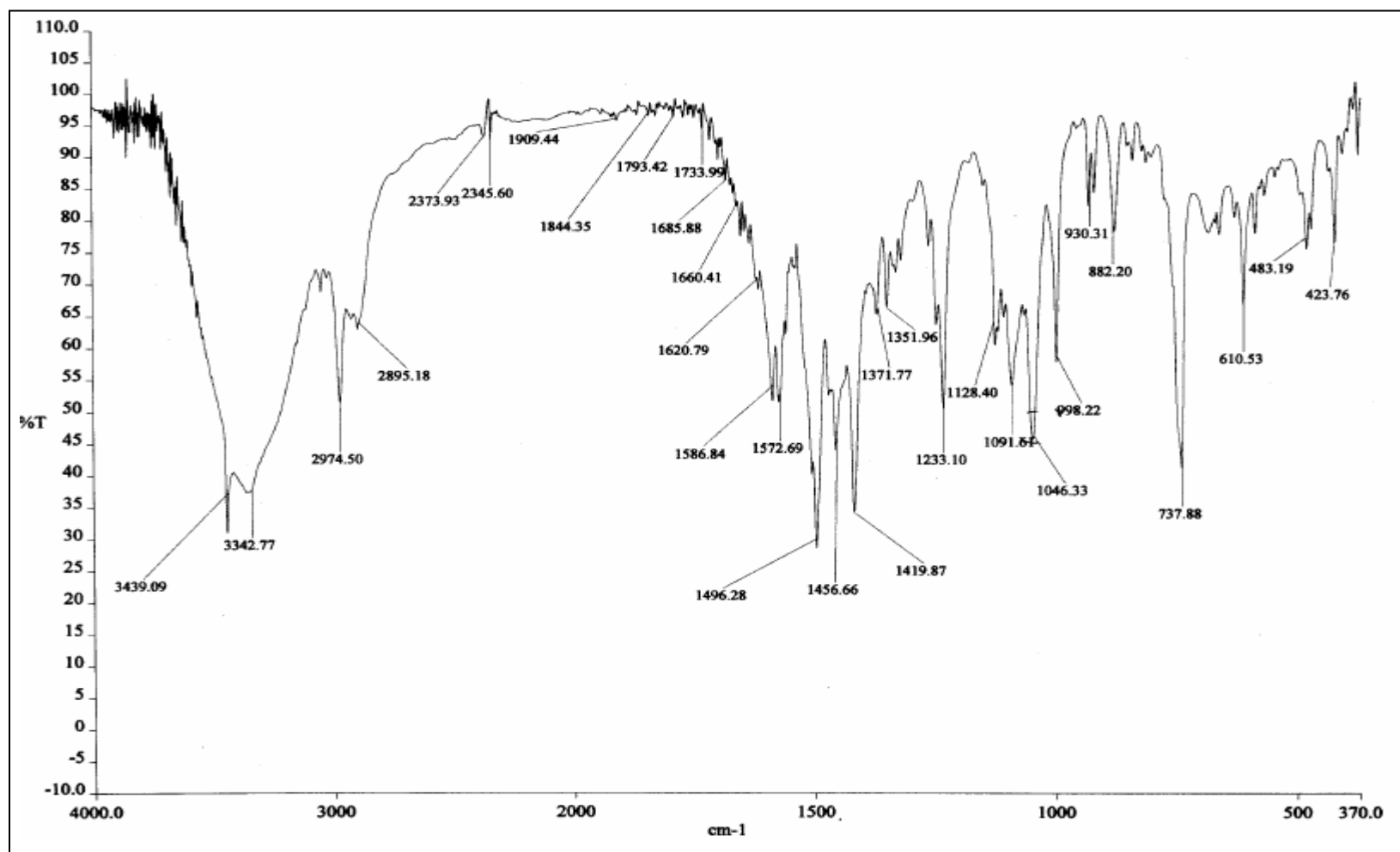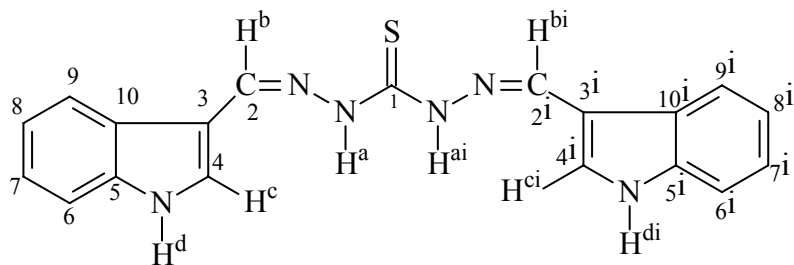
Scheme 4.2: The ligand with atoms numbering

The characteristic resonance peaks of the ^{1}H and ^{13}C-NMR are listed in the Table 4.3 and Table 4.4. The ligand with the atoms numbering is shown in Scheme 4.2.

In the ^{1}H NMR spectrum, peaks were observed around 7.51-7.19 ppm with integration assigned to proton from two phenyl groups. The peaks at 8.09 and 8.07 were attributed to similar protons, H^c and H^{ci} in the ligand. The down field shift (δ= 8.09) of the second peak may be due to the intramolecular hydrogen bonding between H^c or H^{ci} and nitrogen atom from azomethine group (Khlood et al., 2007).

The proton H^b which came from two similar azomethine groups of the ligand can be observed in the region of 8.28-8.25 ppm (Mala et al., 1995). The sharp peak at 9.92 ppm is attributed to the H^a of the ligand while the signal that appears at 11.12 ppm is due to proton H^d.

In the ^{13}C NMR spectrum, the peaks around 176 ppm and 140 ppm are attributed to the thioamide and azomethine atoms, labeled as C1 and C2 in the Scheme 4.2,

respectively (Mala et al., 1995). The carbons of the indole ring which are labelled as C3 and C4 gave signals at the range 131 ppm and 137 ppm, respectively. Besides, the aromatic ring clearly indicated by the peak at the range 125-111 ppm in the ligand spectra (Mala et al., 1995; Golcu et al., 2005).

Table 4.3:
Important ^{1}H NMR data for the bis(1*H*-Indole-3-carbaldehyde)thiocarbohydrazone (ppm)

Compound	N-H^d	N-H^a	H^b-C=N	C-H^c	H$_{aromatic}$
Ind3Thio	11.12	9.92	8.28-8.25	8.10-8.00	7.51-7.19

Table 4.4:
Important ^{13}C NMR data for the bis(1*H*-Indole-3-carbaldehyde)thiocarbohydrazone (ppm)

Compound	C1	C2	C3	C4	C$_{aromatic}$
Ind3Thio	176.54	140.95	131.01	137.08	125-111

Figure 4.3: ^{1}H NMR spectrum of bis(1H-indole-3-carboxaldehyde)thiocarbohydrazone
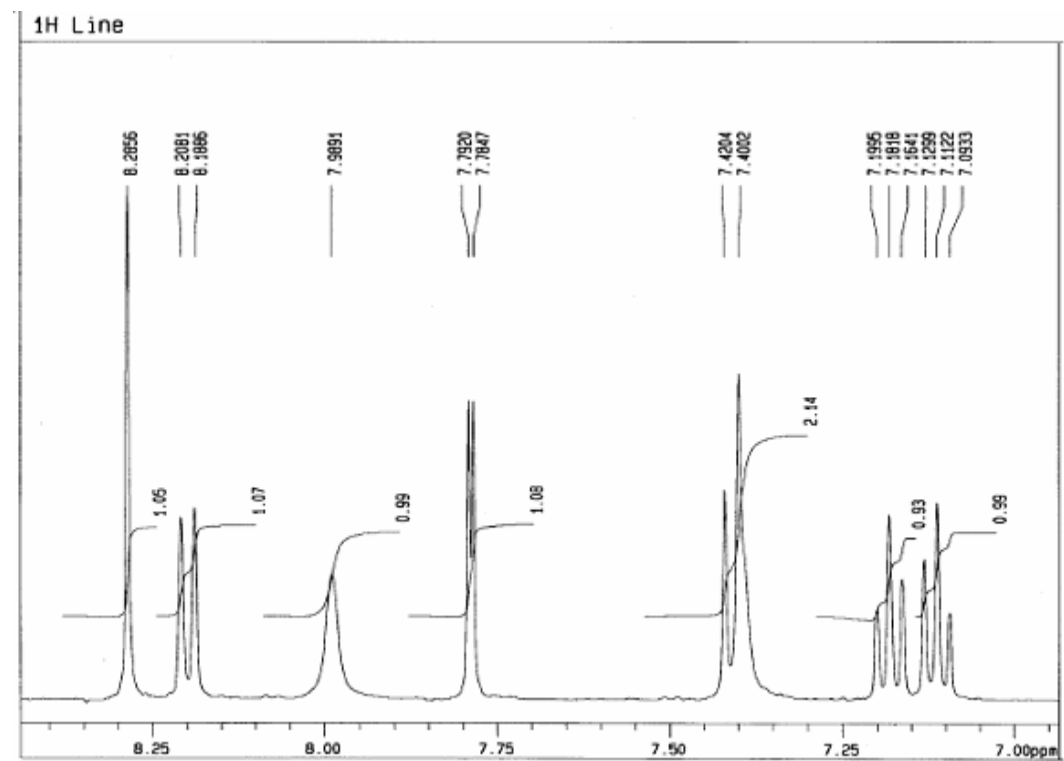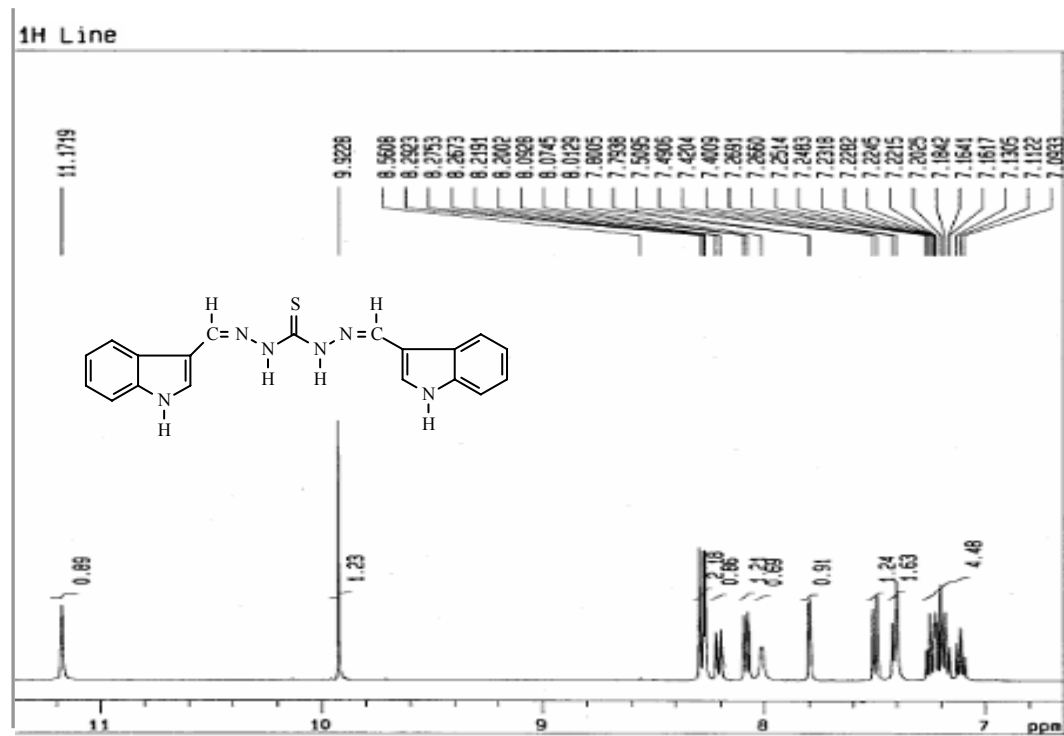
Figure 4.4: ^{13}C NMR spectrum of bis(1*H*-Indole-3-carbaldehyde)thiocarbohydrazone
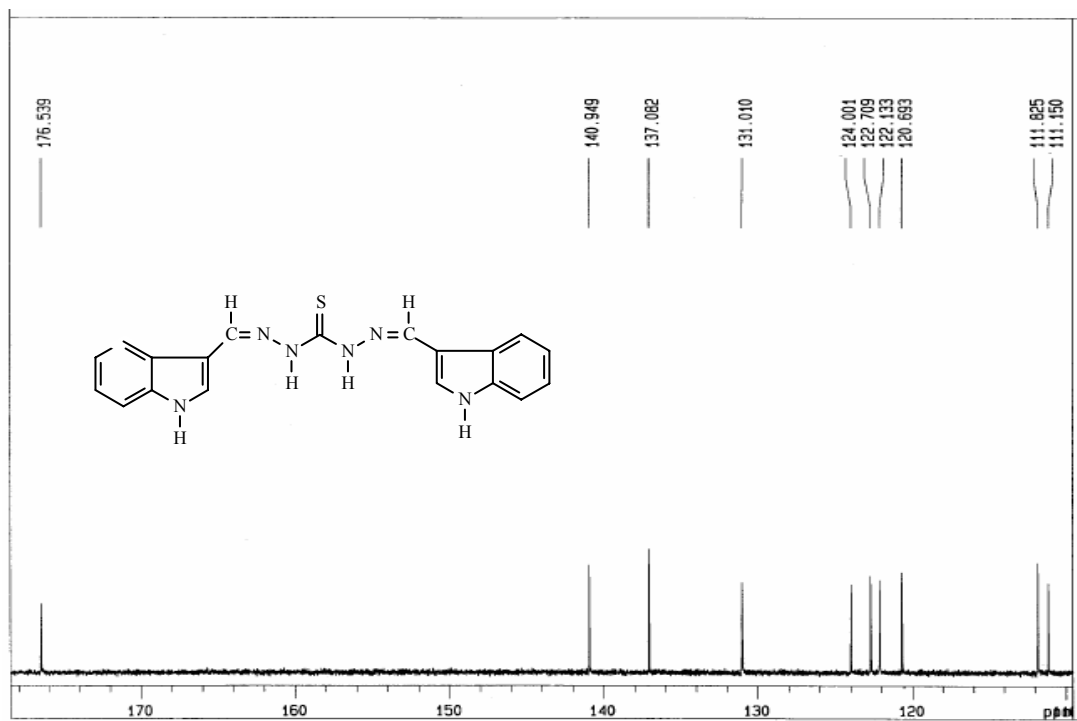
4.1.4 UV-Vis spectra

The electronic absorption of the bis(1*H*-Indole-3-carbaldehyde)thiocarbohydrazone and metal complexes were given in the Table 4.5.

In the Schiff-base electronic spectra, the absorption around 33000 cm^{-1} and less than that were attributed to the $\pi \rightarrow \pi^*$ transition of the benzenoid and the NH-chromophore (Mala et al., 1995). The intense absorption at the range of 33000-32500 cm^{-1} was due to the azomethine chromophore in the ligand. These transitions also appear in complexes spectra but in the higher energy because of hypsochromic shift; confirming coordination of the ligand to the metallic ions (Golcu et al., 2005; Lu, et al., 2000).

In the Ni(II) complex spectra, the low intensity bands exhibit in the range 16500 cm^{-1} and 19950 cm^{-1}. These bands correspond to $^3B_{1g} \rightarrow \,^3A_{1g}$ and $^3B_{1g} \rightarrow \,^3B_{2g}$ transitions, respectively (Chandra et al., 2008). Besides, the *d-d* transitions also clearly indicated at the absorption in the range 25125–24500 cm^{-1} which is attributed to the $^3B_{1g} \rightarrow \,^3E_g$ transition. The high intensity bands clearly appear at the range of 30000-35000 cm^{-1} assignable to the charge transfer transition of the metal-ligand type, between the *d*-orbital of the Ni(II) and the π^* orbital of the N or S atoms from the ligand (Obadović et al., 1997). Thus, these electronic transitions are consistent with square planar geometry for the Ni(II) complex (Lever, 1968).

Besides, in the Cu(II) complex electronic spectra, the intense absorption exhibited at the region 24630 cm^{-1} which is due to the $^3B_{1g} \rightarrow {}^3E_g$ transition. The shifting of the band to lower energy in this metal complex spectrum indicates that the coordination modes of the metal with the ligand (Revankar et al., 2007; Golcu et al., 2005). The *d-d* transition in this metal complex spectrum showed low shoulder around 18100 cm^{-1} which due to the $^3B_{1g} \rightarrow {}^3A_{1g}$ transition. Based on these electron transitions and the absences of the absorption at the region of 12000 cm^{-1} and less, thus indicate that the complexes may exist as a square planar geometry (Zayed et al., 2004; Siddiqi et al., 2007).

In the spectra of Zn(II) and Cd(II) metal complexes, the trends of the bands only appear at the range of 33000-30000 cm^{-1} which indicate the presence of charge-transfer transition between metal and the ligand. These transitions involved the $^3E_g \rightarrow {}^3A_{2u}$ and $^3A_{1g} \rightarrow {}^3A_{2u}$, respectively (Amirnasr et al., 2002). The *d-d* transition in the Zn(II) and Cd(II) complexes were not observed as a result from the full *d* orbital for their d^{10} system.

For conclusions from the electronic spectra, the charge transfer and *d-d* transition in the spectra suggest that the complexes are four-coordinate, most likely forming a square planar geometry for the Ni(II) and Cu(II) and tetrahedral geometry for Zn(II) and Cd(II) complexes (Golcu et al., 2005; Zayed et al., 2004).

Table 4.5:
Electronic spectral data of the bis(1*H*-Indole-3-carbaldehyde)thiocarbohydrazone and its metal complexes (cm^{-1})

Compound	Intraligand and charge transfer (cm^{-1})	*d-d* transition (cm^{-1})
Ind3Thio	33000; 32000	
Ni$_{Ind3Thio}$	32000; 30000	19500; 16500
Cu$_{Ind3Thio}$	30000; 28000	24630; 18100
Zn$_{Ind3Thio}$	33000; 30000	
Cd$_{Ind3Thio}$	33000; 29000	

Figure 4.5: Uv-vis spectrum of bis(1*H*-Indole-3-carbaldehyde)thiocarbohydrazone
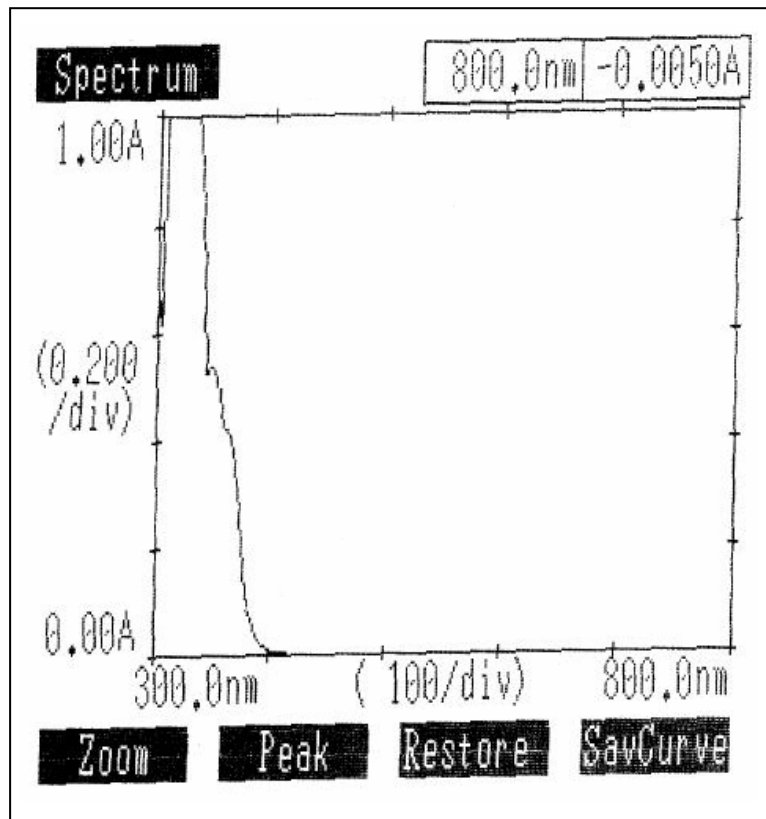
Figure 4.6: Uv-vis spectrum for Cu$_{Ind3Thio}$
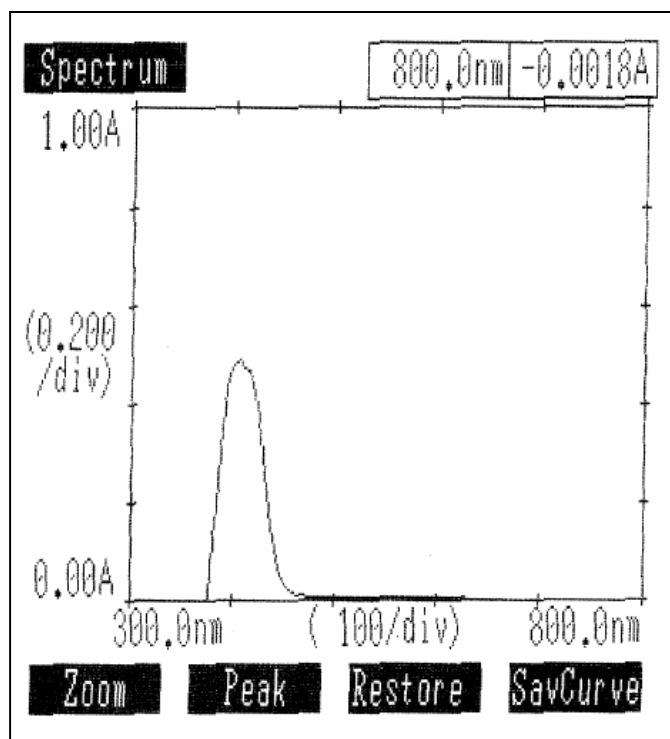
4.1.5 Magnetic Study

The results of the magnetic properties were listed in Table 4.6. The rationality in doing the magnetic study is to know the electron configuration in the metal complexes. Thus, from the electron configuration, the geometry and structure of the complexes can be suggested.

Table 4.6: The magnetic properties of metal complexes. R1 representing bis(1*H*-Indole-3-carbaldehyde)thiocarbohydrazone

Compounds	Mass susceptibility, χ_g $(cm^3\ g^{-1})$	Molar susceptibility, χ_m^{corr} $(cm^3\ mol^{-1})$	Effective magnetic moment, μ_{eff} (B.M.)	Unpaired electron, n	Magnetism
NiR1	0.174×10^{-6}	1.831×10^{-4}	0.779	$0.27 \approx 0$	Diamagnetic
CuR1	1.001×10^{-6}	9.478×10^{-4}	1.509	$0.81 \approx 1$	Paramagnetic
ZnR1	-	-	-	-	Diamagnetic
CdR1	-	-	-	-	Diamagnetic

The calculation of the effective magnetic moment and unpaired electron for the Ni(II) are shown below:

$$\chi_g = 0.174 \times 10^{-6}$$

$$\chi_m^{exp} = \chi_g \times MW$$
$$= 0.174 \times 10^{-6} \times 776.69$$
$$= 1.354 \times 10^{-4}$$

$$\chi_m^{corr} = \chi_m^{exp} - \chi^{dia}$$

$$= 1.354 \times 10^{-4} - (-1.173 \times 10^{-4})$$
$$= 2.53 \times 10^{-4}$$

μ_{eff} $= 2.84\sqrt{\chi_m^{corr} T}$ Bohr Magneton

$= 2.84 \sqrt{\chi_m^{corr} (298)}$ B.M

$= 2.84 \sqrt{2.53 \times 10^{-4} (298)}$ B.M

$= 0.779$

μ_{eff} $= \sqrt{n(n+2)}$ where n is number of unpaired electron

$0.779 = \sqrt{n(n+2)}$

$0.608 = n^2 + 2n$

$n^2 + 2n - 0.608 = 0$

$n = 0.268$ or $n = -2.268$

Negative value is not allowed for the number of electron, so **n = 0.268 ≈ 0**

For the Cu(II) complexes, the number of unpaired electron that was obtained from the experiment is one, indicating the presence of an unpaired electron in the d orbital. Cu(II) is a d^9 system and the electron arrangement in free ion as shown in Figure 4.7.
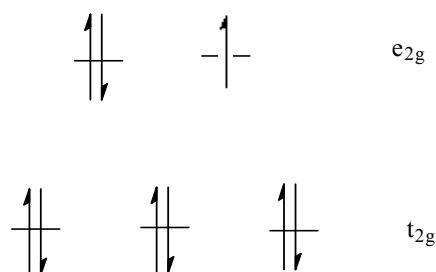
Figure 4.7: Electrons arrangement of Cu(II) as a free ion

The unpaired electron in e_{2g} will be promoted to the $4d$ sub shell to create one empty orbital in e_{2g} that is available for inner complex formation (Zayed et al., 2004). Thus, the d^9 complexes are subjected to the distortion which lowers the local symmetry to D_{4h}. The 8 electrons in the Cu(II) ions will occupied the d_{xz}, d_{yz}, d_{z2} and d_{xy}, thus

satisfied in formation of square planar complexes. As a result, the Cu(II) complex is paramagnetic and may form distorted square planar geometry with dsp^2 hybridization which occupies $3d_{x2-y2}$, $4s$, $4p_x$ and $4p_y$. This observation agrees well with previous reports on Cu(II) ions that showed Cu(II) complexes always adopted paramagnetism although the geometry are square planar, tetrahedral or octahedral (Carlin, 1986; Golcu et al., 2005).

The electron configuration in Ni(II) shows that an unpaired electron does not exist. This indicated that the ligand is a strong field ligand and the complex probably forms square planar geometry with dsp^2 hybridization (Brady and Humiston, 1986).

The Zn(II) and Cd(II) complexes are diamagnetic for being the d^{10} configuration and likely to form a tetrahedral geometry with the sp^3 hybridization of the complexes (Golcu et al., 2005).

4.1.6 Crystal structure and data collection

Recrystallization of Ni(II) complex in dimethyl sulfoxide yielded single crystals suitable for X-ray diffraction analysis. An orange crystal with the size $0.25 \times 0.20 \times 0.20$ mm gave excellent diffraction on the diffractometer. The crystal data with experimental details and structure refinement for the Ni(II) complex are listed in the Table 4.7. The ORTEP-like ellipsoid with bond sticks is depicted in Figure 4.8.
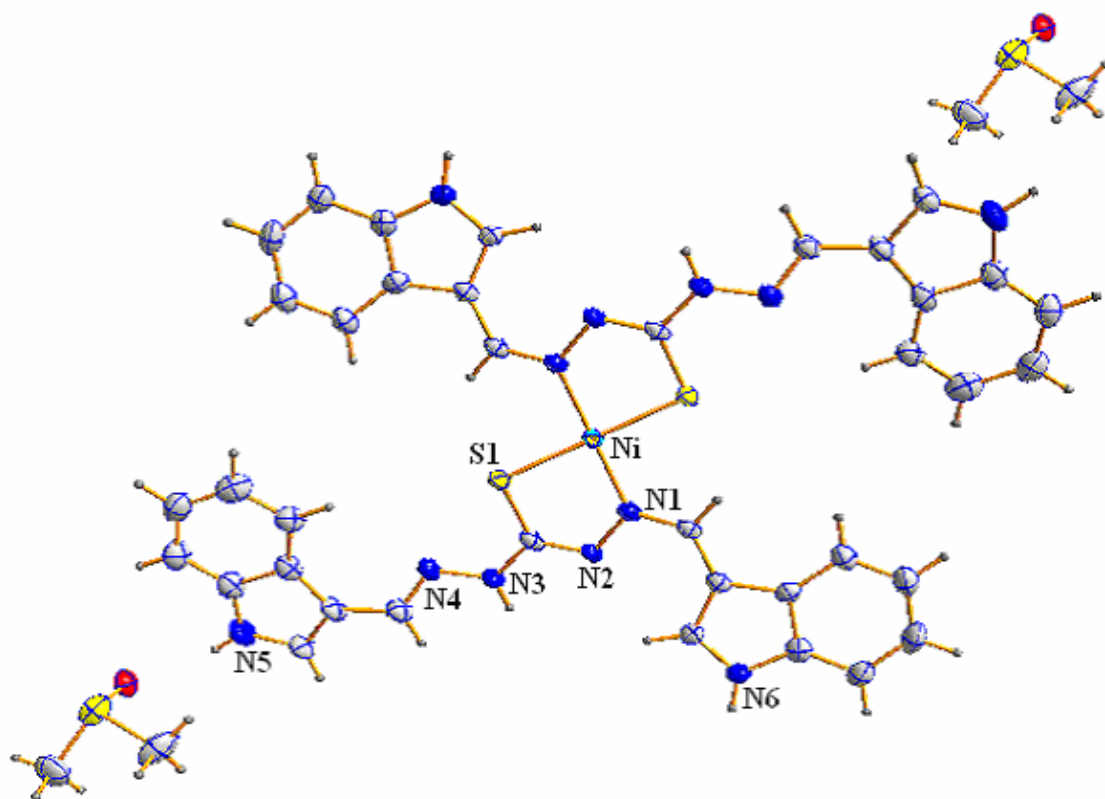
Figure 4.8: The molecular structure of $[Ni(C_{19}H_{15}N_6S)_2] \cdot 2C_2H_6OS$. The hydrogen atoms were refined isotropically.

Table 4.7: Crystallographic data [Ni(C$_{19}$H$_{15}$N$_6$S)$_2$]·2C$_2$H$_6$OS

Crystallographic data for metal complex	
Empirical formula	[Ni(C$_{19}$H$_{15}$N$_6$S)$_2$]·2C$_2$H$_6$OS
Formula weight	933.83
Temperature (K)	100 K
Crystal size (mm)	0.25 X0.020X 0.20
Color	Orange
Shape	Block
Wavelength (Å)	0.71073
Crystal System	Monoclinic
Space group	C2/c
a (Å)	19.0340 (5)
b (Å)	9.1982(3)
c (Å)	25.1374(7)
α (º)	90
β (º)	95.672(2)
γ (º)	90
V (Å^3)	4379.5(2)
Z	4
μ	0.686
F(000)	1944
Theta range for data collection (º)	1.63-27.5
Index ranges	$-24 \leq h \geq 24;\ -11 \leq k \geq 9;\ -32 \leq l \geq 32$
Reflection collected	5030
Independent reflection	3201
R (int)	0.0924
Data/Parameters	5030/277
Final R indices [I>2σ (I)]	0.0481
R indices (all data)	0.1088
Largest diff. peak and hole (e.A^{-3})	0.6000

The crystal structure of the complex showed that the Ni(II) ion is *N,S*- chelated by the deprotonated Schiff bases in a square planar geometry (Rizal et al., 2008). The two complexes are self-assembled *via* intermolecular hydrogen bonds which two indolyl-NH (donor) sites interact with dimethyl sulfoxide to furnish a layer motif. As shown in Figure 4.9, the O1 was connected to two independent complex molecules via hydrogen bonds which presented by the dashed line. The $O1^i$ and $O1^{ii}$ also form hydrogen bonds with other indoyl–NH sites from other complexes like O1. As a result, these hydrogen bonds will form infinite layer structure with dimethyl sulfoxide as bridging molecules.
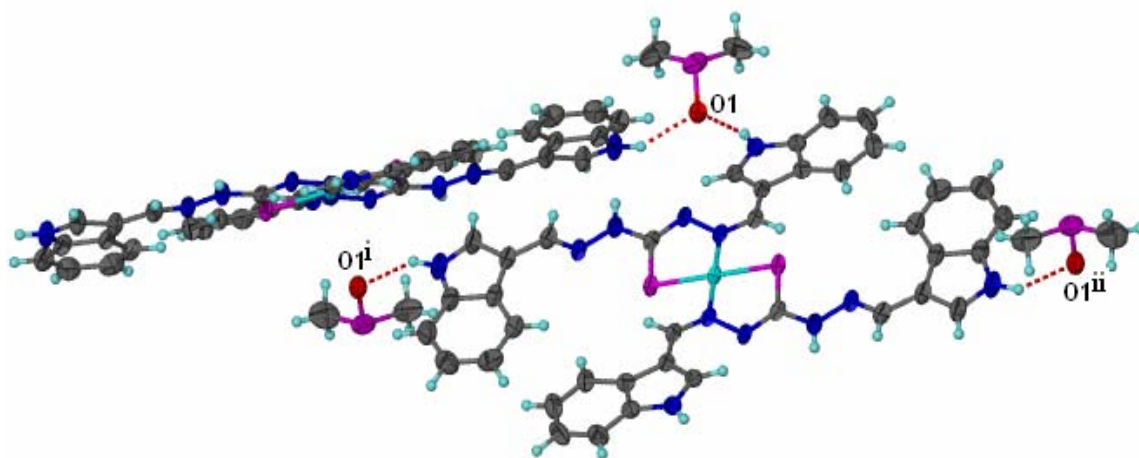
Figure 4.9: The diagram showed the formation of hydrogen bonds in the packing diagram. The connectivity by the hydrogen bonds between dimethyl sulfoxide and complex molecule furnish an infinite layer structure.

From the diagram which was presented before, the Ni(II) formed a square planar complex. The four atoms from two ligands which are two sulphur atoms and two nitrogen atoms were arranged at the corners of a hypothetical square around the central

metal atom. The structure determination shows that the ligand exists in the *thiol* form; supported by the absence of hydrazinic N-H and C-S distance of 1.726(3) Å. The arrangement atoms in square planar were presented in Figure 4.10. The Ni1-S1 is equidistant with Ni1-S2 which is 2.175Å and the distance between Ni1-N1 is same as Ni1-N2 which is 1.906 Å. The same angle between N1-Ni1-N2 and S1-Ni1-S2 indicated that the square planar formed a perfect flat plane. Besides, the *trans-* arrangement in the complex make a good agreement with the value of moment effective for the metal complexes which was proposed before (Obadović et al., 1996).
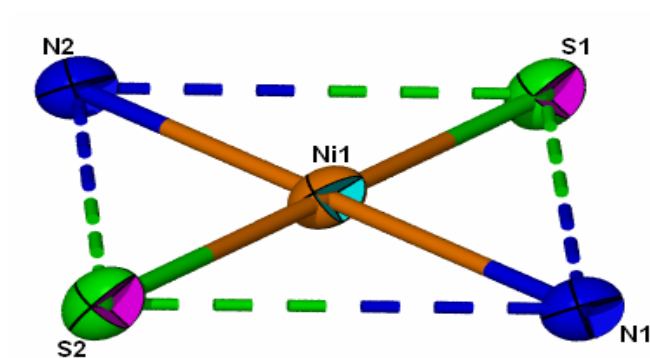
Figure 4.10: The geometry of [Ni(C$_{19}$H$_{15}$N$_6$S)$_2$].

Thus, the above data are consistent with the following suggested structural formula of the metal complexes:
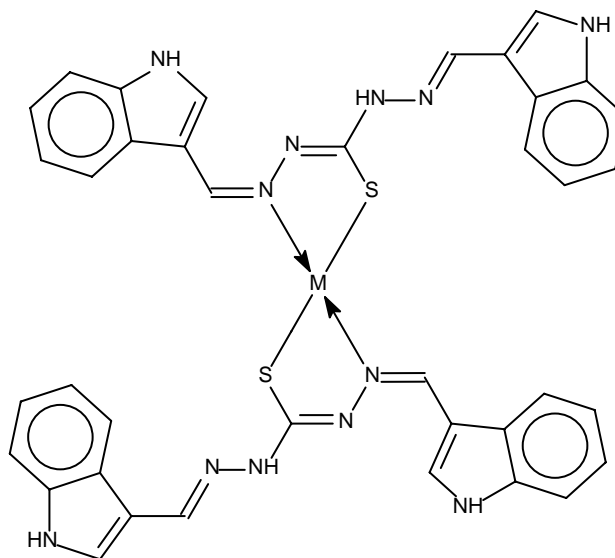
where M can be replaced with nickel, copper, zinc and cadmium. Although all metal complexes formed four coordinated complexes, the nickel and copper normally formed square planar geometries while zinc and cadmium adopted a tetrahedral arrangement (Figure 4.11).
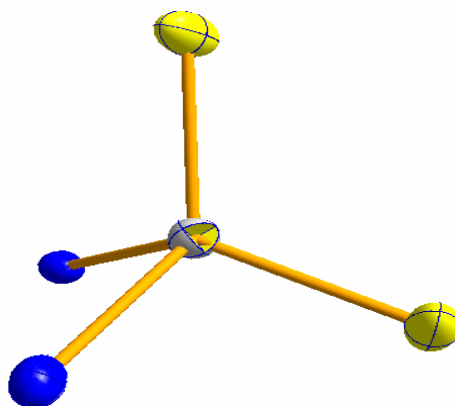
Figure 4.11: The approximate structure of Zinc and Cadmium in tetrahedral geometry. The center atom can be represented as Zn(II) or Cd(II) which chelated to two sulphur atoms and two nitrogen atoms.

4.2 Characterization of 1*H*-Indole-3-carbaldehyde thiosemicarbazone and Its Metal Complexes

4.2.1 Elemental analysis

The elemental analysis data of C, H and N for the 1*H*-Indole-3-carbaldehyde thiosemicarbazone and its metal complexes are in a good agreement with the proposed formulations. The results of the elemental analysis and some physical properties are shown in Table 4.8.

Table 4.8:
The analytical data and some physical properties of 1*H*-Indole-3-carbaldehyde thiosemicarbazone and metal complexes

Compounds	Colour	Melting Point/ °C	Found(Calculated)/%		
			C	H	N
Ind3Thiosemi	Pale Green	235-240	55.07(55.00)	4.73(4.58)	20.51(20.23)
Ni$_{Ind3Thiosemi}$	Orange	>300	48.41(48.49)	4.34(4.04)	25.97(25.67)
Cu$_{Ind3Thiosemi}$	Dark Green	>300	48.11(48.01)	4.15(4.00)	22.39(22.41)
Zn$_{Ind3Thiosemi}$	Yellow	>300	47.93(47.84)	4.03(4.06)	22.73(22.32)
Cd$_{Ind3Thiosemi}$	Pale Yellow	>300	43.71(43.74)	3.54(3.64)	20.43(20.41)

Some of the important IR bands for 1*H*-Indole-3-carbaldehyde thiosemicarbazone and its metal complexes are listed in Table 4.9.

The IR spectrum of 1*H*-Indole-3-carbaldehyde thiosemicarbazone showed the highest frequency band at 3449 cm^{-1}, attributed to the symmetric and asymmetric υ(N-H) stretching vibrations of the terminal NH$_2$ group (Mala et al., 1995). The presence of this band in both ligand and complexes spectra clearly indicate the non-involvement of NH$_2$ group in coordination to metal(II). The sharp and medium intensity bands around 3315-3000 cm^{-1} are due to υ(N-H) and indole N-H vibrations (Tunde and Omolara, 1988). It is important to indicate that the splitting of the band of the N-H group of indole of the metal complexes with respect to ligand is attributed to the existence of a weak interaction between the hydrogen of the N-H group of the indole and the sulphur atom of another molecule, forming a hydrogen intermolecular bonding (Martin R., et al., 1986).
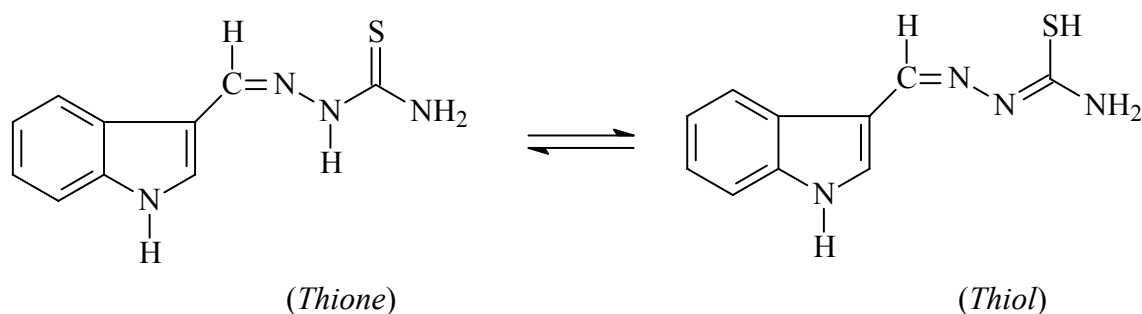
(*Thione*)   (*Thiol*)

Scheme 4.3: Tautomerism structure of *thiol-thione*

The thiosemicarbazone Schiff base can exhibit as either *thione* or *thiol* tautomerism (Scheme 4.3). Determination by harmonic oscillator calculation, the υ(C=S) always observed at two or three different ranges while the υ(C-SH) will appear in the region 2500-2600 cm^{-1} (Nabar, 1966). In the free ligand spectra, a sharp bands in the range 1125-1110 cm^{-1} and 765-750 cm^{-1} can be assigned to the υ(C=S) group, and a weak band around 2500 cm^{-1} suggesting that in the solid state thiosemicarbazones exhibited as a mixture of *thione-thiol* tautomer (Kakul et al., 2007). These bands are shifted to the lower energy in complexes spectra indicating that the *thione* sulphur has participated as a coordinating site.

For Schiff base ligand, the strong bands observed at 1612 cm^{-1} is assigned to the azomethine group vibration, υ(C=N). This band is slightly shifted towards lower frequencies in the complexes, and the change in this frequency shows that the imine nitrogen atom has coordinated to the metal(II) ions (Golcu et al., 2005).

The shifted to higher energy in the complexes spectra for υ(N-N) also indicates coordination of the ligand to the metal (Ugo, et al.,1967). In free ligand, the υ(N-N) in the range of 1120 cm^{-1} while in complex the band has shifted to 1135-1125 cm^{-1}. This is due to reduction in the repulsion between the lone pairs of electrons on the nitrogen atom as a result of the coordination through the azomethine nitrogen atom (Ali et al., 2003).

The bands at 600-450 cm^{-1} in free ligand are assigned to in-plane and out-plane indole ring deformation (Tunde and Omolara, 1988). In all of the present complexes, the medium or weak bands at 500-450 cm^{-1} can be attributed to the υ(M=S) and υ(M=N)

represented by the bands at the range of 450-400 cm^{-1} and thus lending support to the proposed coordination in the complexes.

The preferential coordination of *thionic* sulphur over nitrogen of indole is due to more nucleophilic character of sulphur atom in te ligand. Thus, in the complexes, the metal(II) coordinates to two donor atom, azomethine nitrogen and *thionic* sulphur of the ligand.

Table 4.9:
Important IR data for the 1*H*-Indole-3-carbaldehyde thiosemicarbazone and metal complexes (cm^{-1})

Compound	υ(N-H)	υ(C=N)	υ(C=S)*	υ(C=S)**	υ(N-N)	υ(M-S)	υ(M-N)
Ind3Thiosemi	3311	1612	1251	751	1120	-	-
Ni$_{Ind3\ Thiosemi}$	3371	1594	1234	747	1128	443	427
Cu$_{Ind3\ Thiosemi}$	3365	1595	1233	749	1125	463	420
Zn$_{Ind3\ Thiosemi}$	3372	1597	1232	744	1128	461	424
Cd$_{Ind3\ Thiosemi}$	3367	1605	1230	741	1131	454	421

Figure 4.12: IR spectrum of (1*H*-Indole-3-carbaldehyde)thiosemicarbazone
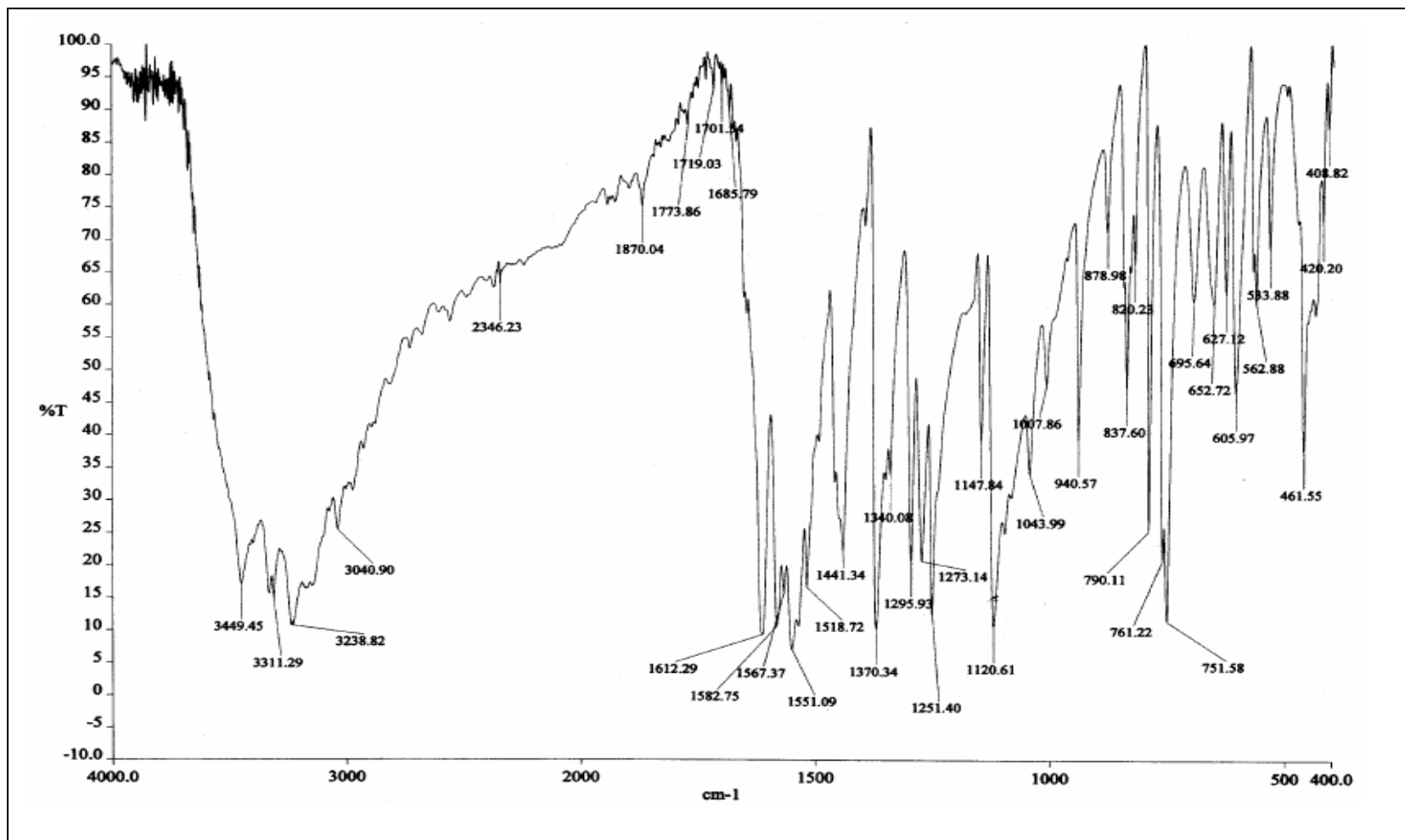
Figure 4.13: IR spectrum of Ni$_{Ind3Thiosemi}$
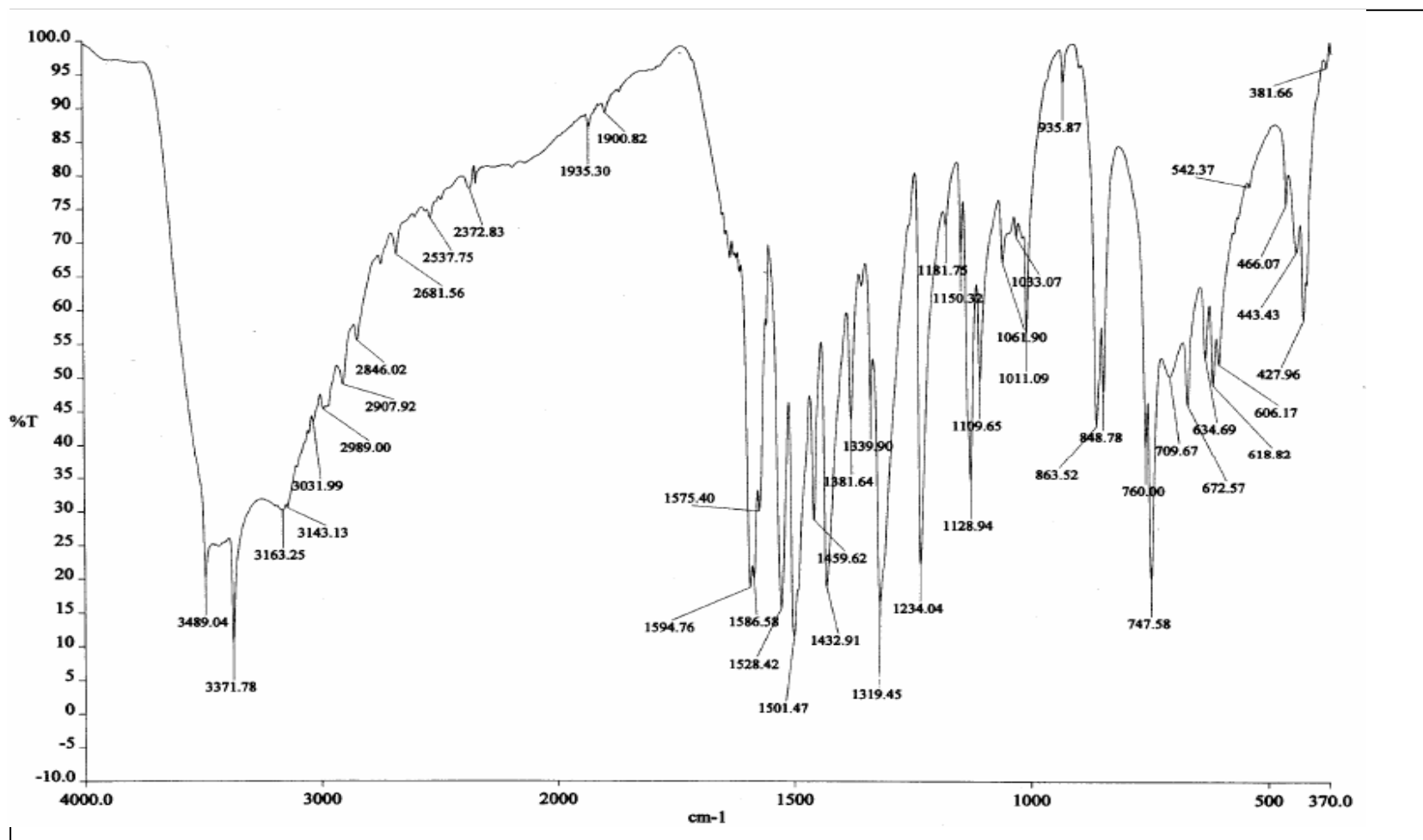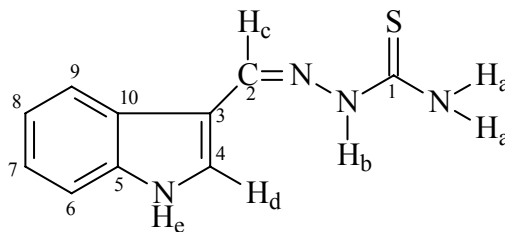
Scheme 4.4: The ligand with atoms numbering

The ^{1}H and ^{13}C-NMR are listed in the Table 4.10 and Table 4.11 respectively. The ligand with the atoms numbering was showed as Scheme 4.4.

The ^{1}H NMR spectrum displays singlet signals at the region 11.58-11.50 ppm and 11.16-11.10 ppm assignable to indole N-H and thioamide N-H respectively. The N-H proton signal clearly indicates that the ligand was in *thione* form in the solution. It is of interest to see that the ^{1}H NMR spectrum exhibits two resonances for the NH_2 protons around 8.30-8.10 ppm, indicating hindered rotation about the C(S)- NH_2 bond due to its partial double bond character (Teoh et al., 1997; Palenik and Shaun, 1990). The partial double bond was observed because of zwitterion resonance in the ligand as shown in Scheme 4.5.

The single signal appearing at 7.90-7.70 ppm is due to the azomethine proton (Mala et al., 1995). The signal of the proton labeled as H_d can be observed at region 7.42 ppm (Golcu et al., 2005). The spectrum showed the aromatic signals at 7.20- 7.00 ppm.

The ^{13}C NMR spectrum of the ligand showed two signals at 185.02 ppm and 176.50 ppm which are assigned to thioamide C1 and azomethine carbon C2, respectively (Mala et al., 1995). The signals around 131-110 ppm are due to indole ring carbons with the signal at 112.42 attributed to C3 and 131.00 assigned to C4. The aromatic carbons can be found at the signals around 140-111 ppm.
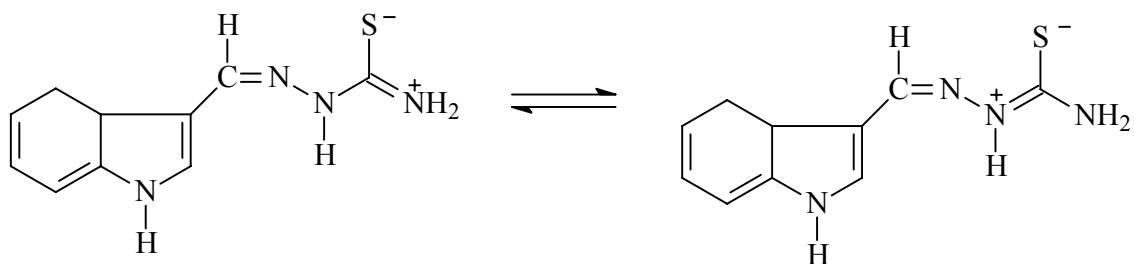
Scheme 4.5: The zwitterionic structures of the Schiff base ligand

Table 4.10:
Important ^{1}H-NMR data for the 1*H*-Indole-3-carbaldehyde thiosemicarbazone (ppm)

Compound	N-H$_e$	N-H$_b$	N-H$_a$	H$_c$-C=N	C-H$_d$	H$_{aromatic}$
Ind3Thiosemi	11.58	11.15	8.20	7.99-7.77	7.42	7.20-7.00

Table 4.11:
Important ^{13}C NMR data for the 1*H*-Indole-3-carbaldehyde thiosemicarbazone (ppm)

Compound	C1	C2	C3	C4	C$_{aromatic}$
Ind3Thiosemi	185.02	176.50	112.42	131.00	140-111

Figure 4.14: ^{1}H NMR spectrum of 1H-Indole-3-carbaldehyde thiosemicarbazone
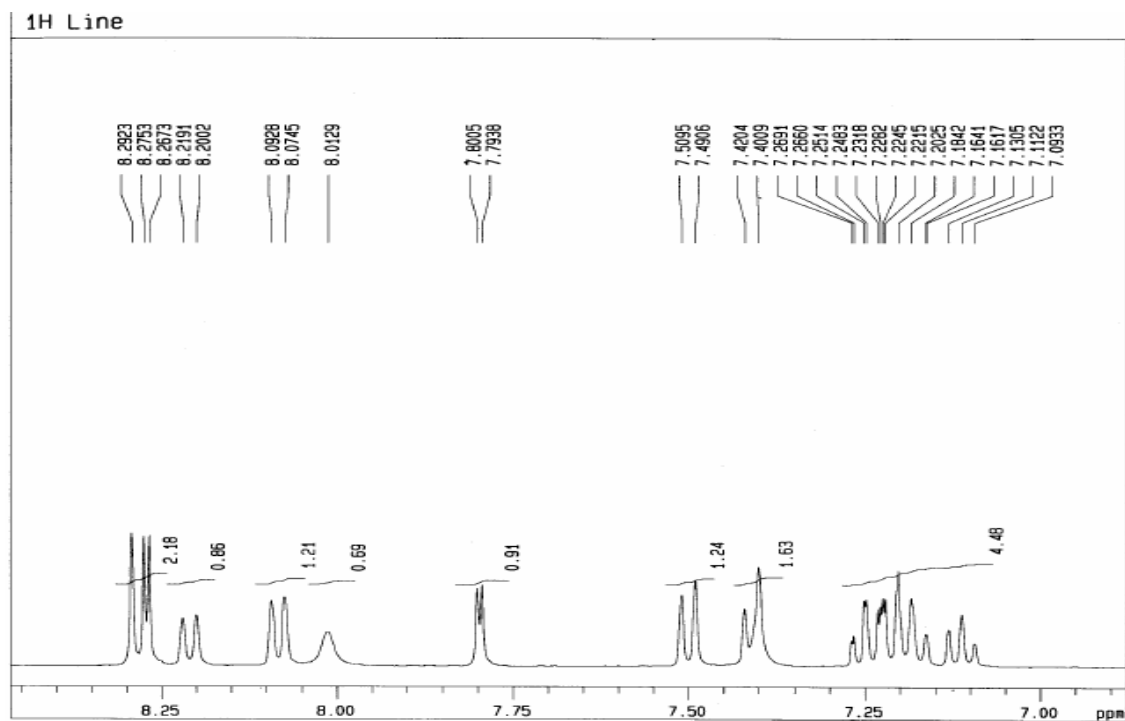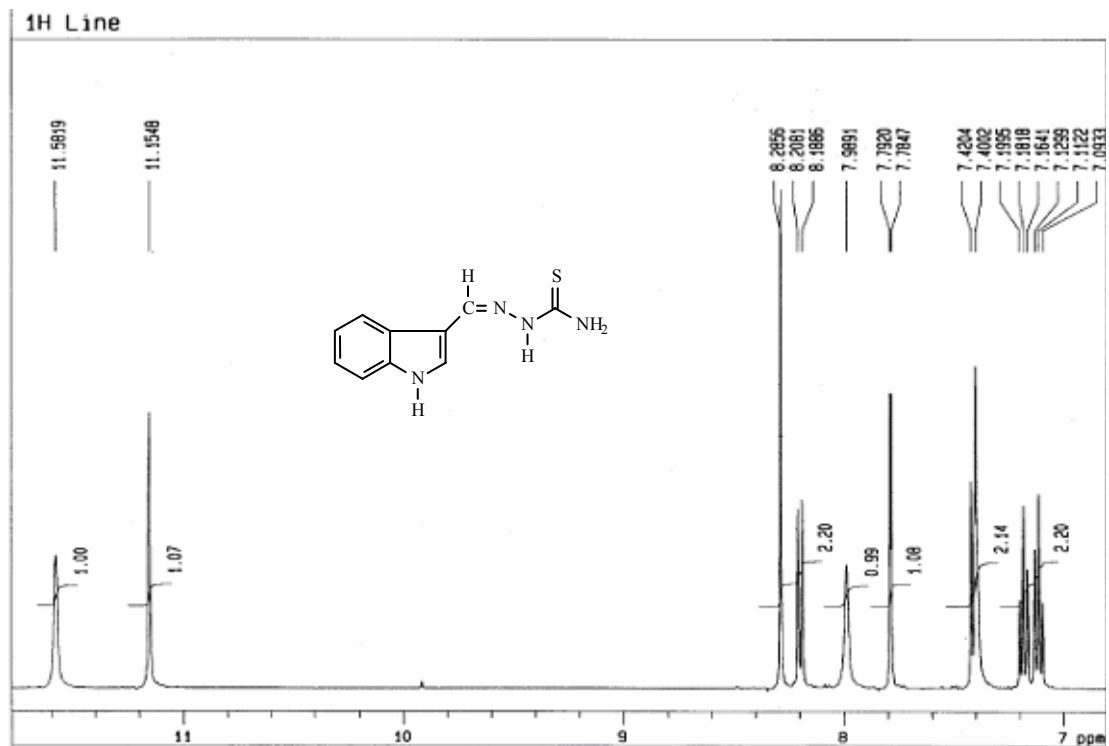
Figure 4.15: ^{13}C NMR spectrum of 1*H*-Indole-3-carbaldehyde thiosemicarbazone
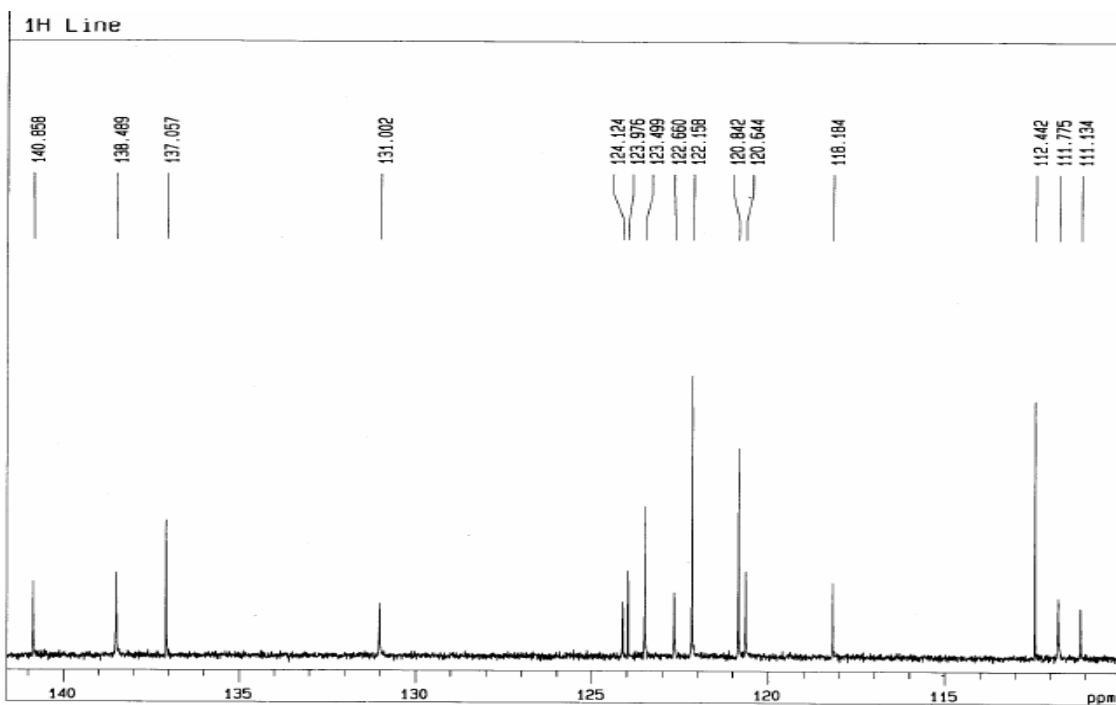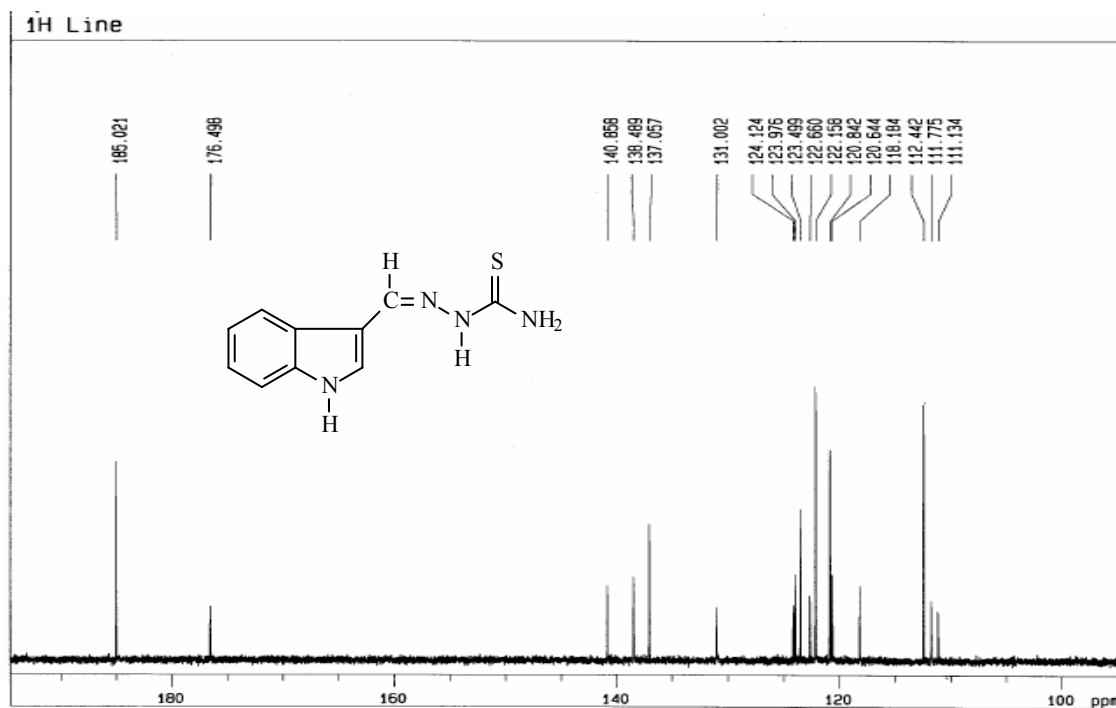
4.2.4 UV-visible spectral data

All the electronic absorptions for the 1*H*-Indole-3-carbaldehyde thiosemicarbazone and complexes in DMSO are listed in the Table 4.12.

In the free ligand, the absorptions that observed after than 33300 cm^{-1} were assigned to the $\pi \rightarrow \pi^*$ transition of the benzenoid and the NH$_2$ chromophore (Mala et al., 1995). The intense band at 33300-32000 cm^{-1} is due to the azomethine chromophore. These transitions also appear in complexes spectra but at higher energy because of the hypsochromic shift, confirming coordination of the ligand to the metallic ions (Golcu et al., 2005; Lu Z.L., et al., 2000).

The important absorption for the metal complexes is the wave number of less than 33300 cm^{-1}. The intense bands in the higher energy around 28500-25000 cm^{-1} can be assigned to charge transfer between ligands and metal(II) (TÜmer, 2000).

In the Ni(II) spectrum, the intense MLCT band in the UV region at 26400 cm^{-1} clearly indicates the coordination of Ni(II) to the ligands (Xavier et al., 2005). This band is attributed to the charge transfer from a p_π orbital on the ligand to the empty *d*-orbitals on the Ni(II), thus suggesting a square planar geometry (Asgedom et al., 1995).

In the electronic spectra of Cu(II) complex, the weak band observed at 18181 cm^{-1} can be assigned to $^2A_{1g} \rightarrow \ ^2B_{1g}$ transition. This band corresponds to a *d-d* transition and therefore suggesting that the Cu(II) complex may form four-coordinated square planar geometry (Golcu et al., 2005).

The electronic absorption spectra of the Zn(II) and Cd(II) complexes in DMSO, are dominated by a broad band in the region 33000-27000 cm^{-1} corresponding to an intra ligand transition and a charge transfer transition (Amirnasr et al., 2002). The *d-d* transitions do not exist as expected for d^{10} system of these metal complexes.

For the conclusion, the charge transfer and *d-d* transition in the metal complexes spectra have provided evidence for the complexation of the metal ions with the Schiff-base (Gupta and Sutar, 2007). The complexation of the Ni(II), Zn(II) and Cd(II) ions with Schiff-base has shown charge transfer transitions at 26455 cm^{-1}, 27777 cm^{-1} and 27472 cm^{-1}, respectively whereas the complexation of Cu(II) ions with the Schiff-base has proved by *d-d* transition at 18181 cm^{-1}. In the metal complexes spectra, the trends of the bands showed more than 15000 cm^{-1} suggesting that all of the metal complexes forming four-coordinate structure.

Table 4.12:
Electronic spectral data for the 1*H*-Indole-3-carbaldehyde thiosemicarbazone and metal complexes (cm^{-1})

Compound	Intraligand and charge transfer (cm^{-1})	*d-d* transition (cm^{-1})
Ind3Thiosemi	32000; 31250	-
Ni$_{Ind3Thiosemi}$	32500; 26455; 24390	-
Cu$_{Ind3Thiosemi}$	33200; 27322; 27027	18181
Zn$_{Ind3Thiosemi}$	33540; 27777	-
Cd$_{Ind3Thiosemi}$	33250; 27472	-

Figure 4.16: Uv-Vis spectrum of 1*H*-Indole-3-carbaldehyde thiosemicarbazone
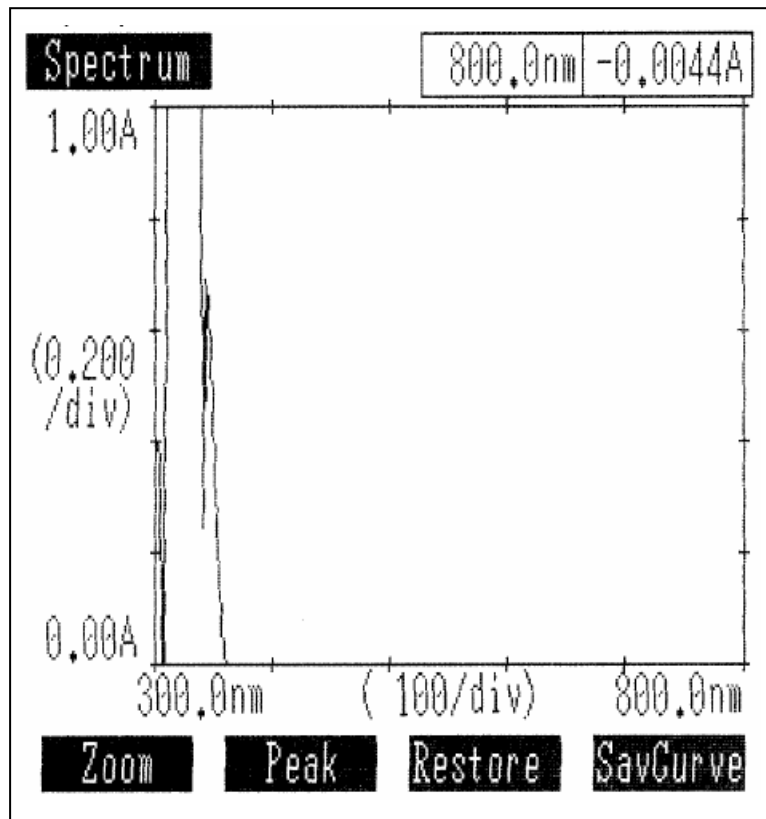
Figure 4.17 : Uv-Vis spectrum of Ni$_{Ind3Thiosemi}$
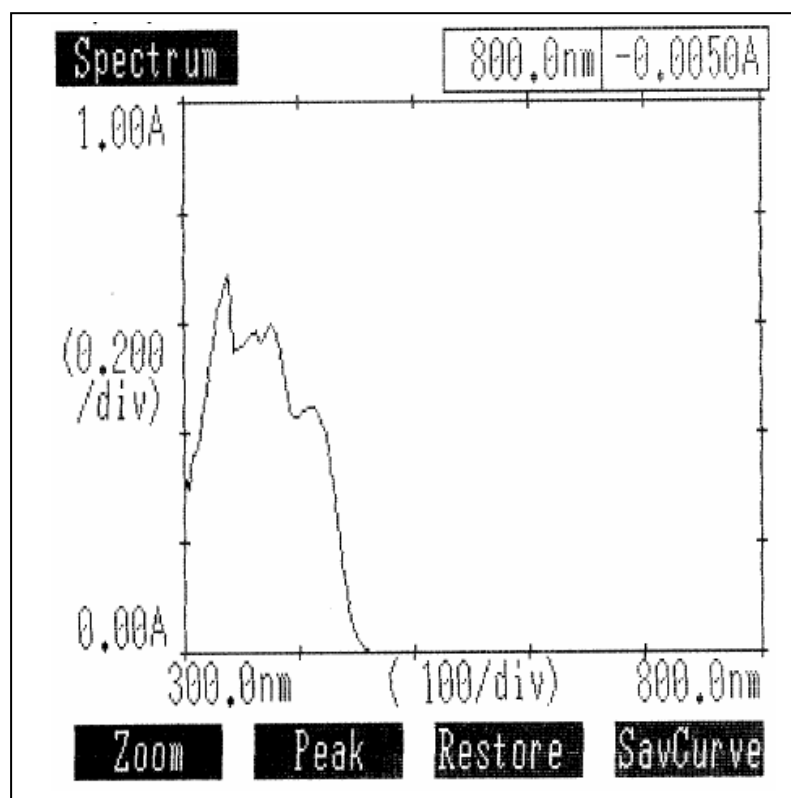
4.2.5 Magnetic Study

The magnetic data of the complexes are listed in the Table 4.13. The calculations of the unpaired electron are same as shown in Section 4.1.5.

Table 4.13: The magnetic properties of metal complexes. R2 representing 1*H*-Indole-3-carbaldehyde thiosemicarbazone

Compounds	Mass susceptibility, χ_g $(cm^3\ g^{-1})$	Molar susceptibility, χ_m^{corr} $(cm^3\ mol^{-1})$	Effective magnetic moment, μ_{eff} (B.M.)	Unpaired electron, n	Magnetism
NiR2	0	0	0	0	Diamagnetic
CuR2	1.283×10^{-6}	7.905×10^{-4}	1.378	$0.78 \approx 1$	Paramagnetic
ZnR2	-	-	-	-	Diamagnetic
CdR2	-	-	-	-	Diamagnetic

For the Ni(II), there are 8 electrons in 3*d* orbitals. The first 6 electrons will occupy the t_{2g} orbital and the remaining 2 electrons will occupy the e_{2g} orbital. Two electrons in e_{2g} will behave as unpaired electrons which occupy the two orbital in e_{2g} state as shown in Figure 4.18.
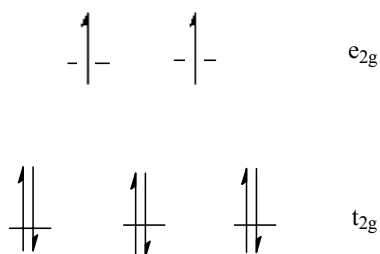
Figure 4.18: Electron arrangement for Ni(II) as free ion

77

Based on the results that obtained from the magnetic susceptibility measurement for the Ni(II) complex, the number of unpaired electron is zero. Assumption can be made that the unpaired electron in e_{2g} orbital will be paired when the ligands are attached to the metal. The electronic arrangement of Ni(II) complex is shown in Figure 4.19.

$$
\begin{array}{ccc}
\uparrow\downarrow & \underline{\quad} & e_{2g} \\[2em]
\uparrow\downarrow \quad \uparrow\downarrow \quad \uparrow\downarrow & & t_{2g}
\end{array}
$$
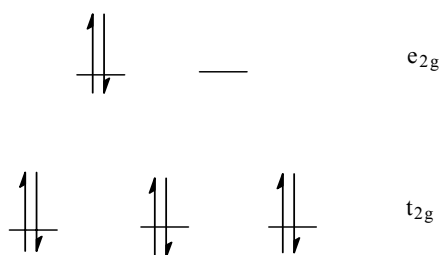
Figure 4.19: The electron arrangement for the Ni(II) ions in the complex

Thus, 1*H*-Indole-3-carbaldehyde thiosemicarbazone is a strong field ligand which forced the unpaired electron in e_{2g} orbital to be paired to become diamagnetic (Brady and Humiston, 1986; James, 1983). This electron configuration is ideal for the formation of square planar geometry. The four pair electrons from the ligands will occupy one 3*d* orbital, one 4*s* orbital and two 4*p* orbital of the metal to form the *dsp²* hybridization as shown in Figure 4.20.

$$
\underbrace{\uparrow\downarrow \quad \uparrow\downarrow \quad \uparrow\downarrow \quad \uparrow\downarrow}_{3d} \quad \underbrace{\overset{\bullet\bullet}{\underline{\quad}}}_{4s} \quad \underbrace{\overset{\bullet\bullet}{\underline{\quad}} \quad \overset{\bullet\bullet}{\underline{\quad}} \quad \overset{\bullet\bullet}{\underline{\quad}} \quad \underline{\quad}}_{4p}
$$
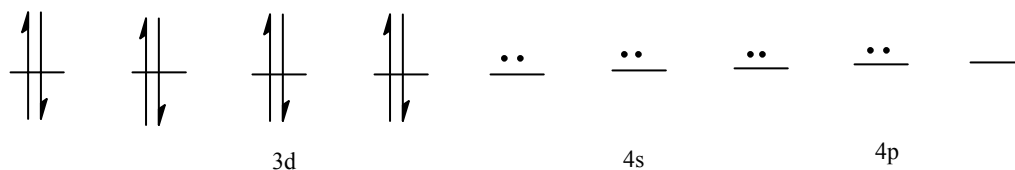
Figure 4.20: Electron arrangement upon the complexation to ligands

For the Cu(II) complex, the number of unpaired electron is one which indicates that the unpaired electron has existed in the electronic configuration. An assumption can be made that the Cu(II) complex in this system exists as mononuclear structure with square planar geometry through a dsp^2 hybridization (Amirnsr et al., 2002). This square planar complex with D_{4h} symmetry operation is expected for d^9 system as this arrangement centers additional stability from the advantageous splitting of the d energy level.

Zn(II) and Cd(II) are diamagnetic because of their d^{10} configuration and likely to form a tetrahedral geometry of the complexes with sp^3 hybridization.

4.2.6 X-ray Study and Data Collection

      The crystal data and details of data collection of 1*H*-Indole-3-carbaldehyde thiosemicarbazone are listed in the Table 4.14. Thermal ellipsoid diagram of the $C_{10}H_{10}N_4S$ is shown as Figure 4.21.

      The pale green crystal that was obtained from recrystallization from ethanol adopted a triclinic system with P-1 space group. The molecules of the title compound, $C_{10}H_{10}N_4S$, are linked by $N\text{-H}_{indole}\cdots S$ hydrogen bonds to form a linear hydrogen-bonded chain as shown in the Figure 4.21. The length of the hydrogen bonds that linked two molecules in an asymmetric unit are shown below:

Elements	H-bond distances (Å)	Angles (°)
$N\text{-H}_{indole}.....S1$	2.56(2)	156(3)
$N\text{-H}_{indole}.....S2$	2.49(2)	157(3)
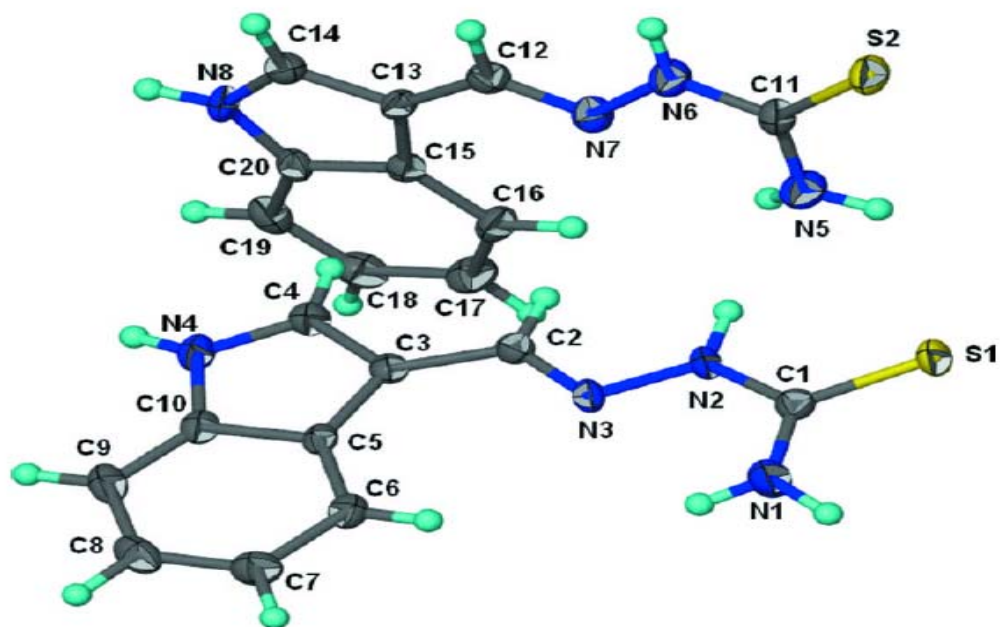
Figure 4.21: Thermal ellipsoid plot of the two independent molecules of the title compound. Displacement ellipsoids are drawn at the 70% probability level, and H atoms are shown as spheres of arbitrary radii.

Table 4.14: Crystallographic data for 1H-Indole-3-carbaldehyde thiosemicarbazone

Crystallographic data for ligand, 1H-Indole-3-carbaldehyde thiosemicarbazone

Empirical formula	$C_{10}H_{10}N_4S$
Formula weight	218.28
Temperature (K)	100 K
Crystal size (mm)	0.44 X0.24 X 0.04
Color	Pale Green
Shape	Wedge
Wavelength (Å)	0.71073
Crystal system	Triclinic
Space group	P-1
a (Å)	7.1893 (1)
b (Å)	11.1654 (2)
c (Å)	13.5373 (3)
α (º)	68.887 (1)
β (º)	85.048 (1)
γ (º)	82.467 (1)
V (Å^3)	1004.07 (3)
Z	4
μ	0.29
F(000)	456
Theta range for data collection (º)	1.6 – 27.5
Index ranges	$-8 \leq h \geq 9;\ -14 \leq k \geq 14;\ -17 \leq l \geq 17$
Reflection collected	9295
Independent reflection	4527
R (int)	0.036
Data/Parameters	4527/303
Final R indices [I>2σ (I)]	0.044
R indices (all data)	0.161
Largest diff. peak and hole (e.A^{-3})	0.45
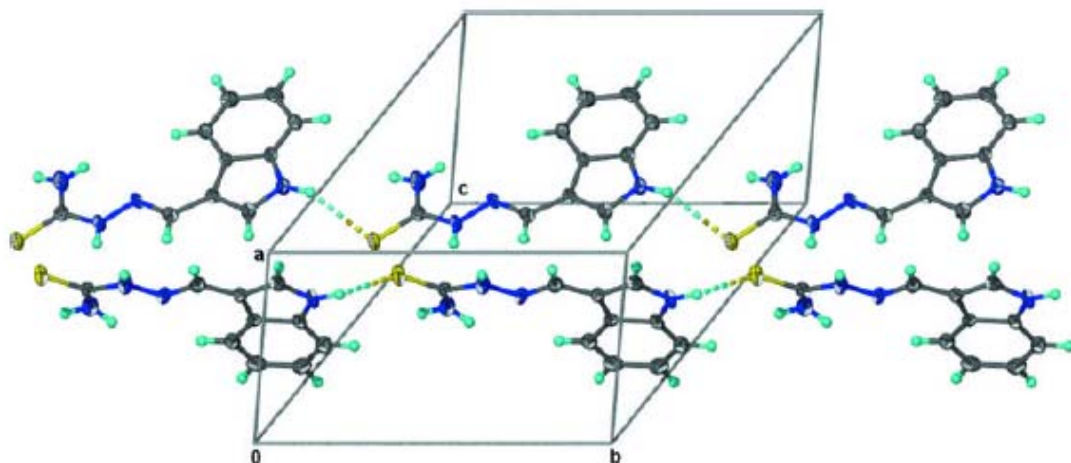
Figure 4.22: The linear chain structure of the ligand formed by hydrogen-bonded. The hydrogen bonds were represented by dashed lines.

The X-ray study on the metal complexes showed that the Ni(II) (Figure 4.23) and Cu(II) (Figure 4.24) complexes are isomorphic and isostructural. The centrosymmetric compound, $[Ni(C_{10}H_9N_4S)_2]$ is *N,S*- chelated by the deprotonated Schiff bases in a square planar geometry (Rizal et al., 2008). The Ni(II) and two thiolato sulphur atoms are equidistant which is 2.167Å. Besides that, the distance between Ni-N1 and Ni-N2 are also same, which is 1.917Å. The flat plane was form between N1, N2, S1, S2 and Ni with the angle of N1-Ni-N2 = 180° and S1-Ni-S2 = 180°.

The Ni(II) complex formed by two 1*H*-Indole-3-carbaldehyde thiosemicarbazone moieties are in a *trans* position, that planarly coordinated to the Ni(II) atom (Figure 4.25). This *trans*-isomer makes a good agreement with the small value of moment effective from Gouy balance measurement (Obadović et al., 1996).

The Cu(II) complex with this bidentate Schiff base ligand also shows square planar geometry but slightly distorted *via* chelation through the *thionic* sulphur and azomethine nitrogen. The Ni(II) and Cu(II) are isostructural, thus the characteristics of these two complexes remain the same. Some of the crystallographic data for the Ni(II) and Cu(II) complexes are listed in the Table 4.15.

Table 4.15: Crystallographic data for $[Ni(C_{10}H_9N_4S)_2]$ and $[Cu(C_{10}H_9N_4S)_2]$

Crystallographic data for metal complexes

	$[Ni(C_{10}H_9N_4S)_2]$	$[Cu(C_{10}H_9N_4S)_2]$
Empirical formula	$[Ni(C_{10}H_9N_4S)_2]$	$[Cu(C_{10}H_9N_4S)_2]$
Formula weight	502.3	527.3
Temperature (K)	100 K	100 K
Crystal size (mm)	0.14 X0.04 X 0.01	0.25 X 0.20 X 0.15
Color	Orange	Green
Shape	Plate	Block
Wavelength (Å)	0.71073	0.71073
Crystal system	Monoclinic	Monoclinic
Space group	P21/c	P21/c
a (Å)	10.4388 (3)	13.4820(1)
b (Å)	5.2604 (1)	8.3192(2)
c (Å)	19.1122(3)	15.3481(2)
α (°)	90	90
β (°)	104.803 (2)	94.251(3)
γ (°)	90	90
V (Å^3)	1014.66 (4)	1127.04 (3)
Z	2	2
μ	1.189	1.108
F(000)	508	453
Theta range for data collection (°)	2.6-24.7	2.1-21.3
Index ranges	$-12 \le h \ge 13; -6 \le k \ge 6; -24 \le l \ge 24$	$-8 \le h \ge 9; -10 \le k \ge 10; -19 \le l \ge 19$
Reflection collected	2326	4387
Independent reflection	1774	2659
R (int)	0.0808	0.1043
Data/Parameters	2326/254	2659/239
Final R indices [$I>2\sigma (I)$]	0.0335	0.0826
R indices (all data)	0.0551	0.1985
Largest diff. peak and hole (e.A^{-3})	0.426	0.801
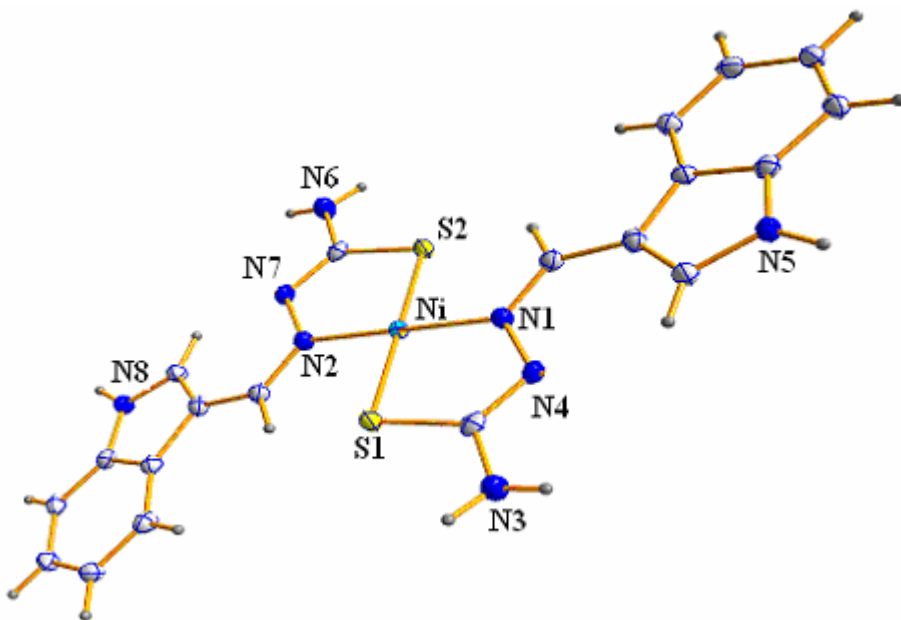
Figure 4.23: The structure of *trans*-Ni complex
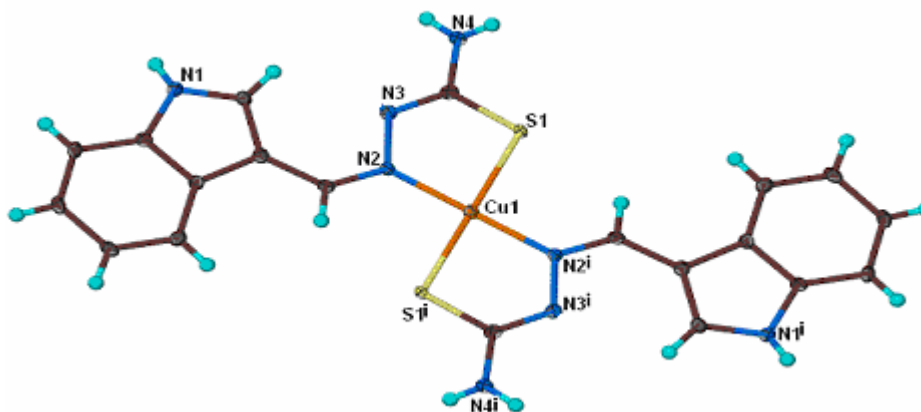
Figure 4.24: The structure of *trans*-Cu(II) complex with 50% probability. The atoms were labeled except for carbon and hydrogen atoms. The hydrogen atoms were refined isotropically.
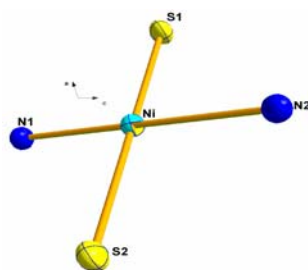
Figure 4.25: The geometry of *trans*-Ni(II) complex. The geometry of the Cu(II) is visually indistinguishable from that of the Ni(II) compound and uses an identical atom numbering scheme, but with 'Ni' replaced by 'Cu'.

Thus, the above data make a good agreement with the proposed structural formula of the metal complexes:
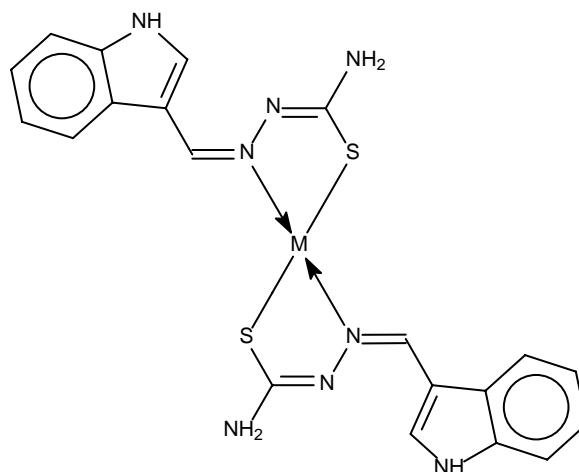
which M can be either Ni(II), Cu(II), Zn(II) or Cd(II) and the metal(II) ions are four coordinated. The Ni(II) and Cu(II) complexes form a square planar geometry while Zn(II) and Cd(II) exist as tetrahedral geometry.

4.3 Characterization of bis(1*H*-Indole-3-carbaldehyde)carbohydrazone and Its Metal Complexes

4.3.1 Elemental Analysis

The elemental analysis data of C, H and N for the bis(1*H*-Indole-3-carbaldehyde)carbohydrazone and their metal complexes are in a good agreement with the proposed formulations and the results with some physical properties are shown in Table 4.16.

Table 4.16: The analytical data and some physical properties of bis(1*H*-Indole-3-carbaldehyde)carbohydrazone and metal complexes

Compounds	Colour	Melting Point/ °C	Found(Calculated)/%		
			C	H	N
Ind3Carbo	White	270-275	66.54(66.41)	4.75(4.66)	24.21(24.47)
Ni$_{Ind3Carbo}$	Orange	>300	61.43(61.18)	4.31(4.28)	22.61(22.54)
Cu$_{Ind3Carbo}$	Green	>300	61.27(61.24)	4.37(4.27)	22.52(22.41)
Zn$_{Ind3Carbo}$	Yellow	>300	60.92(58.59)	4.27(4.26)	21.37(21.34)
Cd$_{Ind3Carbo}$	Pale Green	>300	57.41(57.44)	4.17(4.00)	21.11(21.02)

4.3.2 IR Spectra Data

The assignment of some important IR bands of the Schiff base ligand and metal complexes are listed in the Table 4.17.

In ligand spectra, a broad bands around 3200 cm^{-1} and 3100 cm^{-1} were attributed to –OH and –NH vibrations respectively (Gup and Kirkan, 2006). The ν(O-H) band may be due to the *enolic* form in the ligand tautomerism (Scheme 4.6) or may due to the presence of lattice water in the compound (Gup and Kirkan, 2006). The shifting of ν(N-H) in the metal complexes spectrum could be due to the presence of intramolecular or intermolecular hydrogen bonding (Koh et al., 1998).
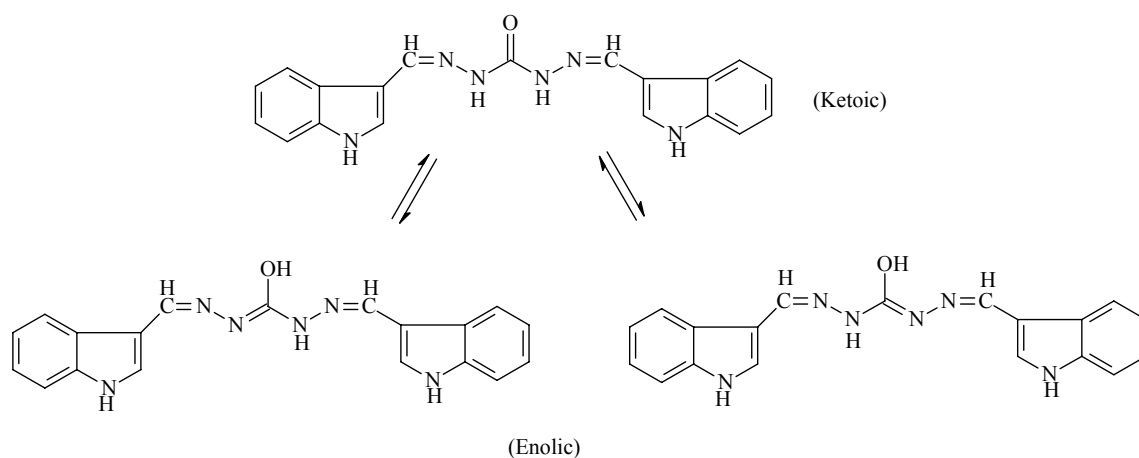
Scheme 4.6: Tautomeric forms of the ligand

The presence of ν(C=O) around 1685-1680 cm^{-1} in ligand spectra indicated that the Schiff base can exist as either *ketoic* or *enolic* forms in solid state (Patil et al., 1982). The ν(C=O) was disappeared during the complexation indicating deprotonation and enolization of the ligands on complexation. The presence of ν(O-H) in metal complexes spectra indicates that the ligand may exist as *enolic* tautomer in the complexes (Iskander et al., 2004).

Coordination of the ligand to the metal(II) can be assigned by the shifting of the ν(C=N) in metal complexes spectra. These vibrations will be shifted about 30-70 cm^{-1} towards lower energy region indicated that the azomethine nitrogen chelated to the metal(II) (Procter et al., 1968). For example, in Zn(II) complex the ν(C=N) is at 1620-1610 cm^{-1} while in the ligand the peak is at 1644 cm^{-1}.

Further support for coordination of azomethine nitrogen in the ligand to metal(II) also can be determined by the higher energy shift of the hydrazinic ν(N-N) in metal complexes spectrum (Ugo, 1967). For example, in Zn(II) complex, the ν(N-N) is at 1107 cm^{-1} while the ν(N-N) in ligand is at 1104 cm^{-1}. This happened because of reduction in the repulsion between the lone pairs of electrons on the nitrogen atom as a result of the coordination through the azomethine nitrogen atom (Ali et al., 2003).

Another evidence which showed chelation of ligand to metal(II) can be observed by the existence of sharp peaks at lower energy in the spectra of metal complexes (Khlood et al., 2007). The observations at this region slightly difficult in the case that the vibrations of the ligand were interfere in this region. Peaks around 600- 470 cm^{-1} are attributed to the in-plane and out-plane ring deformation (Tunde and Omolara, 1988). For the metal complexes, the region around 430-420 cm^{-1} was assigned to the ν(M-O) vibration mode while the region beyond that was assigned as ν(M-N) vibration (Khlood et al., 2007).

In summary for the IR spectra, the trends of the vibration modes indicating that the ligand always existed as *enolic-ketoic* tautomer. The metal(II) ions may chelated the bidentate Schiff bases through the oxygen atom and azomethine nitrogen.

Table 4.17:
Important IR data for the bis(1*H*-Indole-3-carbaldehyde)carbohydrazone and their metal complexes (cm^{-1})

Compound	υ(O-H)	υ(N-H)	υ(C=O)	υ(C=N)	υ(N-N)	υ(M-O)	υ(M-N)
Ind3Carbo	3225	3118	1681	1644	1104	-	-
Ni$_{Ind3Carbo}$	3371	3031	1660	1617	1106	424	386
Cu$_{Ind3Carbo}$	3365	2963	1600	1575	1230	420	400
Zn$_{Ind3Carbo}$	3372	2915	1659	1616	1107	425	408
Cd$_{Ind3Carbo}$	3367	2915	1660	1617	1106	424	407

Figure 4.26: IR spectrum of the ligand bis(1*H*-Indole-3-carbaldehyde)carbohydrazone
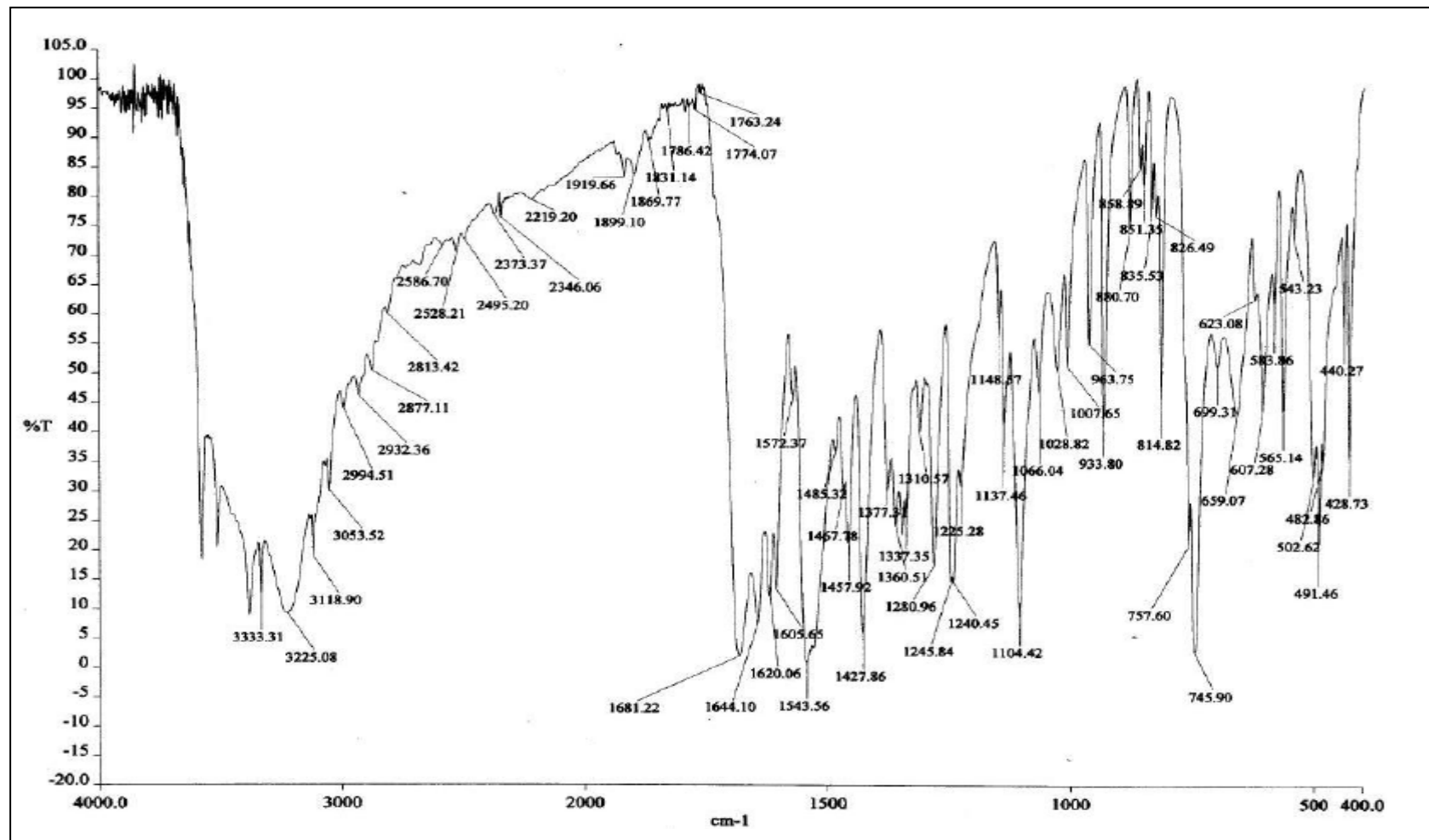
Figure 4.27: IR spectrum of $Cd_{Ind3Carbo}$
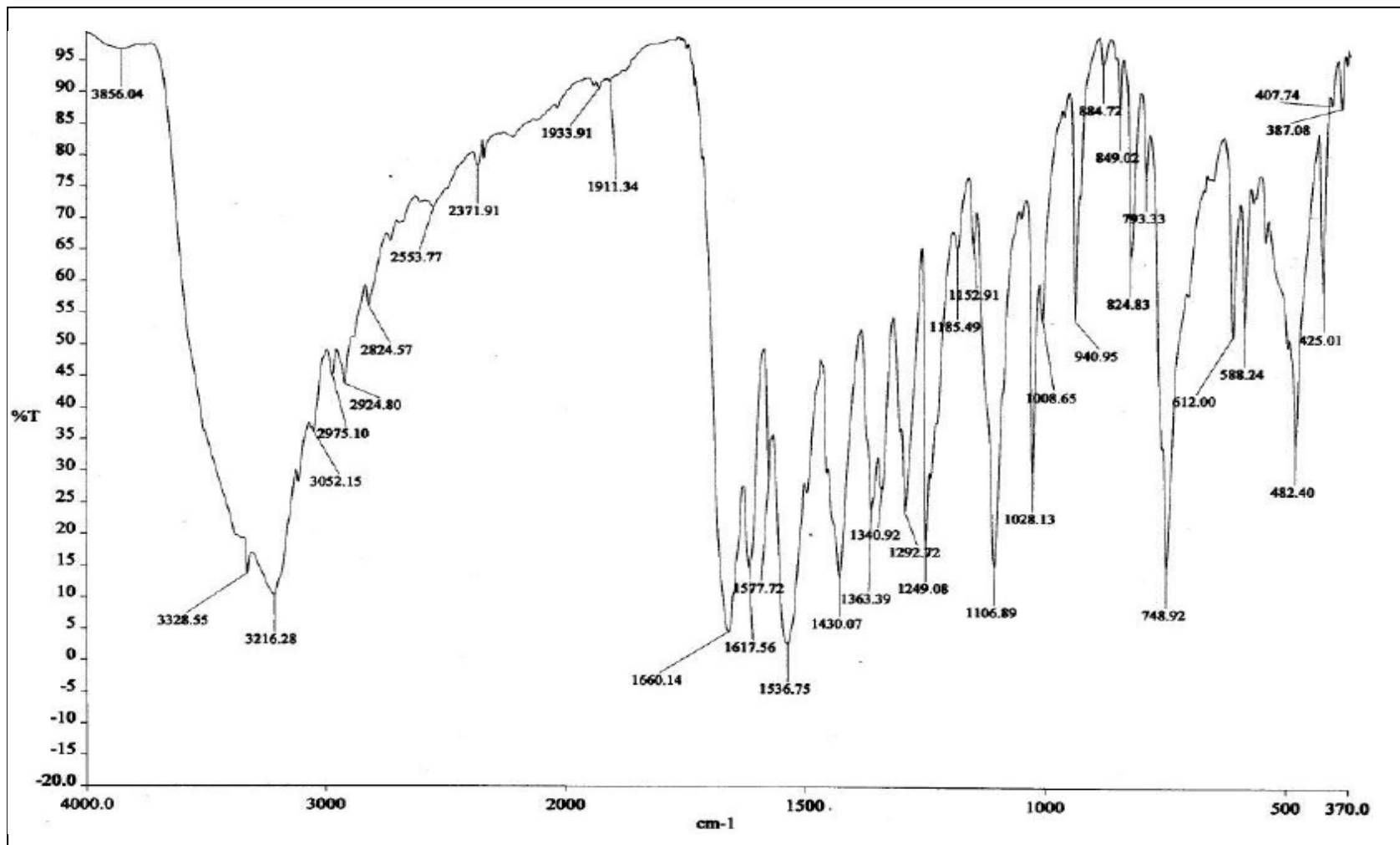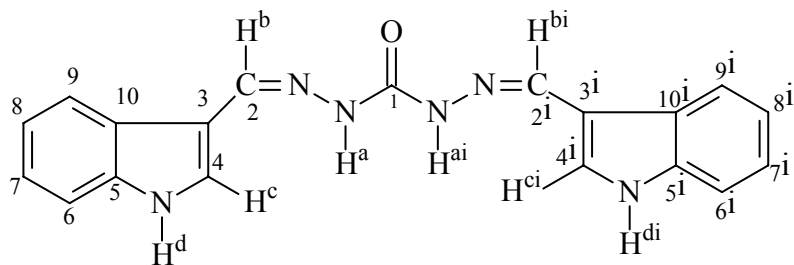
Scheme 4.7: The ligand with atoms numbering

^{1}H and ^{13}C NMR data for bis(1*H*-Indole-3-carbaldehyde)carbohydrazone are listed in the Table 4.18 and Table 4.19, respectively. The Schiff base with proton numbering scheme is shown in Scheme 4.7.

In the ^{1}H NMR spectrum, the signal that appeared around 11.50-11.47 ppm was assigned by the N-H signals representing as H^d and H^{di} in the Scheme 4.7. The sharp peak at 10.05 ppm was attributed to N-H signals, H^a and H^{ai}. The N-H proton signal of the Schiff bases showed that the ligands remain in the *keto* form in solution (Ali et al., 2004).

The signals around region 8.35-8.25 ppm were attributed to H^b and H^{bi} which came from the two similar azomethine groups of the ligand (Mala et al., 1995). In this region, the relative down field appearance (δ= 8.27) of the second peak may be due to the intramolecular hydrogen bonding in the ligand. The h^c and h^{ci} signal can be observed at the peak around 7.75-7.69 ppm and the signals around 7.50-7.30 ppm were attributed to the protons from two phenyl groups.

For ^{13}C NMR spectrum of the ligand, the single peaks at 152.46 ppm and 136.98 ppm were attributed to the C1 and C2, respectively as shown in the Scheme 4.7. The signal at 129.11 ppm was assigned to the C4 and the peak at 124.31 was attributed to the C3 atoms. The aromatic carbons peaks can be observe in the range 123-110 ppm in the spectrum (Golcu et al., 2005).

The ^1H and ^{13}C NMR spectra studies showed that in solution, the Schiff base remain in *keto* tautomeric form. The data that obtained was making a good agreement with the proposed Schiff base ligand structure.

Table 4.18:
Important ^{1}H NMR data for the bis(1*H*-Indole-3-carbaldehyde)carbohydrazone (ppm)

Compound	N-H^d	N-H^a	H^b-C=N	C-H^c	H$_{aromatic}$
Ind3-Carbo	11.50-11.47	10.05	8.35-8.25	7.75-7.69	7.50-7.30

Table 4.19:
Important ^{13}C NMR data for the bis(1*H*-Indole-3-carbaldehyde)carbohydrazone (ppm)

Compound	C1	C2	C3	C4	C$_{aromatic}$
Ind3-Carbo	152.46	136.98	129.11	124.31	123-110

Figure 4.28: ^{1}H NMR spectrum of bis(1H-Indole-3-carbaldehyde)carbohydrazone
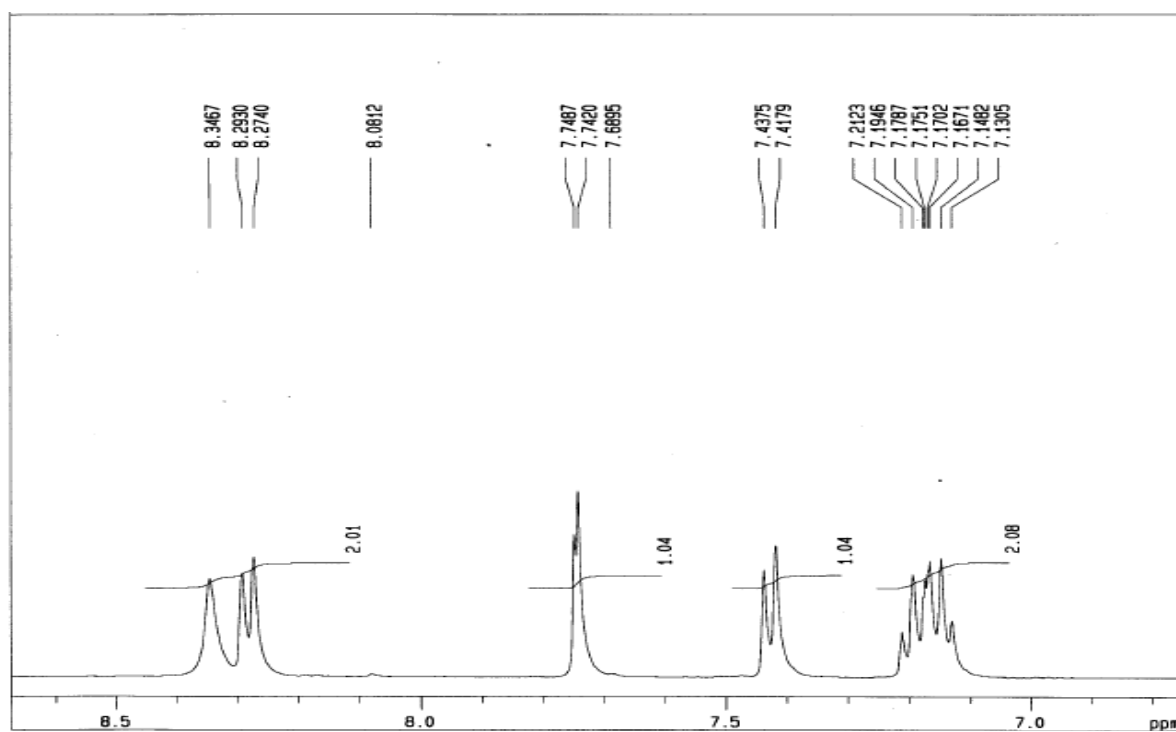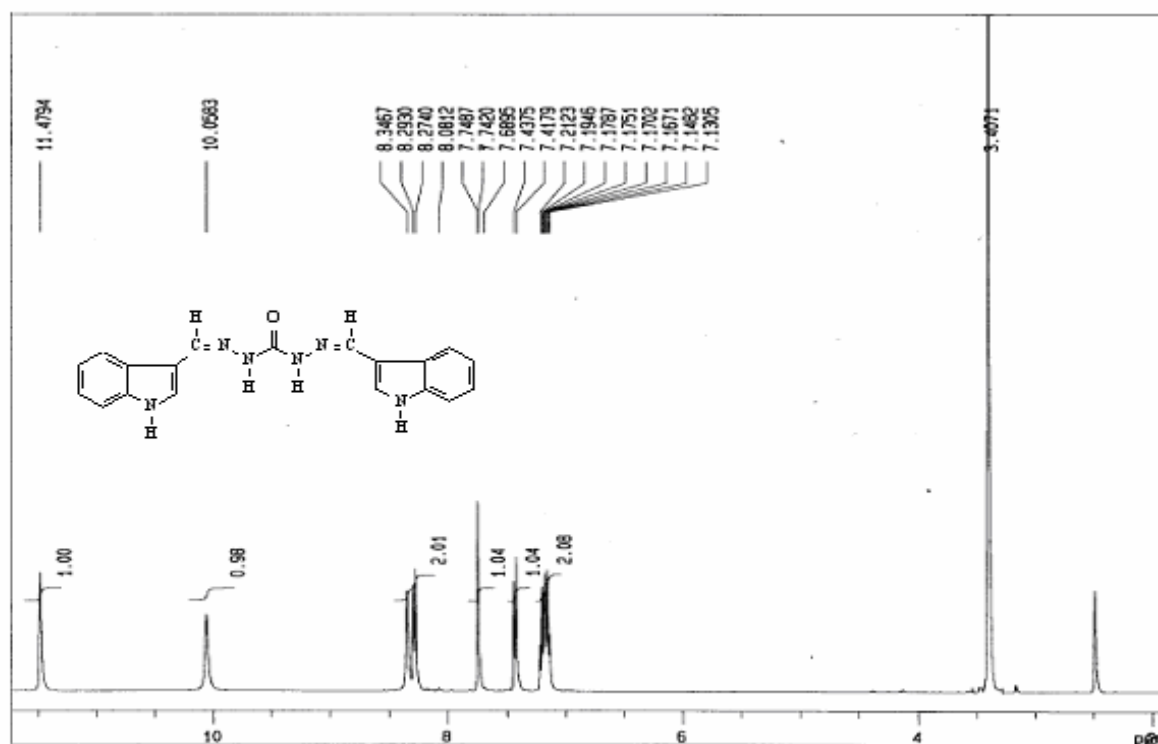
Figure 4.29: ^{13}C NMR spectrum of bis(1*H*-Indole-3-carbaldehyde)carbohydrazone
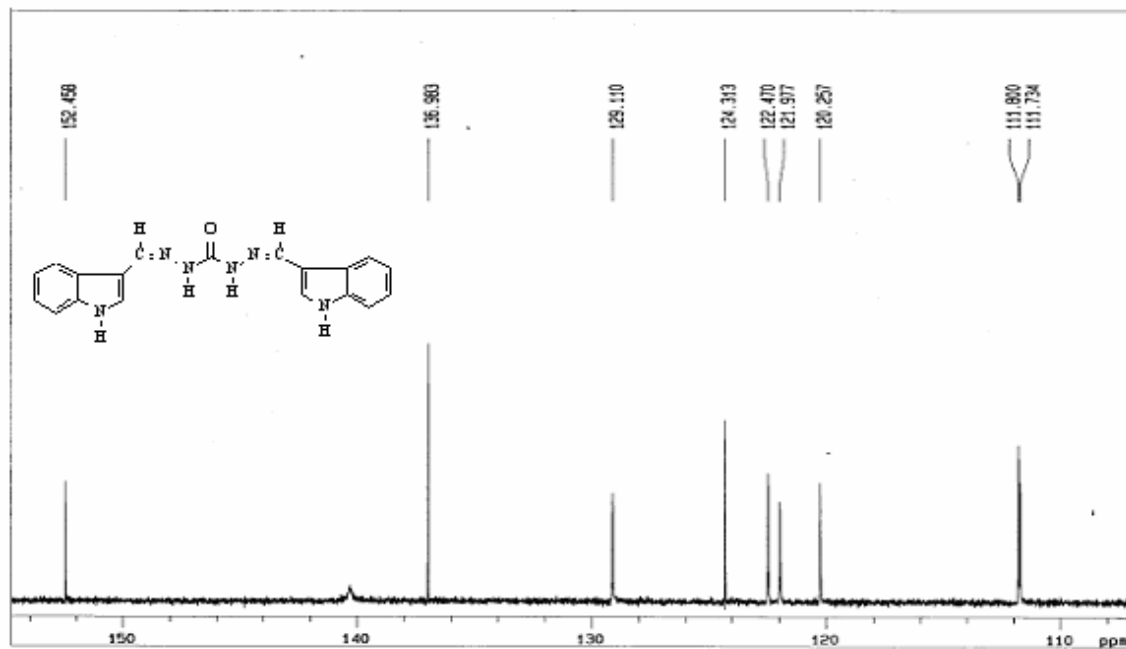
4.3.4 UV-Vis spectra

The electronic absorption data of the Schiff base ligand and metal complexes in DMSO were summarized in the Table 4.20.

The ligand absorptions at the range 33000-30000 cm^{-1} were attributed to the $\pi \rightarrow \pi^*$ transition of the benzenoid and the N-H chromophore (Mala et al., 1995). This broad band overlaps with the bands that assigned to the $n \rightarrow \pi^*$ transitions associated with azomethine chromophore. These bands also can be observed in the high field region of metal(II) complexes spectra indicating the hypsochromic or bathochromic shift, confirming the coordination of the ligands to the metal ions (Lu et al., 2000).

In Cu(II) complex, the sharp and narrow band at the range 27000-25000 cm^{-1} was due to the excitonic nature and related to $\sigma \rightarrow \sigma^*$ transition in the compound (Nešpůrek et al., 2002). The shifting of the absorption bands to lower energy indicates the coordination of Cu(II) complex with the Schiff base ligand (Golcu et al., 2005). This peak also can be considered as charge transfer transition between metal and ligand that involving the *d*-orbital of Cu(II) and π^* orbital of donor atoms (Obadović et al., 1996). Weak absorption at the region 19500-19000 cm^{-1} was attributed to the $^3B_{1g} \rightarrow {}^3A_{1g}$ transition. The trend of the absorption in the spectra showed that the Cu(II) complex may be chelated to four atoms.

For the Ni(II) complex, sharp and short bands at 27500-26000 cm^{-1} is assigned to the excitonic nature and related to $\sigma \rightarrow \sigma^*$ transition in the compound which is analogous to the Cu(II) complex. The chelation of the ligand to the Ni(II) atom have

been proven when the broad band in ligand spectra has shifted to the higher wavelength in the complex spectra (Revankar et al., 2007). The shoulder band at 17500 cm^{-1} can be attributed to the $^3B_{1g} \rightarrow {}^3B_{2g}$ transition. In addition, the tails bands extend up to the visible portion of the spectra, thereby making the expected *d-d* bands which may be assigned to $^3B_{1g} \rightarrow {}^3A_{1g.}$

In Zn(II) and Cd(II) complexes, the *d-d* transition did not occur because of the *d* orbitals have already been filled up with 10 electrons. The absorptions at the range 28000-26000 cm^{-1} are attributed to the ligand metal charge transfer (LMCT) and these bands probably represent the $^3E_g \rightarrow {}^3A_{2u}$ and $^3A_{1g} \rightarrow {}^3A_{2u}$ transitions in the Zn(II) and Cd(II) complexes. The appearance of these absorptions at this range showed chelation of ligand to Zn(II) and Cd(II).

From the spectrum of the complexes, the trends of the transitions indicated that the complexes may form four coordinated structure (Golcu et al., 2005). The *d-d* transitions in the Ni(II) and Cu(II) complexes were confirmed by the weak absorption in the middle of the spectra.

Table 4.20:
Electronic spectral data for the bis($1H$-Indole-3-carbaldehyde)carbohydrazone and its metal complexes (cm^{-1})

Compound	Intraligand and charge transfer (cm^{-1})	d-d transition (cm^{-1})
Ind3Carbo	33000; 30000	
Ni$_{Ind3Carbo}$	27000; 26000	17500
Cu$_{Ind3Carbo}$	27000; 25000	19000
Zn$_{Ind3Carbo}$	28000; 26000	
Cd$_{Ind3Carbo}$	28000; 26000	

Figure 4.30: Uv-Vis spectrum of bis(1*H*-Indole-3-carbaldehyde)carbohydrazone
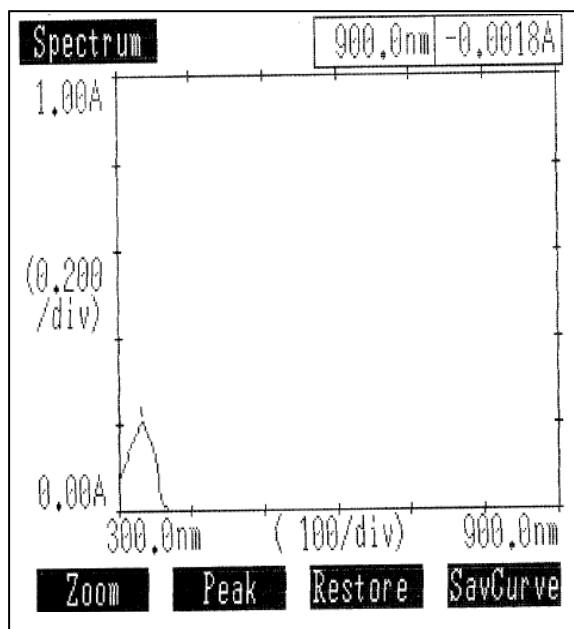
Figure 4.31: Uv-Vis spectrum of Ni$_{IndCarbo}$
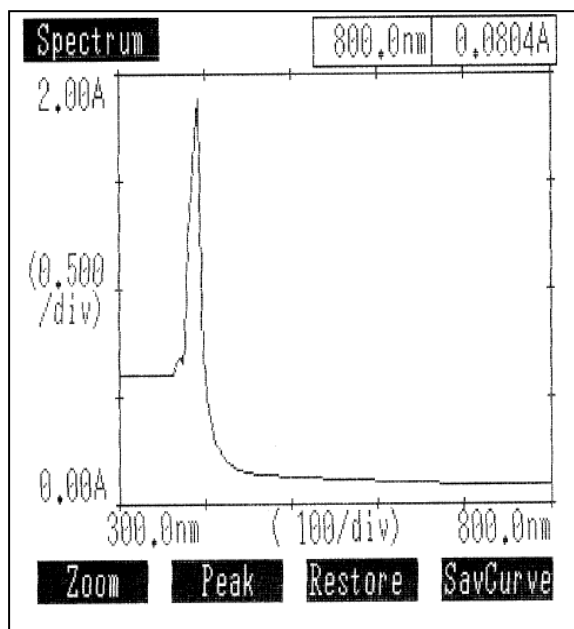
The data of the magnetic study for the metal complexes using the Gouy Balance were listed in the Table 4.21.

Table 4.21: The magnetic properties of metal complexes. R3 represented a bis(1H-Indole-3-carbaldehyde)carbohydrazone

Compounds	Mass susceptibility, χ_g ($cm^3\ g^{-1}$)	Molar susceptibility, χ_m^{corr} ($cm^3\ mol^{-1}$)	Effective magnetic moment, μ_{eff} (B.M.)	Unpaired electron, n	Magnetism
NiR3	0.414×10^{-6}	3.086×10^{-4}	0.860	$0.32 \approx 0$	Diamagnetic
CuR3	0.959×10^{-6}	8.155×10^{-4}	1.403	$0.72 \approx 1$	Paramagnetic
ZnR3	-	-	-	-	Diamagnetic
CdR3	-	-	-	-	Diamagnetic

The absence of unpaired electron in the d orbital for the Ni(II) complex indicated that this ligand behave as strong field ligand and may form a square planar geometry (Schläfer et al., 1967). The empty space in the d orbital, for both Ni(II) and Cu(II) complexes in the molecular orbital facilitates the dsp^2 hybridization. The chelation of ligand to either Ni(II) or Cu(II) atoms occupying the $3d_{x2-y2}$, $4s$, $4p_x$ and $4p_y$ orbitals. This electronic configuration makes a good agreement with the formation of square planar complexes (Brady and Humiston, 1986; James, 1983).

The Zn(II) and Cd(II) complexes only have one electronic configuration as a result of the d orbital been fully occupied. From the electronic spectra, suggest that the Zn(II) and Cd(II) are four coordinated structure, with sp^3 configuration forming tetrahedral geometry (Golcu et al., 2005).

4.3.6 Crystal structure and data collection

The crystal data of bis(1*H*-Indole-3-carbaldehyde)carbohydrazone is summarized in the Table 4.22. The crystal structure of this Schiff base ligand is illustrated as Figure 4.32.

The structure of the Schiff base showed formation of intermolecular and intramolecular hydrogen bonding. The two independent molecules in the asymmetric units were linked with the hydrogen bonds which formed between the N-H....O atoms. These hydrogen bonds then create a one-dimensional zigzag infinite structure as represented in Figure 4.33.
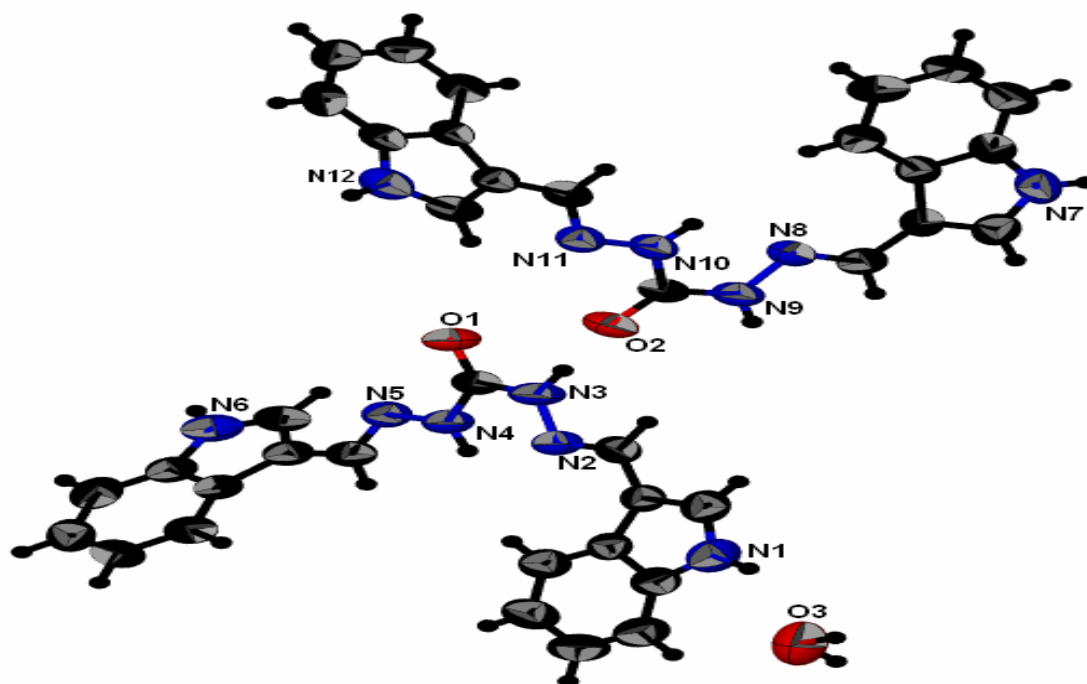
Figure 4.32: Thermal ellipsoid plot of two independent molecules of the title compound. Displacement ellipsoids are drawn at the 50% probability level, and H atoms are shown as spheres of arbitrary radii.
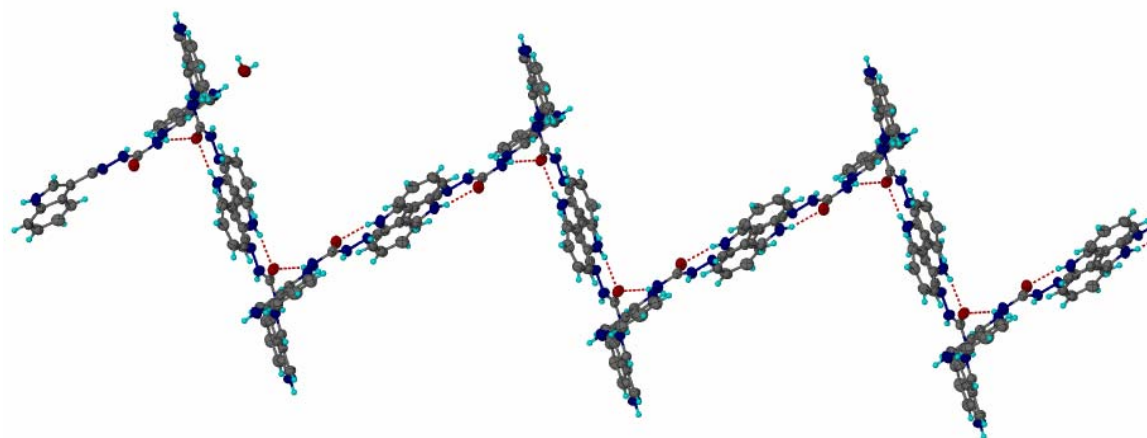
Figure 4.33: The infinite one-dimensional zigzag structure that formed due to hydrogen bonds between the independent molecules.

Table 4.22: Crystallographic data for bis(1*H*-Indole-3-carbaldehyde)carbohydrazone

Crystallographic data for ligand, bis(1*H*-Indole-3-carbaldehyde)carbohydrazone

Empirical formula	$C_{19}H_{16}N_6O_1$
Formula weight	706.77
Temperature (K)	100 K
Crystal size (mm)	0.25 X0.25 X 0.20
Color	Colorless
Shape	Block
Wavelength (Å)	0.71073
Crystal system	Triclinic
Space group	P-1
a (Å)	5.3154 (1)
b (Å)	16.4078 (3)
c (Å)	19.7410 (1)
α (º)	94.939 (1)
β (º)	90.028 (1)
γ (º)	99.316 (1)
V (Å³)	1692.47 (3)
Z	2
μ	0.093
F(000)	740
Theta range for data collection (º)	2.52– 19.58
Index ranges	−6≤ h ≥ 6; −19 ≤ k ≥ 19; −23 ≤ l ≥ 23
Reflection collected	5997
Independent reflection	2006
R (int)	0.072
Data/Parameters	2006/487
Final R indices [I>2σ (I)]	0.073
R indices (all data)	0.181
Largest diff. peak and hole (e.A^{-3})	0.85

Recrystallization of the crude metal complexes either in DMSO or DMF has yielded few crystals that suitable for the X-ray diffraction. Table 4.23 summarizes the crystal data and details of data collection. The X-ray structural study on the Ni(II) and Cu(II) complexes showed that they are isostructural which belong to the similar space group, monoclinic C2/c (Amirnasr et al., 2002).

The centrosymmetric compound $[Ni(C_{19}H_{15}N_6O)_2]$ as shown in the Figure 4.34 is *N,O*- chelated by the deprotonated Schiff bases is slightly distorted square-planar environment (Rizal et al, 2008). The bulky and strong field ligand like bis(1*H*-Indole-3-carbaldehyde)carbohydrazone may effect the geometry of the metal complexes (Onoda et al., 2003). The distance between Ni1-O1 is about 1.952 Å and the distance between Ni1-N5 is around 2.016 Å. The bond distance between Ni1-O1^i and Ni1-N5^i are similar to Ni1-O1 and Ni1-N5, respectively. Although the angle of O1-Ni1-O1^i is 180°, but the angle of N5-Ni1-N5^i is 173.5^o which cause the formation of distorted square planar geometry. Some of the important distances and angles were summarized in Table 4.24.

Table 4.23: Crystallographic data for $[Ni(C_{19}H_{15}N_6O)_2]$ and $[Cu(C_{19}H_{15}N_6O)_2]$

Crystallographic data for metal complexes

	$[Ni(C_{19}H_{15}N_6O)_2]$	$[Cu(C_{19}H_{15}N_6O)_2]$
Empirical formula	$[Ni(C_{19}H_{15}N_6O)_2]$	$[Cu(C_{19}H_{15}N_6O)_2]$
Formula weight	772.3	773.8
Temperature (K)	100 K	100 K
Crystal size (mm)	0.30 X0.24 X 0.10	0.25 X 0.05 X 0.01
Color	Orange	Green
Shape	Irregular	Plate
Wavelength (Å)	0.71073	0.71073
Crystal system	Monoclinic	Monoclinic
Space group	C2/c	C2/c
a (Å)	23.5169 (2)	25.1936(2)
b (Å)	4.2374(2)	3.196(1)
c (Å)	20.3873(1)	18.530(1)
α (º)	90	90
β (º)	93.43 (2)	101.36(2)
γ (º)	90	90
V (Å^3)	3245.27 (4)	3347.31(3)
Z	4	4
μ	1.07	1.16
F(000)	1032	971
Theta range for data collection (º)	2.3-22.6	2.1-24.7
Index ranges	$-14 \le h \ge 14$; $-5 \le k \ge 5$; $-22 \le l \ge 23$	$-10 \le h \ge 10$; $-13 \le k \ge 12$; $-18 \le l \ge 19$
Reflection collected	8347	15361
Independent reflection	1759	3371
R (int)	0.0710	0.0814
Data/Parameters	1759/170	3371/293
Final R indices [I>2σ (I)]	0.0652	0.0714
R indices (all data)	0.0971	0.1025
Largest diff. peak and hole (e.A^{-3})	0.55	0.84
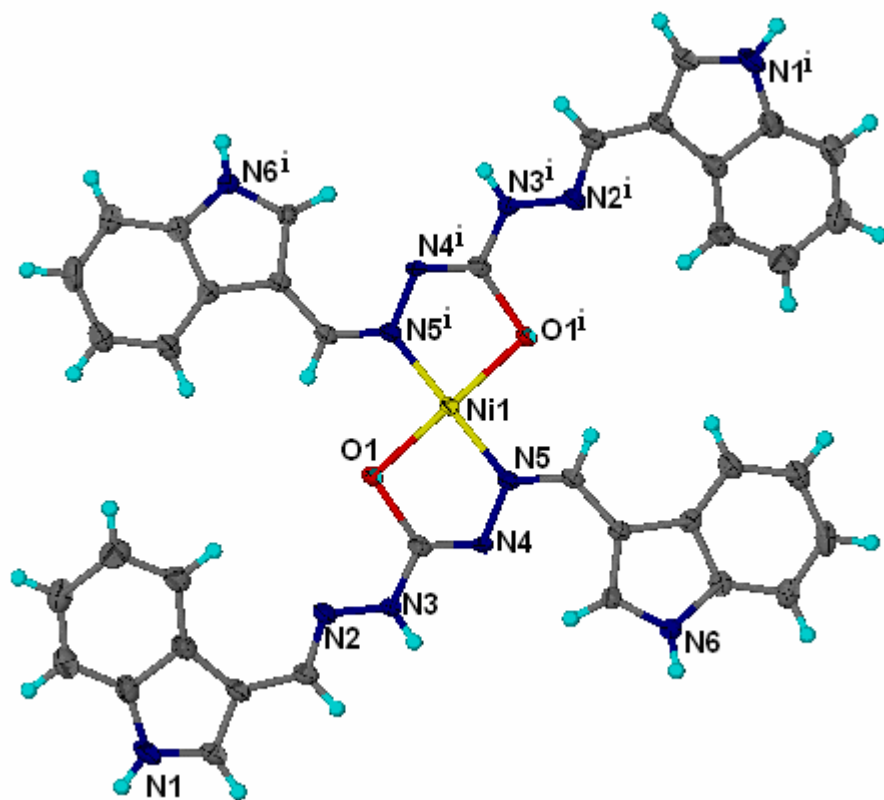
Figure 4.34: Thermal ellipsoid of *trans*-Ni(II) complexes. The atoms were labeled except for the carbon and hydrogen atoms. All atoms were refined anisotropically except for hydrogen.

Table 4.24: Selected geometric parameters (Å, °)

Distances:			
Ni1-O1	1.951(1)	Ni1-N5	2.016(2)
Angles:			
O1-Ni1-N5	83.68(2)	O1^i-Ni1-N5	94.26(2)
O1-Ni1-O1^i	180.0(1)	N5-Ni1-N5^i	175.5(1)

The Cu(II) complex which represent in the Figure 4.35 show that the crystal also exists as a distorted square-planar. This crystal adopted a monoclinic system with C2/c space group with β is 101.36°. This space group then allowed the Cu(II) to lie down on the special position of the structure. The negative charge of the monoanionic ligand is

localized over the (1*H*-Indole-3-carbaldehyde)carbohydrazone and the C-O bond distance is consistent with increased single bond character, while the imine C-N distances and both thioamide C-N distances indicate consider double bond character. Since the Cu(II) and Ni(II) complexes were isostructure, then the characteristics of the Cu(II) complex were similar to the Ni(II) complex that discussed before. Some of the important distances and angles were stated in the Table 4.25.

Table 4.25: Selected geometric parameters (Á, º)

Distances:			
Cu1-O1	1.951(1)	Cu1-N2	2.016(2)
Angles:			
O1-Cu1-N2	83.68(2)	O2 -Cu-N8	94.26(2)
O1-Cu1-O2	180.0(1)	N2-Cu1-N8	178.5(1)
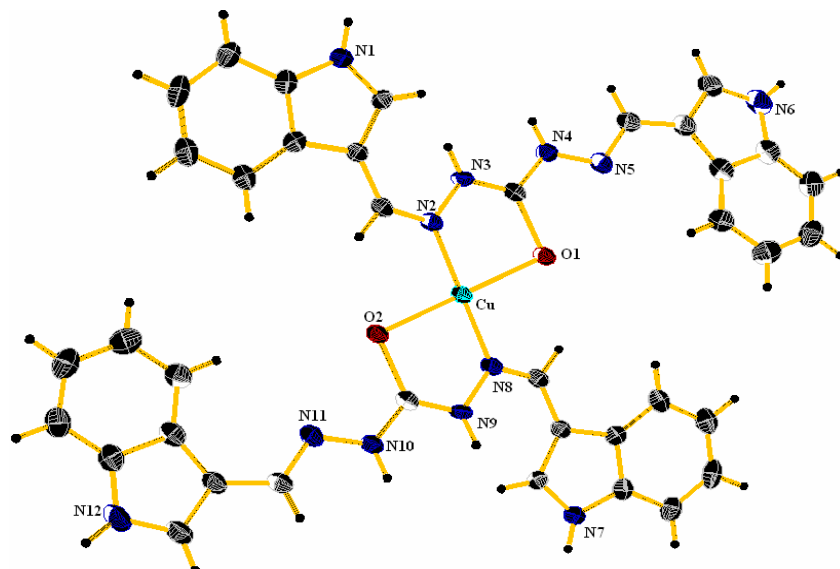
Figure 4.35: Thermal ellipsoid diagram of *trans*-Cu(II) complex. The atoms were 50% probability displacement and hydrogen atoms were refined isotropically.

Thus, from x-ray data, it suggested the following structural formula of metal complexes:
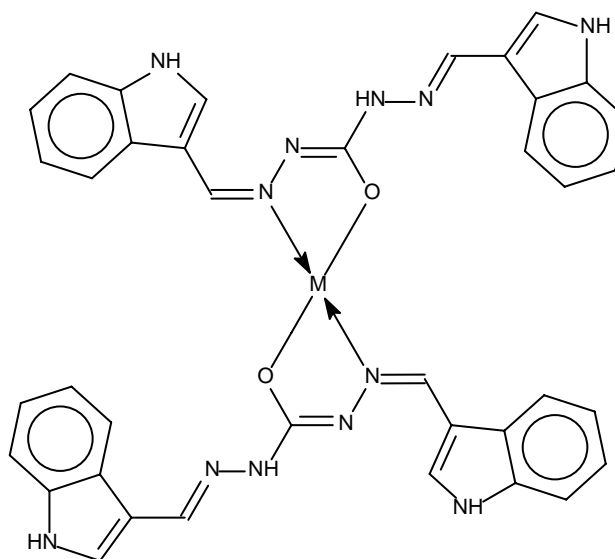
which M can be nickel(Ni), copper(Cu), zinc(Zn) or cadmium(Cd). All metal complexes form four coordinates with Ni(II) and Cu(II) exhibited as square planar geometry and Zn(II) and Cd(II) existed as tetrahedral geometry.

4.4 Toxicology Study

Toxicology study is mandatory for the newly produced drugs in order to establish it is safely. Toxicity is defined as any harmful effect of a chemical or a drug on a target organism. The purpose of toxicity study is to observe any toxicity profile that may occur following exposure to the tested substance for a certain period. No further study using higher dose level is required if no mortality observed at this dose level.

The results for acute toxicity for *Sprague-Dawley* rats are summarized in Table 4.26. This study has shown that acute oral toxicity studies in male and female rats documented no deaths at low and high dosages.

Table 4.26: The observations data for toxicology study of the ligands

	High Dose (5g/kg)				Low Dose (2g/kg)			
	10min	30min	3h	24h	10min	30min	3h	24h
Male Found Death	0	0	0	0	0	0	0	0
Found Ataxia	0	0	0	0	0	0	0	0
Female Found Death	0	0	0	0	0	0	0	0
Found Ataxia	0	0	0	0	0	0	0	0

The toxicology study has been done for all ligands, bis(1*H*-Indole-3-carbaldehyde)thiocarbohydrazone, 1*H*-Indole-3-carbaldehyde thiosemicarbazone and bis(1*H*-Indole-3-carbaldehyde)carbohydrazone. The rats that were fed with these three Schiff bases ligands showed same characters; no signs of discomfort, no unusual

115

changes in behavior or in locomotor activity, no ataxia and no sign of intoxication during 5 hour periods of observation on the rats through the experiments.

These observations then are similar to those for the control group. The control group was treated with only 10% Tween 20 which was used as the vehicle for the test compounds. This study then suggested that all Schiff bases synthesized in this work are nontoxic in rats following oral administration.

4.5 Antiulcerogenic activity

The series of Schiff base ligands and their metal complexes were tested for antiulcerogenic properties on *Sprague Dawley* rats to observe their ability to protect the gastric mucosa against injuries caused by the necrotizing agent, ethanol. The lesions were characterized by multiple-hemorrhage red bands of different sizes along the long axis of the glandular stomach. The control group treated orally with ethanol clearly produced the expected characteristic zone of necrotizing mucosal lesions.

It has been reported that the gastric mucosal lesions by necrotizing agents, such as ethanol involves the depression of gastric defensive mechanisms (Kinoshita et al., 1995). According to oral ethanol induce administration, the reduction in flow of blood contributing the development of hemorrhage red bands and necrosis (Szabo,1987).

Table 4.27:
Gastroprotective effect of the Schiff base ligands and their metal complexes and cimetidine on ethanol induced gastric ulcer in rats

Pretreatment	Mucus Weight	pH	Ulcerative Lesion Index (mm^2) (Mean ± S.E.M)	Inhibition (%)
Control (Negative)	3.50	4.43	1510.26 ± 468.28	-
Cimetidine (Positive Control)	3.63	6.63	170.40 ± 25.17	89.50
Ind3Thio	1.66	5.32	218.75 ± 35.62	85.82
Ni$_{Ind3Thio}$	1.84	5.12	267.27 ± 42.14	82.35
Cu$_{Ind3Thio}$	2.14	4.72	202.34 ± 32.15	86.82
Zn$_{Ind3Thio}$	2.12	5.25	147.98 ± 45.18	90.20
Cd$_{Ind3Thio}$	1.98	5.28	75.5 ± 22.15	95.02
Ind3Thiosemi	1.83	5.52	203.85 ± 42.11	86.25
Ni$_{Ind3Thiosemi}$	2.38	4.32	226.53 ± 32.25	85.02
Cu$_{Ind3Thiosemi}$	1.85	5.16	202.65 ± 35.74	86.58
Zn$_{Ind3Thiosemi}$	2.52	5.08	45.26 ± 15.12	98.26
Cd$_{Ind3Thiosemi}$	2.55	4.72	105.73 ± 25.64	93.48
Ind3Carbo	1.48	4.73	271.83 ± 45.27	82.51
Ni$_{Ind3Carbo}$	2.23	5.13	151. 63 ± 28.93	90.50
Cu$_{Ind3Carbo}$	1.74	4.86	120.18 ± 27.65	92.26
Zn$_{Ind3Carbo}$	1.82	4.62	60.41 ± 18.42	96.32
Cd$_{Ind3Carbo}$	2.56	4.84	70.97 ± 24.17	95.36

Data are reported as mean ± S.E.M of six rats per group.
The pre-treatment tests were done at dose 62.5 mg kg^{-1}.

Pre-treatment with Schiff base ligands and metal complexes at a dose of 62.5 mg/kg diminished the lesion index compared with the control group. The results showed that the ligands and metal complexes generally possess gastroprotective activity as evidenced by their significant inhibition in the formation of ulcer induced by ethanol. For the positive control group, treatment with 50 mg/kg of cimetidine, presented a 89.50% reduction of lesion.

Among the three Schiff bases, the 1*H*-Indole-3-carbaldehyde thiosemicarbazone showed the highest property towards peptic ulcer with 86.25% reduction of lesion compared to control value. It was followed by bis(1*H*-Indole-3-carbaldehyde)thiocarbohydrazone and bis(1*H*-Indole-3-carbaldehyde)carbohydrazone with 85.82% and 82.51% reduction of lesion, respectively. Interestingly, the Schiff bases with sulphur-containing compounds have shown higher ability to prevent mucosal lesion rather than oxygen-containing compound. This finding was not surprising because the recent drugs that available in market; cimetidine and omeprazole are also sulphur-containing drugs. The sulphur-containing compounds have been proven before to have anticancer properties by detoxification, which helps the liver to breakdown carcinogenic substances (Oommen et al., 2004; Sawant et al., 2006).

The pH value of acid in the stomach for 1*H*-Indole-3-carbaldehyde thiosemicarbazone suggested that the compound inhibits the production of acid in the stomach. Although the compounds' mechanism of action does not explain well, the pH value has indicated that this type of compound probably reacted as H_2-receptor antagonist; block the action of histamine on parietal cells in stomach, which decreasing

the production of acid in the stomach. The high quantity of acid in stomach probably can irritate the lining and cause a sore or peptic ulcer.

In the pre-treatment with metal complexes, the percentage of inhibition indicated that the complexes also prevent gastric ulceration in the stomach. In this study, we have found that the Zn(II) and Cd(II) complexes demonstrate excellent inhibition against gastric ulcer with the highest is $Zn_{Ind3Thiosemi}$ with 98.26% reduction of lesion in stomach followed by $Zn_{Ind3Carbo}$ and $Cd_{Ind3Carbo}$ with 96.32% and 95.36%, respectively. Most of the metal complexes show significant reduction in gastric lesion rather than their ligands indicating that complexation enhance the property of the compounds.

The higher amount of mucus in the stomach that was pretreated with metal complexes suggests that the metal complexes may stimulate gastric cells to secrete some products acting as a shield for the mucosa; which the shield is so effective that it prevents damage by strong chemicals (Robert et al., 1979). Besides, the mucus also can provide a viscous physical barrier between the damaging agents and the surface epithelium. These results then suggest that a possible cytoprotective mechanism in this study may involve the production of prostaglandins and/or mucus (Barros et al., 2008).

The results of this study show that the synthesized Schiff bases and metal complexes display antiulcer activity. Although the actual mechanism of this study were not explained deeply, the value of stomach juice and higher amount of mucus in stomachs of the rats pretreated with the active compounds suggest that the compounds are able to induce an adaptive cytoprotection mechanism which prevents formation of gastric ulcer. Further studies are needed to investigate the mechanisms that involved in gastric cytoprotection provided by the active compounds.
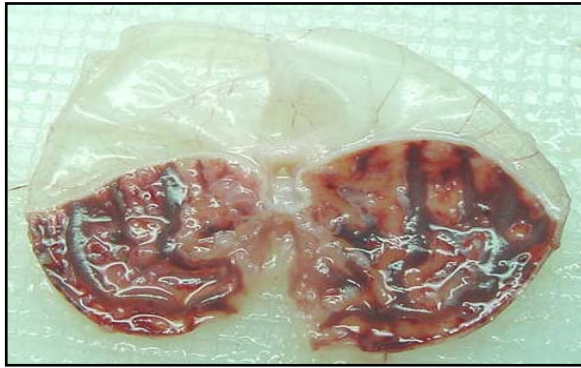
Figure 4.36: Macroscopic appearance of the gastric mucosa in a rat pre-treated with only 10% Tween 20 (negative control). Severe macroscopic hemorrhagic necroses of the gastric mucosa are visible following induction by absolute alcohol.

Figure 4.37: Macroscopic appearance of the gastric mucosa in a rat pre-treated with cimetidine (50 mg kg^{-1}). Compared to the negative control, the gastric mucosal injuries are visibly much milder following induction by absolute alcohol.

Figure 4.38: Macroscopic appearance of the gastric mucosa in a rat pre-treated with $Zn_{Ind3Thiosemi.}$ (62.5 mg kg^{-1}). Compared to the negative control, the gastric mucosal injuries are visibly much milder following induction by absolute alcohol.

Edema with leucocytes infiltration of submucosa

Severe destruction of gastric mucosa
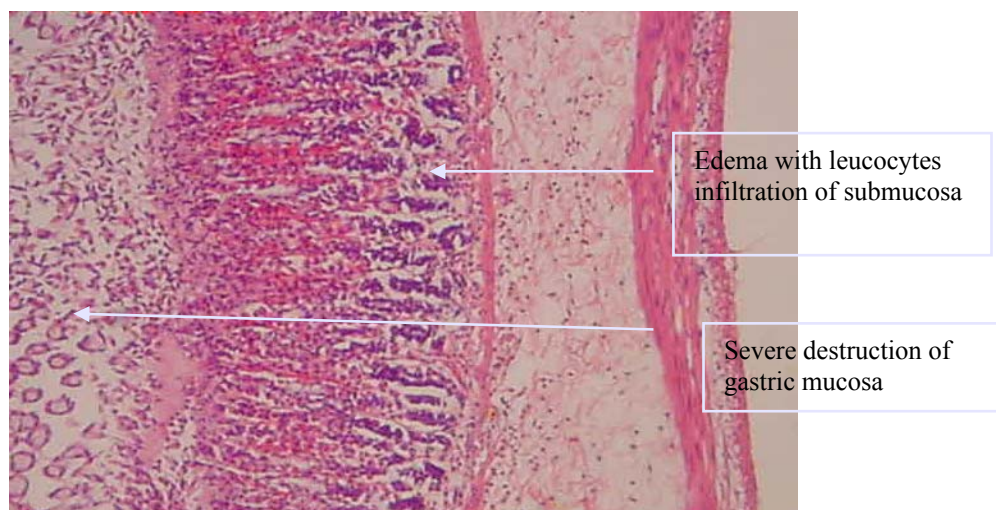
Figure 4.39: Histological section of the gastric mucosa in a rat pre-treated with only 10% Tween 20 (negative control). There is severe disruption of the surface epithelium, deep penetration of necrotic lesions into mucosa and edema of the submucosal layer with leukocyte infiltration of ulcerative tissues (H&E stain, 40x).

Mild disruption of gastric mucosa
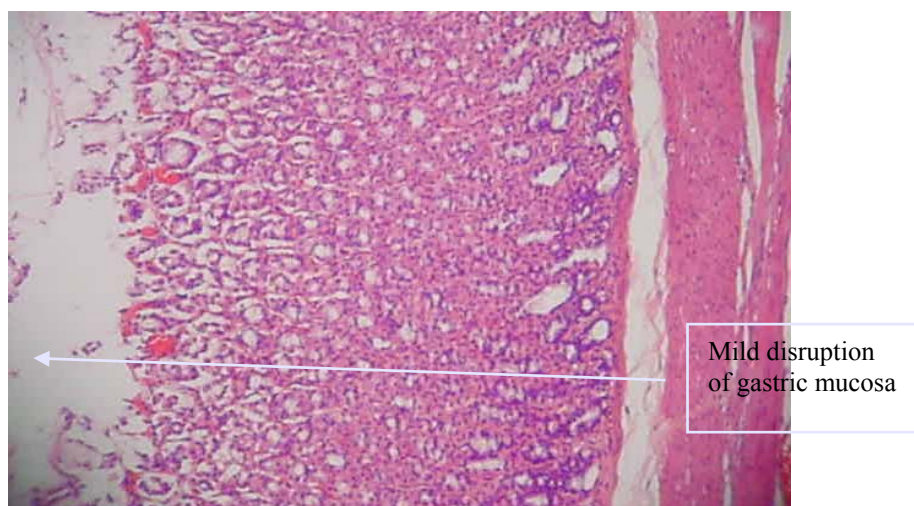
Figure 4.40: Histological section of the gastric mucosa in a rat pre-treated with $Zn_{Ind3Thiosemi.}$ (62.5 mg kg^{-1}). Compared to the negative control, the disruption to the surface epithelium is very mild, and there is no submucosal edema and no leucocytes infiltration (H&E stain, 40x).

Conclusion

The formation of Schiff bases ligand derived from the indole-3-carboxaldehyde and thiocarbohydrazide was confirmed by presence of imino v(C=N) bands between range 1605-1610 cm^{-1}. The data was obtained from the IR study indicated that the bis(1*H*-Indole-3-carbaldehyde)thiocarbohydrazone displays as *thione-thiol* tautomerism in the solid state condition. In solution, data from ^{1}H and ^{13}C spectra showed that the ligand exhibited as *thione* tautomerism. For the metal complexes, the deprotonated ligand exhibited as *thiol* tautomerism as indicated by the longer distance between carbon and sulphur atoms. The magnetic susceptibility study showed that the Ni$_{Ind3Thio}$, Zn$_{Ind3Thio}$ and Cd$_{Ind3Thio}$ are diamagnetic compounds while Cu$_{Ind3Thio}$ is paramagnetic compound. Because of the indole group does not possess a suitable donor coordinating atom, we have suggested that the Schiff base usually acts as a bidentate ligand through one of the azomethine nitrogen and the sulphur atom for every metal(II) ions. The limitation of donor atoms in this Schiff base then may allow Zn(II) and Cd(II) complexes exhibit as monomer complexes; with bidentate Schiff base in tetrahedral geometry. The formulae for the metal complexes are [M(C$_{19}$H$_{15}$N$_6$S)$_2$], with M assigned to Ni(II), Cu(II), Zn(II) and Cd(II). Recrystallization of Ni(II) complexes in DMSO is in good agreement with the proposed formula. Thus, the Ni(II) and Cu(II) complexes exhibit as square planar geometry while the Zn(II) and Cd(II) exhibit tetrahedral geometry.

The 1*H*-Indole-3-carbaxaldehyde thiosemicarbazone exhibited in the mixture of *thione* and *thiol* forms in solid state but *thione* tautomer is the major component. This

conclusion is supported by the crystal structure that showed the distance between C=S to be about 1.536 Å; the ideal value for the short interaction between carbon and sulphur. However, in solution, the Schiff base ligand exists in zwitterionic form. In the solid state of the complexes, the deprotonated Schiff base ligand exhibited as *thiol* form which was confirmed by the longer distance of C-S compared to C=S. The crystal structure of the Ni(II) and Cu(II) complexes reveal that the complexes exhibit as a square planar geometry with *N,S-* coordination. Then, we suggested that the formula for the metal complexes is $[M(C_{10}H_9N_4S)_2]$ with M is attributed to Ni(II), Cu(II), Zn(II) and Cd(II).

Bis(1*H*-Indole-3-carbaldehyde)carbohydrazone in the solid state, exists as *ketoic* and *enolic* tautomers. X-ray crystallographic data for the Schiff base ligand indicated that the *keto* tautomer is the major component in this tautomerism structure. Based on the data from ^{1}H and ^{13}C NMR spectra, the ligand exists as *keto* tautomer in solution. For metal complexes, data from IR spectra suggested that the deprotonated Schiff base ligand may chelate with the metal(II) ions through azomethine nitrogen and oxygen atom. Thus the ligand exists as an *enolic* tautomer with the negative charge of the monoanionic ligand delocalized over the ligand. The crystal structure of some metal complexes showed that the complexes existed as monomeric structure that coordinated with two monoanionic ligands in purpose to balance the charges. The limitation of donor atoms for coordinate and also steric effect caused by two azomethine groups in this Schiff base allowed the ligand to behave as bidentate with *N,O-* chelation. Thus the complexes possessed a $[M(C_{19}H_{15}N_6O)_2]$ formula with M represented Ni(II), Cu(II), Zn(II) and Cd(II).

The antiulcerogenic study showed that synthesized Schiff bases and their metal complexes possessed significant inhibition against ulceration compared with the standard drug. Moreover, we also found that most of the metal complexes are more active than their respective ligands indicating that the complexation enhances the activity of the ligand. Futhermore, the Zn(II) and Cd(II) have shown significantly higher potency compared to other metal complexes suggesting that the Zn(II) and Cd(II) complexes are biologically active form of the carbazone derivatives. We suggest that the metal complexes which exist in tetrahedral form can inhibit ulcers better than complexes that exist in square planar form. However, the reason of this result is not really clear because of the mechanism of Zn(II) and Cd(II) in ulcerogenic activity has not been investigated yet and is limited by the scope of our research that only focused on the ability of the compounds in prevent ethanol-induced gastric lesion in the *Sprague-Dawley* rats.

The present study suggests that the synthesized Schiff base and their metal complexes are new alternatives in antiulcerogenic activities. This was strengthened by discovery that the Schiff base ligands are non-toxic compounds. Thus, these molecules can be very useful for further study in medical research.

Figure I.1: IR spectra of Ni$_{Ind3Thio}$
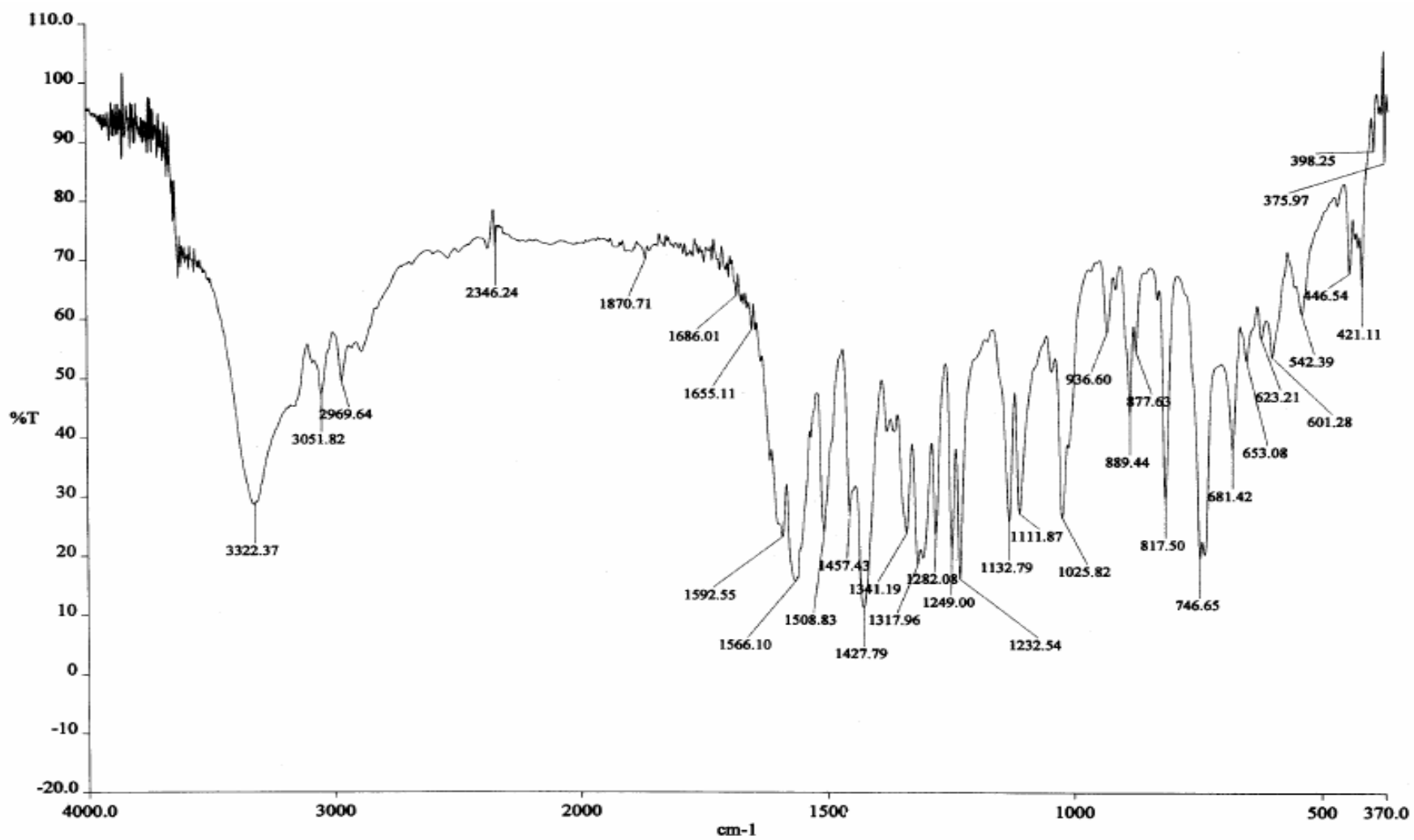
Figure I.2: IR spectra of Zn$_{Ind3Thio}$
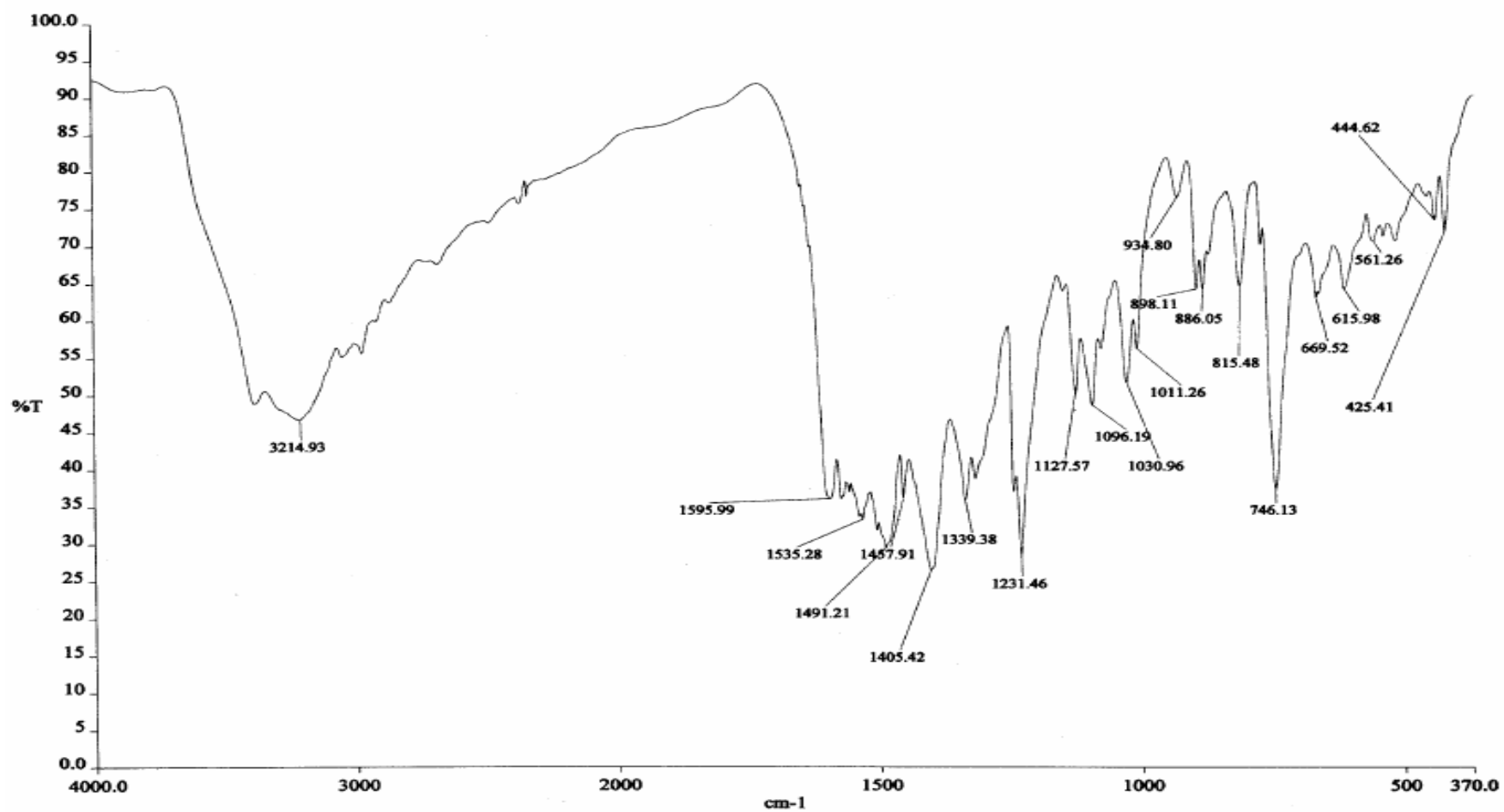
Figure I.3: IR spectra of Cd$_{Ind3Thio}$
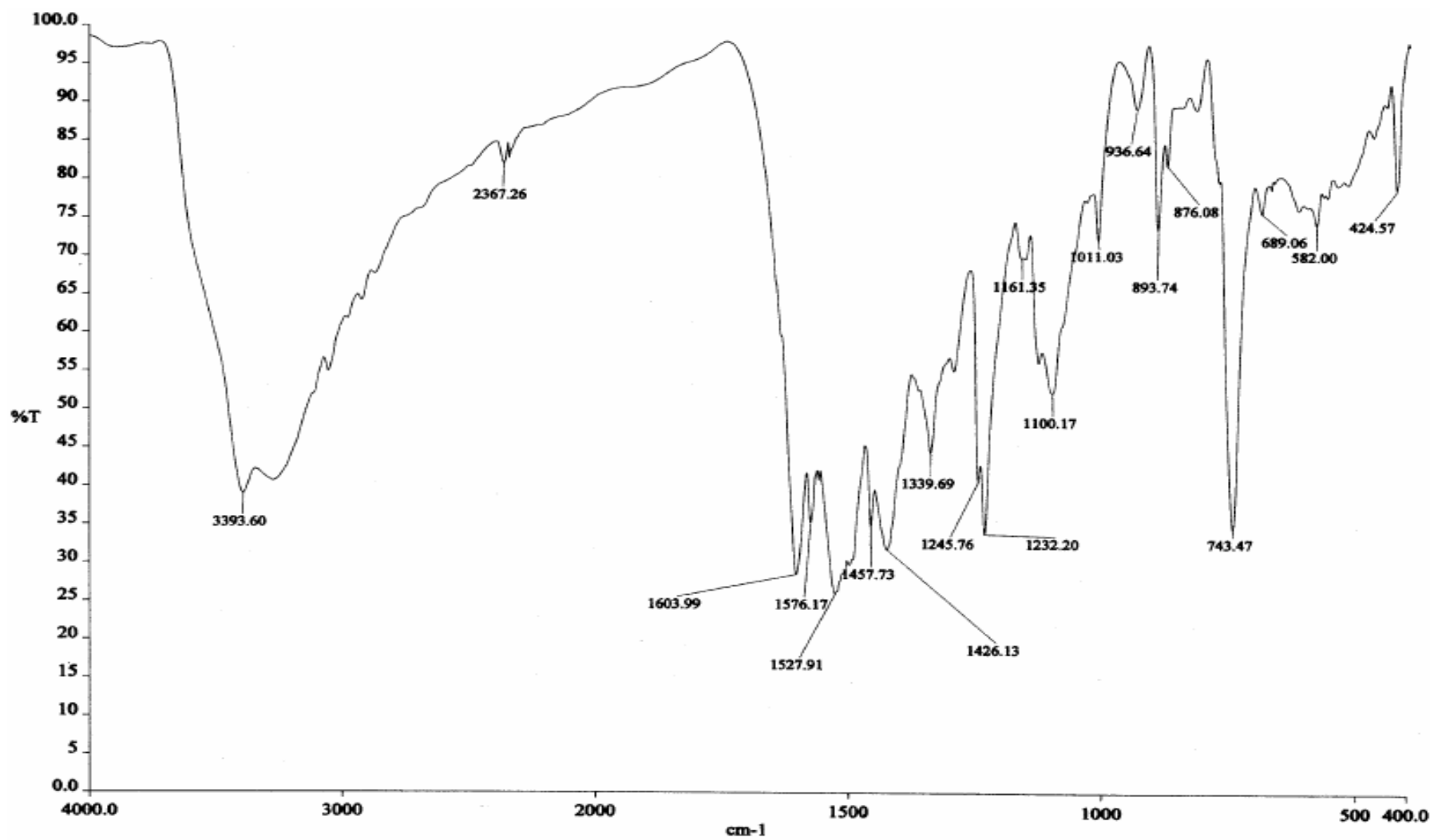
Figure I.4: IR spectra for Cu$_{Ind3Thiosemi}$
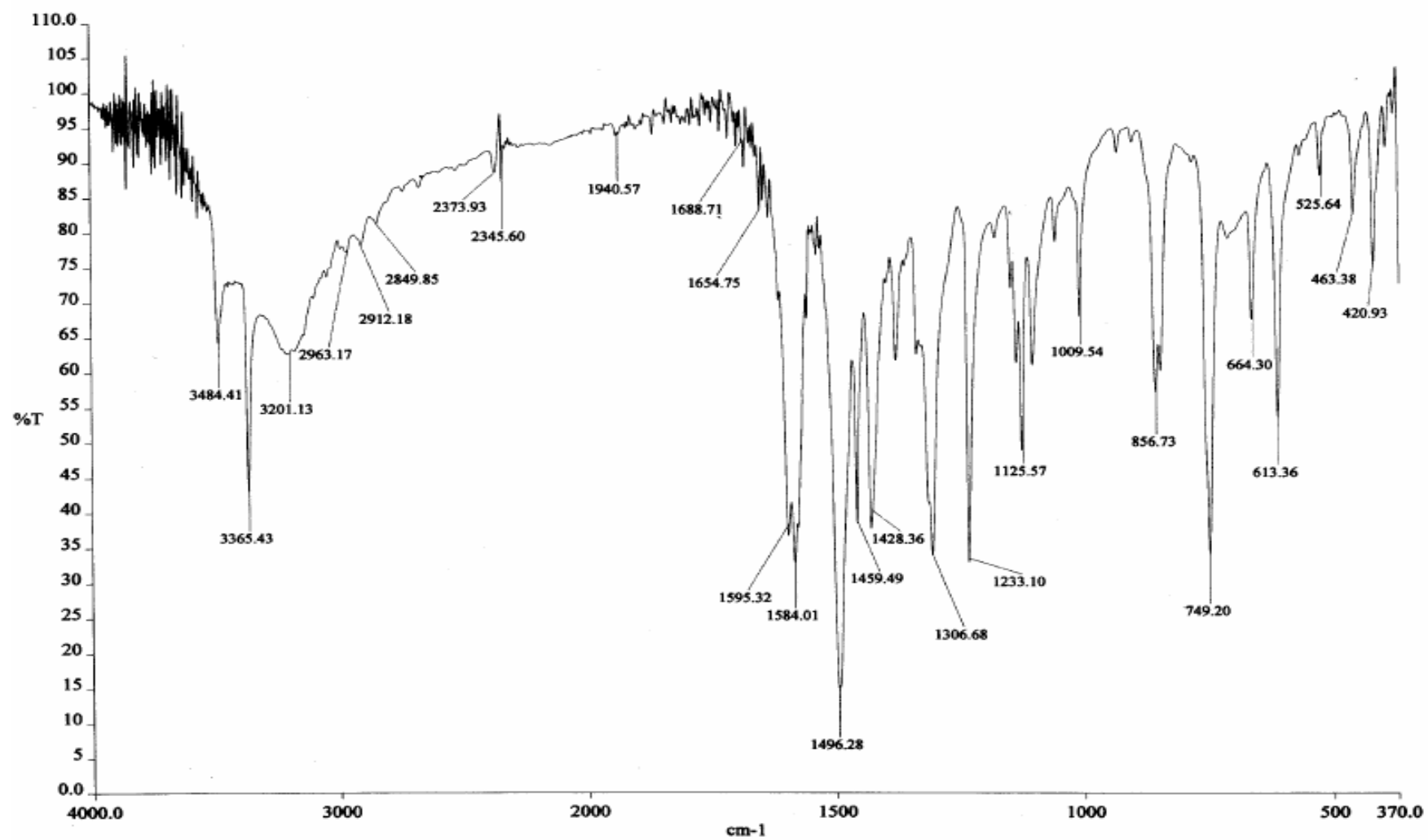
Figure I.5: IR spectra for Zn$_{Ind3Thiosemi}$
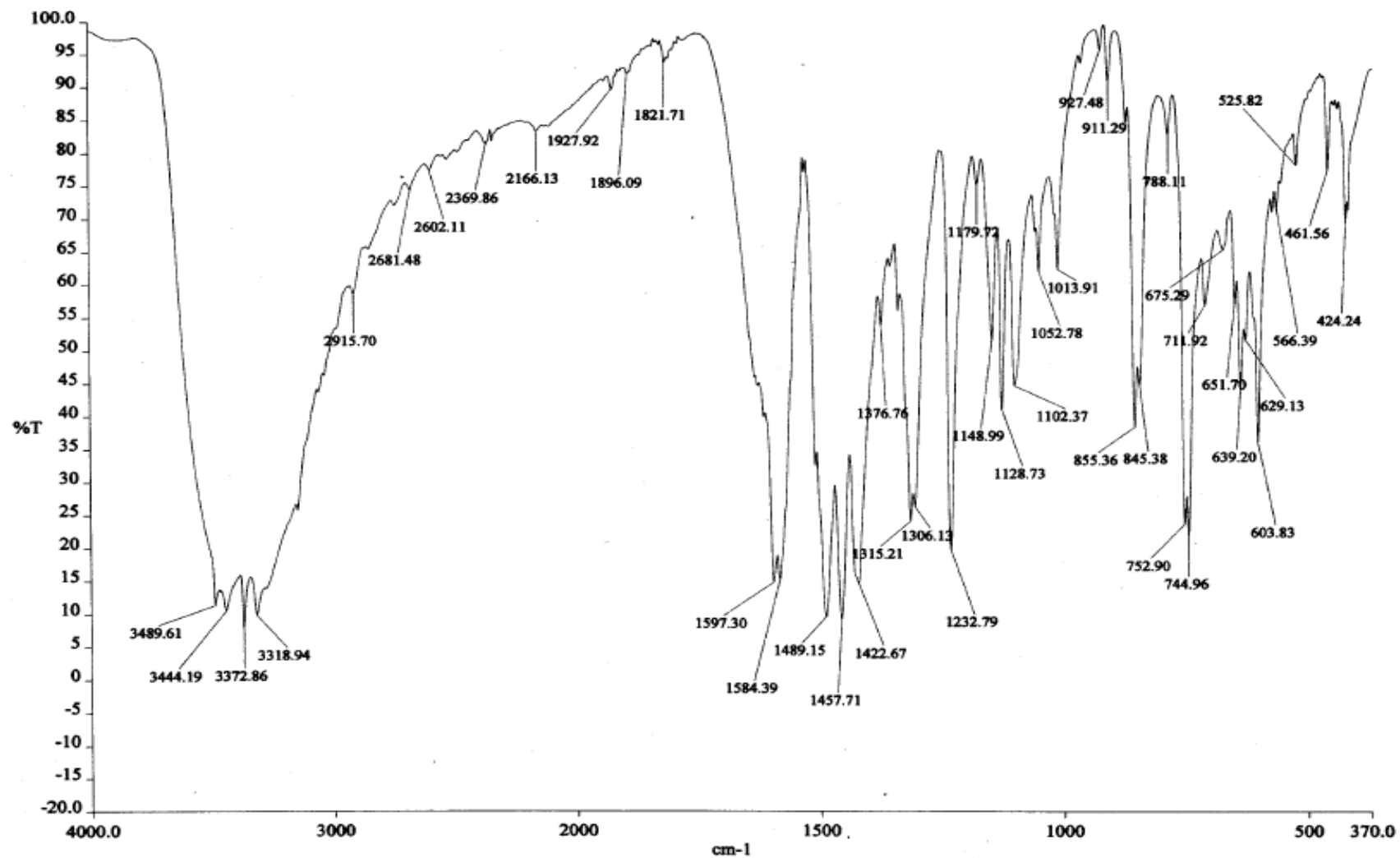
Figure I.6: IR spectra for Cd_Ind3Thiosemi
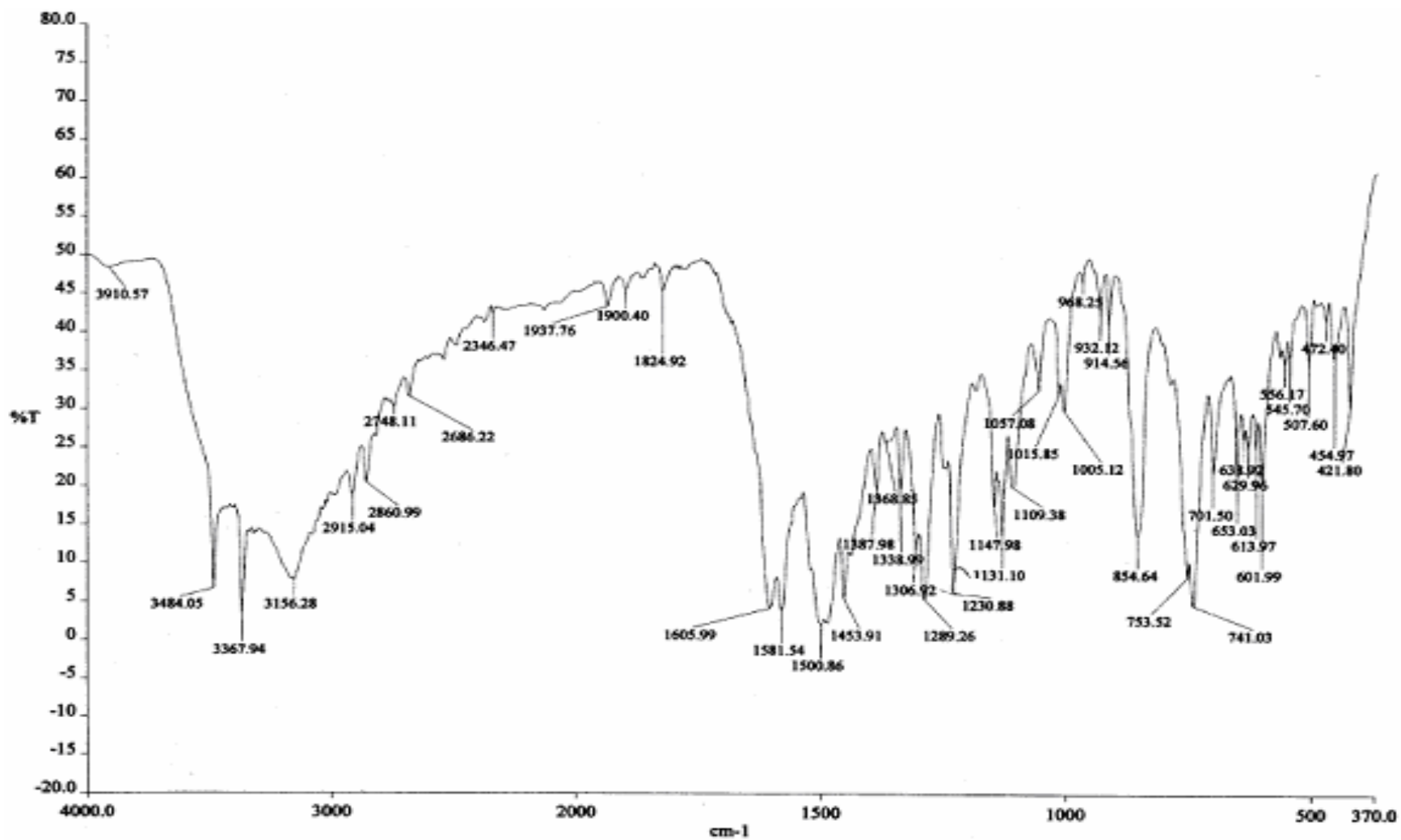
Figure I.7: IR spectra for Ni$_{\text{Ind3Carbo}}$
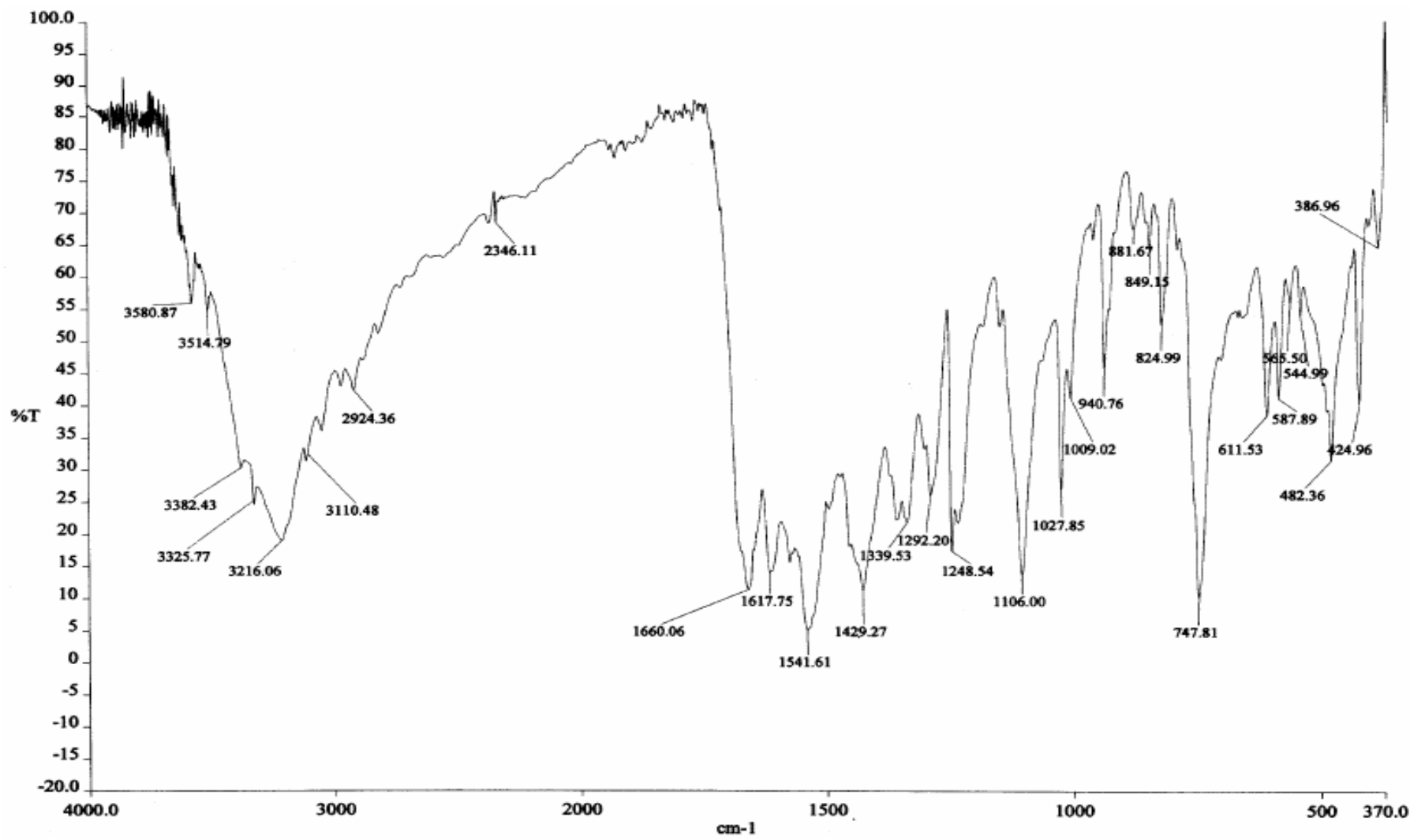
Figure I.8: IR spectra for Cu$_{Ind3Carbo}$
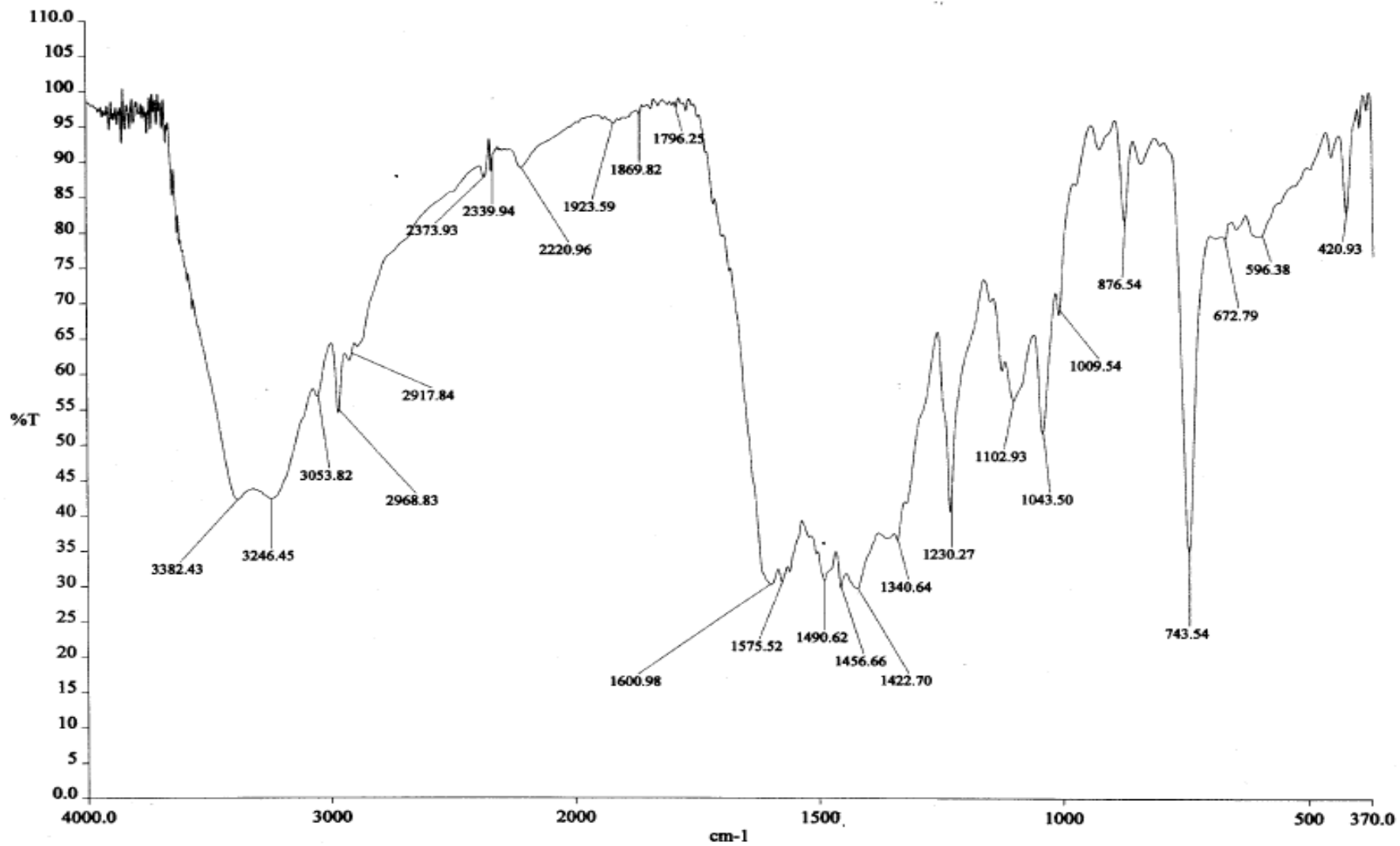
Figure I.9: IR spectra for $Zn_{Ind3Carbo}$
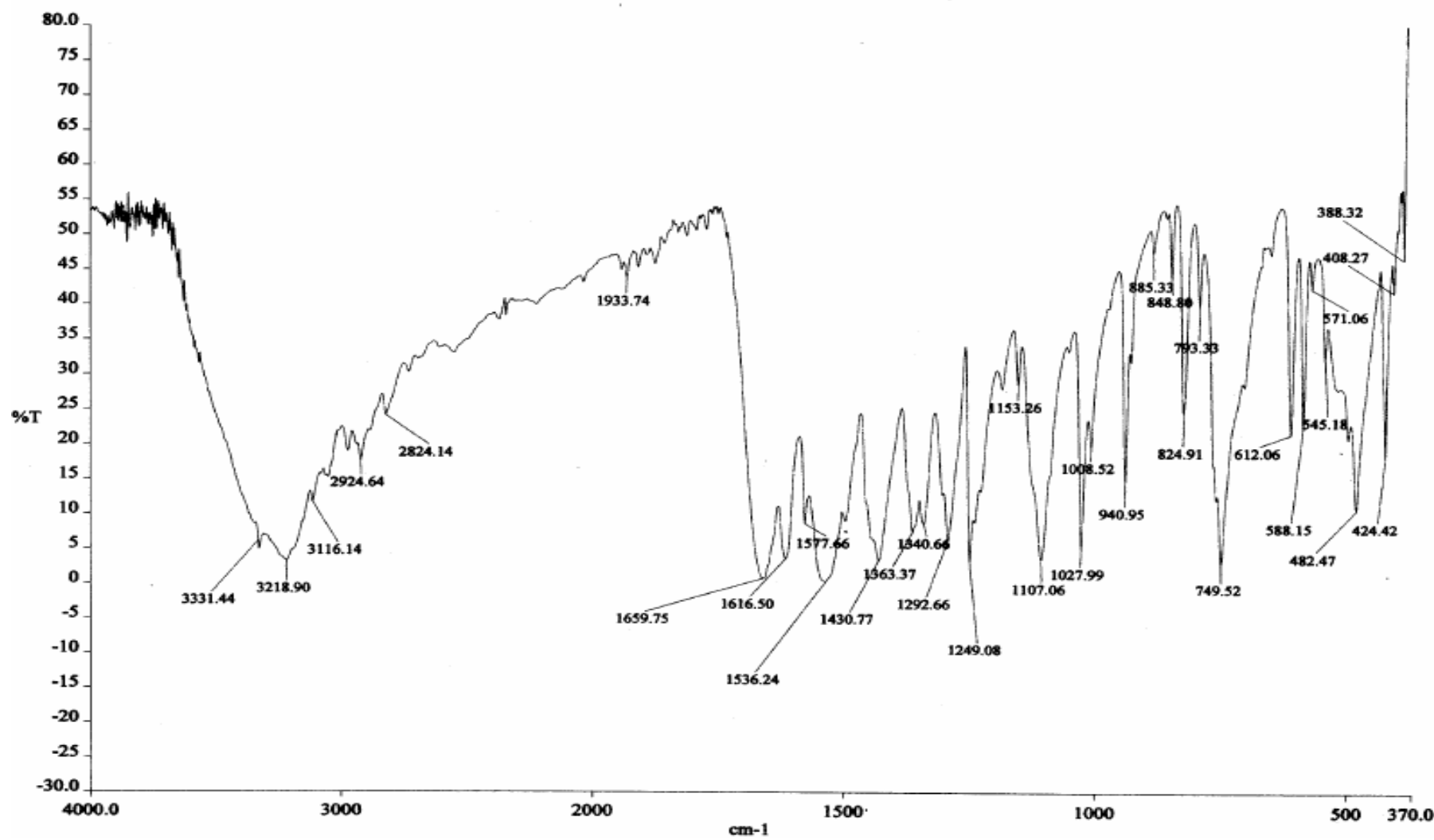
Figure E.1: Uv-vis spectrum of Ni$_{Ind3Thio}$
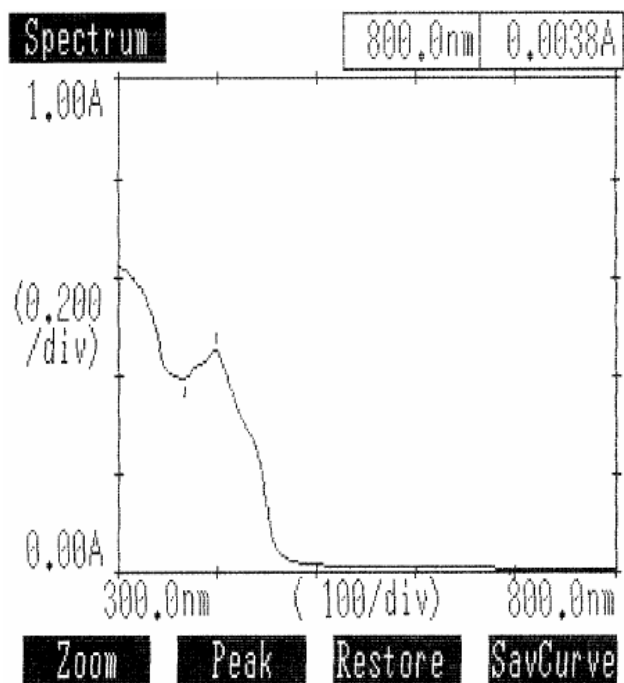
Figure E.2: Uv-vis spectrum of Zn$_{Ind3Thio}$
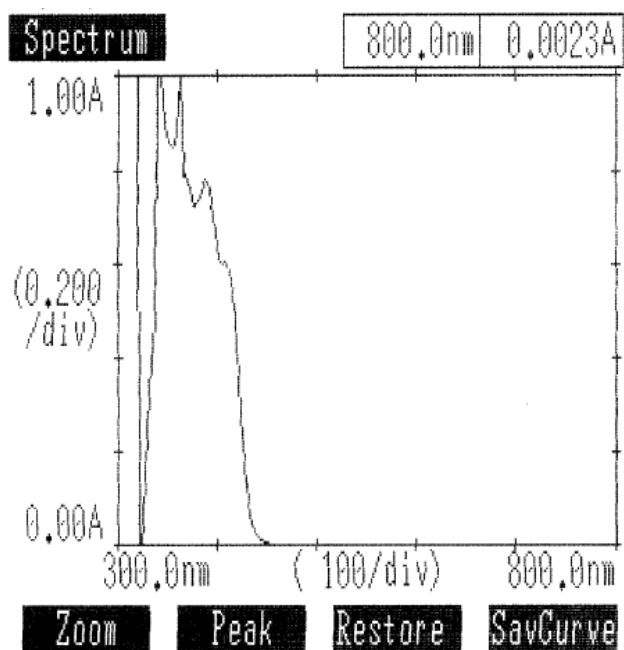
Figure E.3: Uv-vis spectrum of Cd$_{Ind3Thio}$
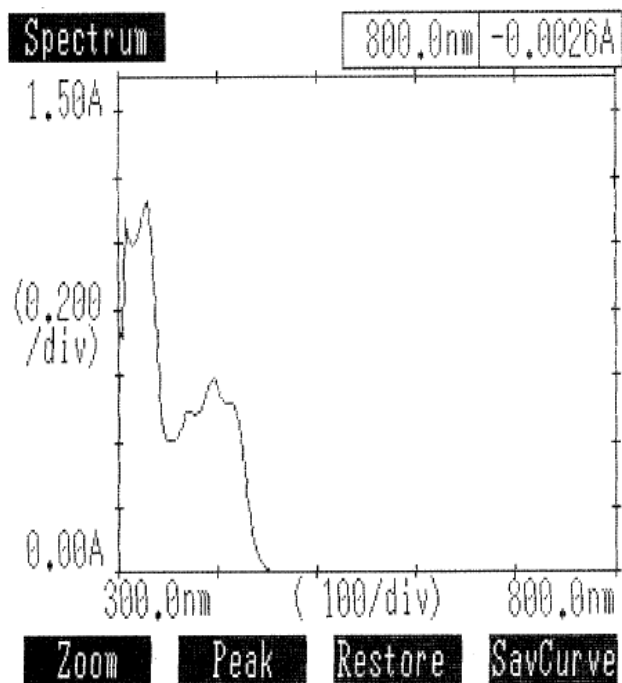
Figure E.4: Uv-vis spectrum of Cu$_{Ind3Thiosemi}$
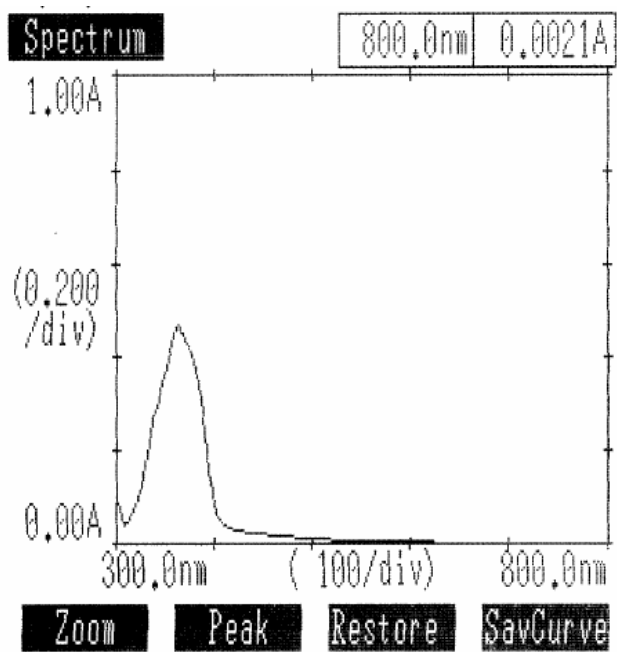
Figure E.5: Uv-vis spectrum of $Zn_{Ind3Thiosemi}$
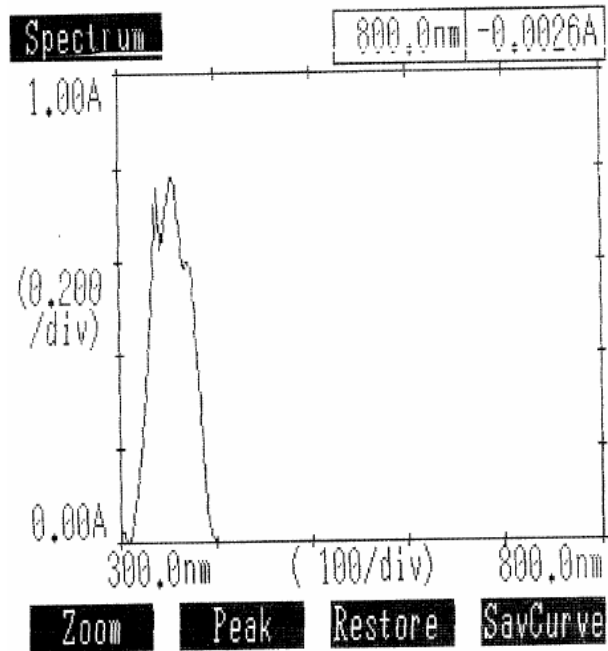
Figure E.6: Uv-vis spectrum of $Cd_{Ind3Thiosemi}$
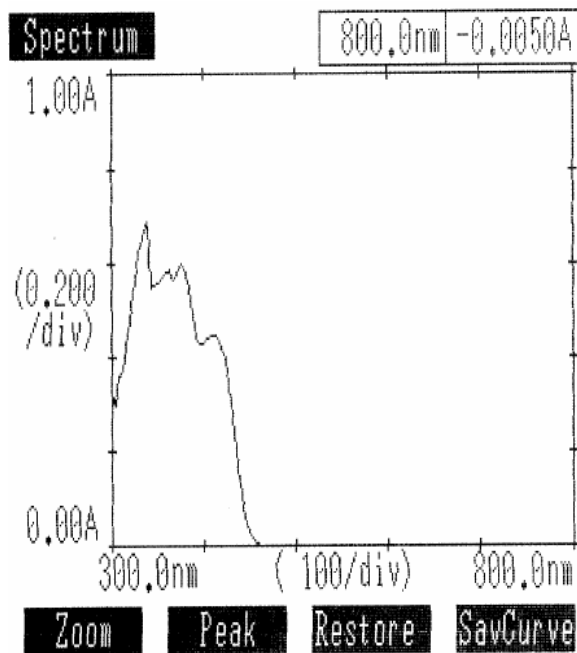
Figure E.7: Uv-vis spectrum of Cu$_{Ind3Carbo}$
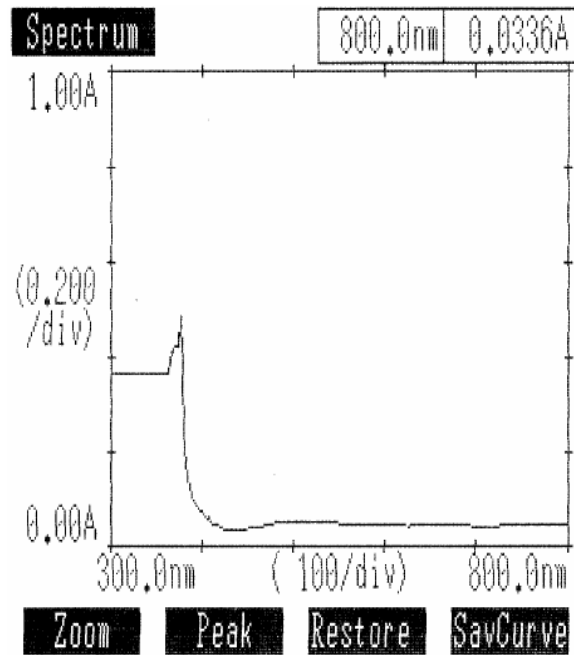
Figure E.8: Uv-vis spectrum of Zn$_{Ind3Carbo}$
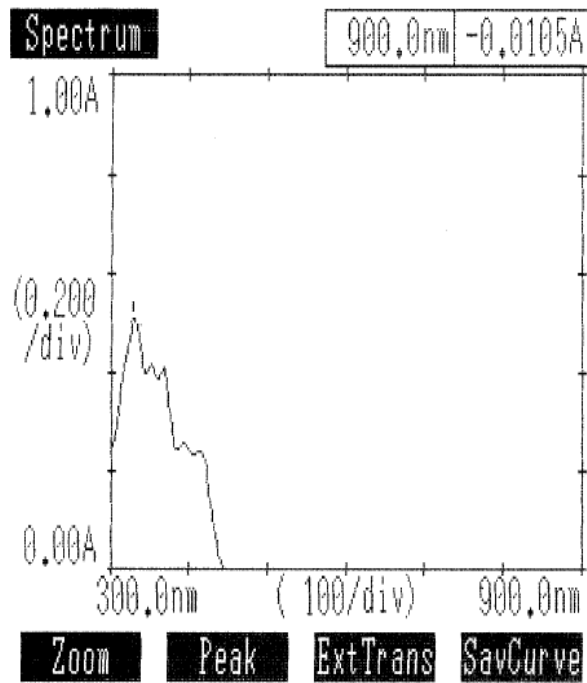
Figure E.9: Uv-vis spectrum of Cd$_{Ind3Carbo}$
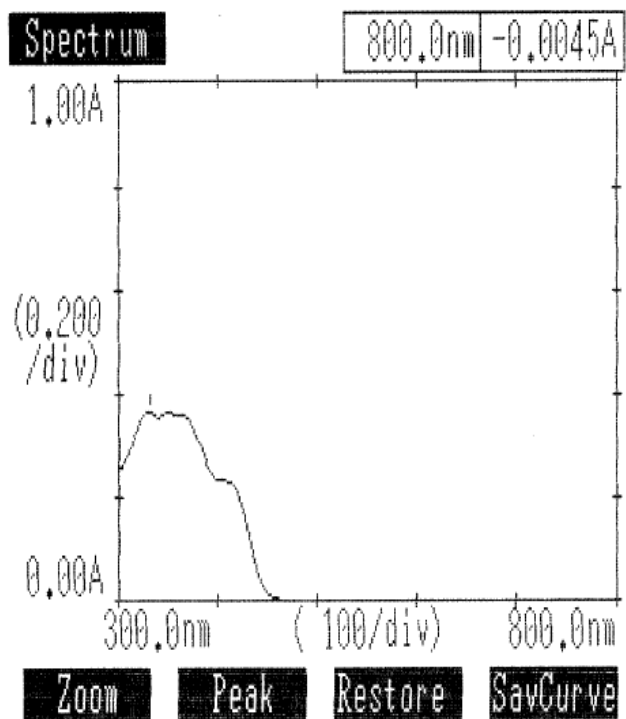
References

Afrasiabi Z., Sinn E., Lin W., Ma Y., Champana C. and Padhye S., *Journal of Inorganic Biochemistry*, **99** (2005) 1526-1531.

Ahmed I. T., *Spectrochimica Acta Part A: Molecular and Biomolecular Spectroscopy*, **63** (2006) 416-422.

Akthar M. S., Akthar A. H. and Khan M. A., *Journal of Pharmacognosy*, **30** (1992) 97-104.

Ali M. A., Mirza, A. H., Voo, C. W., Tan, A. L. and Bernhardt, P. V., *Polyhedron*, **22** (2003) 3433-3438.

Ali M. A., Mirza, A. H., Tan, A. L., Wei, L. K. and Bernhardt, P. V., *Polyhedron*, **23** (2004) 2037-2043.

Amirnasr M., Amir H.M., Alireza G., Saeed D. and Hamid R. B. *Polyhedron*, **21** (2002) 2733-2742.

Asgedom G., Sreedhara, A. and Rao, C. P., *Polyhedron*, **14** (1995) 1873-1879.

Bandhopadhyay U., Biswas, K., Chatterjee, R., Kumar Ganguly, I. C. C., Bhattarcharya, K. and Banerjee, R., *Life Science*, **71** (2002) 2845-2865.

Barros M. P., Lemos M., Maistro E. L., Leite M. F., Barreto J. P., Bastos J.K. and Andrade S. F., *Journal of Ethnopharmacology*, **120** (2008) 372-377.

Batista L. M., de Almeida, A. B., de Pietro-Magri, L., Toma, W., Calvo, T. R., Vilegas, W. and Souza-Brito, A. R., *Biological and Pharmacological Bulletin*, **27** (2004) 328-332.

Bauer D.J., *Annals of New York Academy of Science,* **130** (1965) 110–117.

Bauer D.J., Dumbell K.R., Fox-Hulme P. and Sadler P.W., *Bulletin World Health Organ* **26** (1962) 727–732.

Bauer D.J., L. St. Vincent, C.H. Kempe and A.W. Downie, *Lancet,* **II** (1963) 494–496.

Bauer D.J., St. Vincent L., Kempe C.H., Young P.A. and Downie A.W., *American Journal of Epidemiol.* **90** (1969) 130–145.

Betten A., Dahlgren, C., Hermoddson, S. and Hellstrand, K., *Journal of Leukocyte Biology*, **70(1)** (2001) 65-72.

Brady J. E and Humiston G. E., *General Chemistry*, 1986. Wiley-Interscience, New York. Pg 784-788.

Borrelli F. and Izzo, A. A., *Phytotherapy Research*, **14** (2000) 581-591.

Boutina J. A., Audinot, V., Ferry G. and Delagrange, P., *Trends in Pharmacological Sciences*, **26 (8)** (2005) 412-419.

Campbell M.J., *Coordination Chemistry Review*, **15** (1975) 279.

Carlin R. L., *Magnetochemistry*, 1986. Springer Verlag, Berlin. Page 2.

Chan F. K. and Leung W. K., *Lancet*, **360** (2002) 933-941

Chandra S., Jain D. and Sharma A. K., *Spectrochimica Acta Part A: Molecular and Biomolecular Spectroscopy,* **14** (2009) 851-857.

Chien L. K., Ruey C. W., Jow L. H., Chuan P. L., Yi F. L., Cheng Y. W. and Hung C. C., *Journal of Nanotechnology*, **19** (2008) 393-401.

Chohan Z. H., Pervez H., Khalid K. M. and Supuran C. T., *Journal of Enzyme Inhibition and Medicinal Chemistry*, **20** (2005) 81-89.

Das D. and Banerjee R. K., *Molecular and Cellular Biochemistry*, **125** (1993) 115-125.

Demertzi D.K., Yadav P. N., Wiecek J., Skoulika S., Varadinova T. and Demertzis M.A., *Journal of Inorganic Biochemistry*, **100** (2006) 1558-1567.

Diana D., Anthony W.A., Matthias Z., Laurence K.T., Dushyanti H., Mihail D.R. and Allen D.H., *European Journal of Inorganic Chemistry,* 16 (2008) 2530-2436.

Domagk G., Behnisch R., Mietsch F. and Schmidt H., *Naturwissenschaften,* **10** (1946) 315.

Earnshaw A. A., *Introduction to Magnetochemistry*, 1968. London Academic Press, London. Page 5.

El-Abhar H. S., Abdallah D. M. and Saleh S., *Journal of Ethnopharmacology*, **84** (2003) 251-258.

Ettling C., *Annalen der Chemie und Pharmacie*, **35** (1840) 241.

Fukutomi J., Fukuda, A., Fukuda, S., Hara, M., Terada, A. and Minoru, Y., *Life Sciences*, **80** (3) 254-257.

Gaber M., Shar S. A., *Scientific Journal of King Faisal University (Basic and Applied Sciences)*, **5 (2)** (2004) 181-195.

Gili P., Martin Z. P., Palacios M. S., Rodriguez M.L., Ruiz-Perez C. and Rodriguez-Romero F. V., *Inorganica Chimica Acta*, **176** (1990) 261-265.

Gili P., Palacios M. S., Martin R. M.G. and Martin Z. P., *Polyhedron*, **11(17)** (1992) 2171-2178.

Golcu A., Tumer M., Demirelli H. and Wheatley R. A., *Inorganica Chimica Acta.,* **358** (2005) 1785-1797.

Gracioso J., Vilegas, W., Hiruma-Lima, C., and Souza-Brito, A. R., *Biological and Pharmacological Bulletin*, **25** (2002) 487-491.

Gup R. and Kirkan B., *Spectrochimica Acta Part A: Molecular and Biomolecular Spectroscopy,* 64 (2006) 809-815.

Gupta K.C. and Sutar A.K., *Journal of Molecular Catalysis*, **272** (2007) 64-74.

Guth P. H., Paulsen G. and Nagatha H., *Gastroenterology*, **87** (1984) 1083-1090.

GÜzel A., Sakalar Y.B. and Su K., Unlu K., *Turkiye Klinikleri Journal of Ophtalmol*, **17** (2008) 252.

Hardeland R., Reiter R. J., Poeggeler B. and Tan D. X., *Neuroscience and Biobehavioral Reviews*, **17** (1993) 347-357.

Hussen A.A. and Azza A.A., *Journal of Coordination Chemistry*, **57** (2004) 973-987.

Iskander M. F., El-Sayed L., Salem N. M. H., Haase W., Linder H. J. and Foro S., *Polyhedron*, **23** (2004) 23-31.

James E.H, *Inorganic Chemistry: Principles of Structure and Reactivity, Third Edition,* 1983. Harper & Row Publishers, New York. Page 363-368.

Kakul H., Abid M. and Azam A., *European Journal of Medicinal Chemistry,* **42** (2007) 393-403.

Khlood S. A., and Nashwa M. E., *Spectrochimica Acta Part A: Molecular and Biomolecular Spectroscopy,* **70** (2007) 277-283.

Kinoshita M., Tsunehisa N. and Tamaki H., *Biological and Pharmaceutical Bulletin,* **18** (1995) 223–226.

Klayman D.L, Scovill J.P., Bartosevich J.F. and Bruce J., J*ournal of Medicinal Chemistry*, **26(1)** (1983) 35–39.

Koh L. L., Kon O. L., Loh Y. C., Ranford J. D., Tan A. L. C. and Tjan Y. Y., *Journal of Inorganic Biochemistry,* **72** (1998) 155.

Kovala D.D., Boccarelli A., Demertzis A. and Coluccia M., *International Journal of Experimental and Clinical Chemotherapy*, **53** (2007) 148-152.

Lever A. B. P, *Inorganic Electronic Spectroscopy,* 1968. Elsevier, Netherlands. Page 25-30.

Lewis D. A., and Hanson D., *Progress in Medicinal Chemsitry*, **28** (1991) 201-231.

Lu Z.-L., Xiao, W., Kang, B.-S., Su, C.-Y. and Liu, J., *Journal of Molecular Structure,* **523** (2000) 133-141.

Macchi M. M. and Bruce J. N., *Frontiers in Neuroendocrinology*, **25(3-4)** (2004) 177-195.

Mala N., Neelam S. and Sharma C.L., *Synthesis and Reactivity in Inorganic and Metal Organic Chemistry,* **20** (1990) 623-643.

Mala N., Neelam S., Sharma C.L., *Main Group Metal Chemistry,* **18** (1995) 1565.

Marisa B. F., Franco B., Giorgio P., Pieralberto T. Roberto A., Pier P. D., Silvana P., Alberta B. and Gianni S., *Journal of Inorganic Biochemistry*, **98** (2004) 301-312.

Marisa B.F., Franco B., Giorgio P., Silvana P. and Pieralberto T., *Polyhedron*, **26** (2007) 5150–5161.

Martin R. M. G., Gili, P., Martin Z. P., Medina O. A. and Diaz G. M. C., *Inorganica Chimica Acta*, **116** (1986) 153-156.

Martin Z. P., Gili P., Mederos, A. and Medina, A., *Thermochimica Acta*, **156** (1989) 231-238.

Martelli A., Mattlioli F., Mereto E., Brambilla C. G., Sini D., Bergamaschi R. and Brabilla G., *Toxicology*, **30** (1998) 19-41.

Mincis M., Chebli J. M. F., Khouri S. T. and Mincis R., *Arquivos of Gastroenterology*, **32** (1995) 131-136.

Nabar M.A., *Bulletin of the Chemical Society of Japan*, **1** (1966) 1067-1069.

Nagaraja B.R., Prakash G.A., Prema S.B. and Patil S.A., *Journal of Saudi Chemical Society*, 11 (2007) 253-268.

Nešpůrek S., Kadashchuk A., Skryshevski Y., Fujii A. and Yoshino K., *Journal of Luminescence,* 99 (2002) 131-140.

Noamesi B. K., Mensa J. F., Bogale M., Dange E. and Adotey J., J *Journal of Ethnopharmacology*, **42** (1994) 13-18.

Noda Y., Mori A., Liburdy R. and Packer L., *Journal of Pineal Research*, **27(3)** (1999) 159-163.

Obadović D. Ž., Divjaković V. and Leovac V. M., *Polyhedron*, **16** (1996) 3631-3634.

Obadović D. Ž., Petrović A. F. and Lukić F., *Review Research, Physics Series,* **411** (1981) 51-54.

Obadović D. Ž., Petrović A. F., Leovac V. M. and Chundak S. Y., *Journal of Physical Chemistry,* **42** (1990) 225-232.

Oommen S.,Anto R.J., Srinivas G. and Karunagaran D., *European Journal of Pharmacology*, **485** (2004) 97-103.

Onoda A., Kawakita K., Okamura T., Yamamoto H. and Ueyama N., *Acta Crystallography Section E.*, **59** (2003) 291-293.

Palenik G.J. and Shaun O.S., *Inorganica Chimica Acta,* **183** (1990) 217-220.

Patil S., Kantak U. and Sen D., *Inorganica Chimica Acta*, **63(2)** (1982) 261-265.

Patil B.G., Havinale B.R., Shallom J.M. and Chitnis M.P., *Journal of Inorganic Biochemistry*, **36** (1989) 107–113.

Pelttari E., Karhumaki E., Langshaw J. and Elo H., *Zeitschrift für Naturforschung. C, Journal of Biosciences*, **62** (2007) 483-486.

Peskar B. M. and Maricic N., *Digestion Disease Science*, **43** (1998) 23-29.

Pfeiffer P., Bucholz E. and Bauer O., *Journal für Praktische Chemie*, ***129*** (1931) 163.

Pfeiffer P., Breith E., Lübbe E. and Tsumaki T., *Justus Liebigs Annalen der Chemie*, **503** (1933) 84.

Pfeiffer P., Christeleit W., Hesse T., Pfitzinger H. and Thielert H., *Journal für Praktische Chemie*, **150** (1938) 261.

Pfeiffer P., Thielert H. and Glaser H., *Journal für Praktische Chemie*, **152** (1939) 145.

Pfeiffer P., Offermann W. and Werner H., *Journal für Praktische Chemie*, **159** (1942) 313.

Piper D. W. and Stiel D. D., *Medical Program Technology*, **2** (1986) 7-10.

Poeggeler B., Saarela, S., Reiter, R. J., Tan, D. X., Chen, L. D., Manchester, L. C. and Barlow-Walden, L. R., *Annals of the New York Academy of Sciences*, **738** (1994) 419-420.

Procter I., Hathaway B. and Nicholls P., *Journal of American Chemical Society*, **7** (1968) 1678.

Ramesh C., and Deepali J., *Synthesis and Reactivity in Inorganic, Metal Organic and Organic Chemistry,* **23** (1993) 767-776.

Ranjit M.B. and Sangita G., *AAPS Pharmaceutical Sciences,* **6** (2004) 14.

Raymond C. and Shiufun P., *The University of Hong Kong, Ultra Biotech Ltd., China Patent Agent,* 2004.

Revankar V. K., Sathisha M. P., Shetti U. N. and Pai K.S.R., *Journal of Medicinal Chemistry* **9** (2007) 536-544.

Rizal M.R, H.M. Ali and S.W. Ng, *Acta Crystallography Section E*, **64** (2008) m824.

Rizal M.R, H.M. Ali and S.W. Ng, *Acta Crystallography Section E*, **64** (2008) m755.

Rizal M.R, H.M. Ali and S.W. Ng, *Acta Crystallography Section E*, **64** (2008) o918.

Robert A., Nezamis J. E., Lancaster C. and Hanchar A. J., *Gastroenterology*, **77** (1979) 433-443.

Rosenberg B., *Platinum Metal Review*, **15** (1971) 42-51.

Sathisha M.P, Revankar V.K. and Pai K.S.R., *Metal Based Drugs*, **ID 362105** (2008) 1-11.

Sathisha M.P., Shatti U.N., Revankar V. K. and Pai K.S.R., *European Journal of Chemistry,* **9** (2004) 713-727.

Sawant S.S., Sylvester P.W., Avery M.A., Desai P., Youssef D.T.A. and El-Sayed K.A., *Chemistry Pharmacology Bulletin*, 54 (2006) 1119-1123.

Schiff H., *Annalen der Chemie und Pharmacie*, **3** (1864) 343.

Schläfer H.L., Gausmann H. and Witzke H., *Journal of Chemical Physics*, 46 (1967) 1423.
Sérgio F.A., Marivane L., Eros C., Vânia F.N., Valdir C.F. and Rivaldo N., *Journal of Ethnopharmacology*, **113** (2007) 252-257.

Sheldrick G. M. (1997) *SHELXS97* and *SHELXL97,* University of Göttingen, Germany.

Sheldrick G. M. (2008) *Acta Crystallography Section A,* **64** (2008) 112-122.

Siddiqi K.S., Sadaf K., Shahab A.A.M. and El-ajaily M.M., *Spectrochimica Chimica Acta: Part A,* **67** (2007) 995-1002.

Singh N. K., Kushawaha S.K. and Thomas M.J.K., *Transition Metal Chemistry*, **25**, (2000) 648.

Singh S.B., Zink D.L., Polishook J.D., Dombrowski A.W., Darkin-Rattray S. J., Schmatz D. M. and Goetz M. A., *Tetrahedron Letter,* **37** (1996) 8077.

Sundberg R.J., *The Chemistry of Indoles,* New York Academic Press (1970). Page 10-50.

Syamal A. and Maurya M.R., *Synthesis and Reactivity in Inorganic, Metal Organic and Organic Chemistry*, **16** (1986) 39.

Szabo S., *Scandinavian Journal Gastroenterology,* **22** (1987) 21-28.

Teoh S.G., Ang S.H., Teo, S.B., Fun H.K., Khew K.L. and Ong C.W., *Dalton Transactions*, **6** (1997) 2827-2834.

Terano A., Hiraishi H., Ota S., Shiga J. and Sugimoto T., *Gastroenterologia Japonica*, **24** (1989) 488-493.

Toma W., Gracioso J., Andrade F., Hiruma-Lima C., Vilegas W. and Souza-Brito A. R., *Biological and Pharmacological Bulletin*, **25** (2002) 1151-1155.

TÜmer M., *Synthesis and Reactivity in Inorganic, Metal Organic and Organic Chemistry,* **30** (2000) 803-813.

Tunde T.B. and Omolara A.B., *Inorganica Chimica Acta,* **144** (1988) 249-252.

Ugo R., *J. Organometallic Chemistry*, **9** (1967) 395.

Ureña J., Lopez B.J., Lopez J.R. and Gonzalez C., *Science*, **241** (1998) 580-582.

Walter M., Kolarz B. and Zgorniak-Nowosielska I., *Archivum Immunologiae Et Therapiae Experimentalis,* **29** (1981) 187–194.

Williams D.R., *Chemical Reviews*, **72** (1972) 203-213.

Wolfe M. M., and Sachs G., *Gastroentorolgy*, **118** (2000) S9-S31.

Xavier O., Ally A., Yves J., Rosa C., Joan C., Beatriz C., Isabel C., Simona C., Munoz M. C., Antonio L. R., Bernardino S. and Rafael R., *Dalton Transactions*, **15** (2005) 2516-2526.

Zayed M. A., El-Dien. F. A., Mohamed G.G. and El-Gamel N.E.A., *Spectrochimica Acta Part A: Molecular and Biomolecular Spectroscopy,* **60** (2004) 2215.

Zahid C.H., Khalid K.M. and Claudid S.T., *Applied Organometallic Chemistry,* **18** (1987) 305-310.

Zgornaik-Nowosielska A., Gatkiewicz A., Veckenstedt and Beladi I., *Acta Virologica,* **24** (1980) 439–444.

List of publications

1. **M.R. Rizal**, H.M. Ali and S.W. Ng, *trans*-bis(1H-indoe-3-carbaldehyde thiosemicarbazonato-$\kappa^2 N^1$, *S*)nickel(II). Acta Cryst. (2008), E**64**, m824.

2. **M.R. Rizal**, H.M. Ali and S.W. Ng, Bis[1,5-bis(1*H*-indol-3-ylmethylene) thiocarbazonato-$\kappa^2 N$,*S*]nickel(II) dimethyl sulfoxide disolvate. Acta Cryst. (2008), E**64**, m755.

3. H. M. Ali, M. I. Mohamed Mustafa, **M. R. Rizal** and S. W. Ng, Dichloridobis(2-{1-[2-(1*H*-indol-3-yl)ethyliminio]ethyl}phenolate-κO)zinc(II)-2-{1-[2-(1*H*-indol-3-yl)ethyliminio]ethyl}phenolate (1/2). *Acta Cryst.* (2008). E**64**, m718-m719.

4. H. M. Ali, M. Laila, **M. R. Rizal** and S. W. Ng, *N*'-(5-Fluoro-2-oxo-2,3-dihydro-1*H*-indol-3-ylidene)benzenesulfonohydrazide. *Acta Cryst.* (2008). E**64**, o921.

5. H. M. Ali, M. I. Mohamed Mustafa, **M. R. Rizal** and S. W. Ng, Bis{2-[2-(1*H*-indol-3-yl)ethyliminomethyl]phenolato-$\kappa^2 N$,*O*}nickel(II) *N*,*N*-dimethylformamide disolvate, *Acta Cryst.* (2008). E**64**, m787.

6. **M.R. Rizal** and S.W. Ng, 4'-Fluoro-2'-hydroxyacetophenone. *Acta Cryst.* (2008). E**64**, o916.

7. H. M. Ali, M. I. Mohamed Mustafa, **M. R. Rizal** and S. W. Ng, Bis{4-chloro-2-[2-(1*H*-indol-3-yl)ethyliminomethyl]phenolato-$\kappa^2 N$,*O*}zinc(II). *Acta Cryst.* (2008). E**64**, m421.

8. H. M. Ali, M. Laila, **M. R. Rizal** and S. W. Ng, Bis{μ-*N*'-[1-(5-bromo-2-oxidophenyl)ethylidene]benzenesulfonohydrazidato}-$\kappa^3 O^2$,*N*':*N*;$\kappa^3 N$:*O*^{2},*N*'-bis[(dimethyl sulfoxide-κO)copper(II)]. *Acta Cryst.* (2008). E**64**, m414

9. H. M. Ali, M. I. Mohamed Mustafa, **M. R. Rizal** and S. W. Ng, 2-[2-(1*H*-indol-3-yl)ethyliminiomethyl]-4-nitrophenolate. *Acta Cryst.* (2008). E**64**, o913

10. H. M. Ali, K. Zuraini, B. Wan Jeffrey, **M.R. Rizal** and S.W. Ng, 1-(2-Hydroxy-5-methylphenyl)ethanone [(1*H*-indol-3-yl)acetyl]hydrazone. *Acta Cryst.* (2008). E**64**, o912.

11. H.M. Ali, J. Yusnita, **M.R. Rizal** and S.W. Ng, *N*'-(2,5- Dihydroxybenzylidene) benzenesulfonohydrazide. *Acta Cryst.* (2008). E**64**, o522.

12. **M.R. Rizal**, H.M. Ali and S.W. Ng, 5-Bromo-1H-indole-3-carbaldehyde thiosemicarbazone. Acta Cryst. (2008). E**64**, o918.

13. **M.R. Rizal**, I. Azizul, S.W. Ng, Low-temperature predetermination of 3,4,5,6-tetrahydropyrimidine-2(1H)-one. Acta Cryst. (2008). E**64**, o914.

14. **M.R. Rizal**, I. Azizul, S.W. Ng, 4-Hydroxy-3-nitrobenzaldehyde. Acta Cryst. (2008). E**64**, o915.

15. **M.R. Rizal**, H.M. Ali, S.W. Ng, 1H-Indole-3-carbaldehyde azine. Acta Cryst. (2008). E**64**, o555.

16. **M.R. Rizal**, S.W. Ng, 4'-Fluoro-2'-hydroxyacetophenone. Acta Cryst. (2008). E**64**, o916.

17. A.M. Graisa, Y. Farina, M. Kassim, **M.R. Rizal**, S.W. Ng. Acta Cryst. (2008) E**64**, o251.

18. H.M. Ali, J. Yusnita, **M.R. Rizal** and S.W. Ng, [2'-(5-Chloro-2-oxidobenzylidene) benzenesulfonohydrazide-$\kappa^2 N,O$][2'-(2-oxidobenzylidene)benzenesulfonohydrazide-$\kappa^2 N,O$]copper(II). *Acta Cryst.* (2007). E**63**, m2937.

19. H.M. Ali, S.J. Nazzatush, **M.R. Rizal** and S.W. Ng, Bis{2'-[(5-chloro-1*H*-3-indolyl)methylene]-2-(1*H*-3-indolyl)acetohydrazido-$\kappa^2 N,O$}nickel(II) dimethyl sulfoxide disolvate. *Acta Cryst.* (2007). E**63**, m3033.